Spectroelectrochemical Studies of Molecular Association with Polyamidoamine Dendrimers at Liquid | Liquid Interfaces

Spectroelectrochemical Studies of Molecular Association with Polyamidoamine Dendrimers at Liquid|Liquid Interfaces

Division of Material Sciences, Graduate School of Natural Science & Technology, Kanazawa University

Submitted by Hiroki Sakae
(ID: 1323132002)
Certified by Hirohisa Nagatani
January, 2016

ABSTRACT

Dendrimers are non-traditional polymers which have a well-defined molecular structure and have attracted much attention as molecular capsule for drug delivery systems (DDS) and separation sciences. It is worth investigating molecular encapsulation behavior and charge transfer reaction of dendrimers at an interface between two immiscible electrolyte solutions (ITIES) where metal ions and organic molecules are transferred. In order to evaluate the potential ability of dendrimers as molecular capsule, molecular encapsulation behavior of amino and carboxylate-terminated polyamidoamine (PAMAM) dendrimers and the interfacial behavior at the polarized water|1,2-dichloroethane (DCE) interface were investigated through potential modulated fluorescence (PMF) spectroscopy. The association between the dendrimers and the porphyrins or bioactive species was significantly dependent on the pH condition and the generation of dendrimers. In aqueous solutions, the spectroscopic results indicated that zinc(II) 5,10,15,20-tetrakis(4-sulfonatophenyl)porphyrin ($ZnTPPS^{4-}$) associated with the positively charged fourth generation (G4) PAMAM dendrimer was highly stabilized without protolytic demetalation in a wide range of pH. On the other hand, the free base porphyrin (H_2TPPS^{4-}) was readily protonated under acidic conditions even in the presence of the dendrimers accompanied by forming the J-aggregates of diprotonated species, $(H_4TPPS^{2-})_n$. PMF measurement at the water|DCE interface revealed that the dendrimers incorporating porphyrin molecules were transferred across the positively polarized interface accompanied by the adsorption process, whereas the porphyrins released from the dendrimers were transferred at the negatively polarized interface. The ion association stability between the dendrimer and the porphyrin estimated from the negative shift of the transfer potential of the porphyrins exhibited relatively strong interaction between $ZnTPPS^{4-}$ and the higher generation dendrimer. In the bioactive species systems, ionizable drugs, i.e. dipyridamole (DIP), propranolol (PRO) and warfarin (WAR), were

not effectively associated with the dendrimers in the aqueous solutions. PMF results of the fluorescent DIP indicated that the monoprotonated form, $HDIP^+$, was transferred across the water|DCE interface accompanied by the adsorption process and the interfacial mechanisms of the DIP species were significantly modified by the dendrimers, depending on the pH conditions. Flavin derivatives, especially riboflavin (RF) and lumichrome (LC), were effectively associated with the dendrimer in the aqueous solution. The interfacial adsorption of the anionic flavin derivatives was inhibited by forming associates with the dendrimer, while the associates were transferred across the interface in the positive potential region. Present results demonstrated that the potential ability of the dendrimers as molecular capsule and drug transporter.

CONTENS

PART I
Spectroelectrochemical Characterization of Dendrimer-Porphyrin Associates at Polarized Liquid|Liquid Interfaces

PART II
Ion Transfer and Adsorption Behavior of Bioactive Species Affected by PAMAM Dendrimers at the Water|1,2-Dichloroethane Interface

1 INTRODUCTION

1-1 Liquid|Liquid Interface

A liquid|liquid interface consisted of two immiscible liquids is a two-dimensional specific reaction field, where a solvent structure, electrostatic potential, intermolecular interaction could be drastically changed as compared with bulk solution phase.[1-3] In the solvent extraction system, an ion in the aqueous phase is extracted to the organic phase via the ion association and complexation with ligands. It is important for effective extraction to enhance the phase transport efficiency, e.g., the ion selectivity of ligand at interfaces.[4] In addition, amphiphilic species such as surfactants and phospholipids are adsorbed and assembled at the liquid|liquid interface. Therefore, mass transfer reactions at liquid|liquid interfaces have been studied extensively for analytical sciences, synthesis of thin-layer materials, and biochemical applications. Especially, an interface between two immiscible electrolyte solutions (ITIES) has been studied as a model of biomembrane to investigate the cell membrane permeability of ion species and enzymatic reaction.[5-8] Charge transfer, adsorption and heterogeneous reactions could be controlled as a function of the Galvani potential difference at ITIES (**Fig. 1**). The ion-

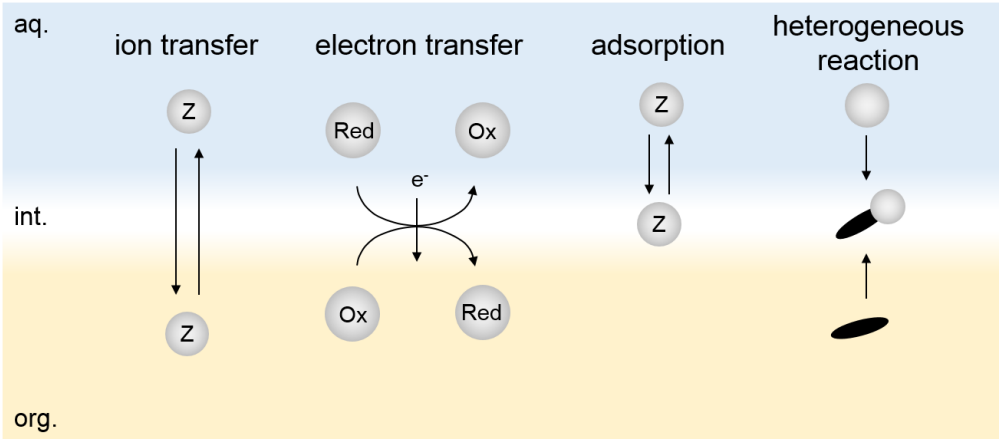

Fig. 1 Schematic representation of elementary steps at a polarized liquid|liquid interface.

partitioning property of species under electrochemical control is particularly useful to evaluate the pharmacokinetic distribution of drugs. Ion transfer voltammetry and related electrochemical techniques allow us to access fundamental information on the charge transfer reaction across ITIES. The ionic partition diagram is one of the most important data to evaluate the distribution property of ionic species.[9-13] The diagram is analogous to Pourbaix's pH-potential diagrams widely used in the electrochemistry on solid electrodes. The ionic partition diagram indicates the dominant species at given potential differences and pH values. Basically, the ionic partition diagram is constructed by three types of boundary lines. For instance, the partition diagram of a basic species (HB^+) provide us to trace the ion transfer potential and distribution equilibria of HB^+ and B in the liquid|liquid system as a function of pH (**Fig. 2**). Furthermore, in order to investigate the interfacial molecular structure and the mechanism including an ion transfer and adsorption with a specific orientation, surface-sensitive spectroscopic techniques, e.g. second harmonic generation (SHG) and potential modulated fluorescence (PMF) spectroscopy, have been employed.[14-16]

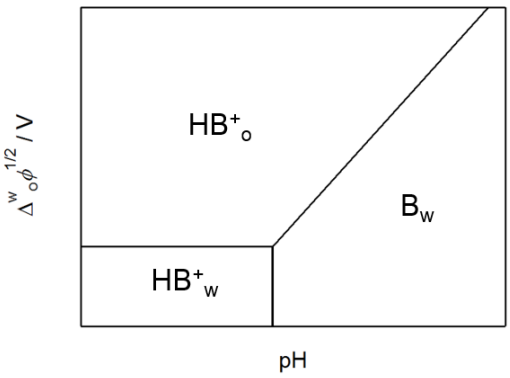

Fig. 2 Schematic representation of the ionic partition diagram of a basic species (HB^+).

1-2 Dendrimers

Dendritic polymers have a three dimensional structure repeating multifunctional monomers. Dendritic polymers are roughly categorized into dendrimers and hyperbranched polymers. Dendrimers should have an accurate structure with a monodispersed molecular weight, while hyperbranched polymers have repeated branch units with a polydispersed one. Dendritic polymers have attracted much attention over the years for light-harvest devices, molecular recognition and drug delivery systems (DDS) and so on.[17-23] Dendrimers first defined by Tomalia in 1985 are unique and nontraditional polymers with a well-defined macromolecular architecture consisting of a core, iterative branch units, and terminal groups.[24] The repeat of branch units is called generation (G). Dendrimers have been synthesized by divergent and convergent methods.[25] In the divergent method, an internal core is grown up to outside by attaching branch units. On the other hand, in the convergent method, dendrons which compose peripheral moiety are synthesized and then these dendrons are attached by a core. The former is used to a large-scale synthesis, although a lot of building blocks are needed to proceed reaction perfectly. The latter has the advantage of achieving the dendrimer with an accurate monodispersed molecular weight. Modification of the terminal and/or branching units leads to adjustment of shape, solubility, flexibility, viscosity and functionality.[26] For instance, the density and size of the interior of the dendrimer is important for the host/gest chemistry. Various organic molecules and metal ions have been reported to be accommodated into the internal cavity and captured on the peripheral region of the dendrimer by hydrophobic and electrostatic interactions.[27-29]

The most widely studied polyamidoamine (PAMAM) dendrimer is constructed based on an ethylenediamine core and amino (full generation) or carboxyl (half generation) terminal groups. The net charges and conformation of the PAMAM dendrimer are significantly affected by the pH condition owing to the protonation equilibria of

terminal groups and tertiary amines in the interior. The molecular configuration of the PAMAM dendrimer tends to be a spherical shape from a flat-elliptical according to the increase of the generation.[26, 30-33] Structural characteristics of the G2 and G4 PAMAM dendrimers are shown in **Fig. 3** and **Table 1**. The molecular encapsulation features of a guest molecule thus would be affected by the generation of the dendrimer. The ion association and transfer mechanisms of the dendrimer in liquid|liquid biphasic systems are very important to estimate a capability of the dendrimer in DDS and separation sciences. ITIES is a useful model as biomembrane systems, in which charge transfer and adsorption reactions are took place by applying potentials. However, there are only a few reports for the simple interfacial behavior of dendrimers in the absence of the coexisting species at ITIES. Berdque and coworkers investigated the electrochemical behavior of the polypropylenimine (DBA-AM-*n*) and polyamidoamine (PAMAM) dendrimer with a different generation at the water|1,2-dichloroethane (DCE) interface.[34] Recently, the ion transfer mechanism of the PAMAM dendrimer incorporating a fluorescence probe was studied in detail at the polarized water|DCE.[35, 36] Spectroelectrochemical analysis demonstrated that the amino-terminated fourth-generation (G4) PAMAM dendrimer was transferred across the interface accompanied by the adsorption processes including the facilitated ion transfer of the organic electrolyte anion in the positively polarized interface.[36] In addition, molecular encapsulation behavior of the carboxylate-terminated G3.5 PAMAM dendrimer for 8-anilino-1-naphthalenesulfonate (ANS^-) and its bimolecular derivative (bis-ANS^{2-}) was investigated at the polarized the water|DCE interface.[35] It was demonstrated that the molecular encapsulation behavior could be controlled as a function of pH and the Galvani potential difference.

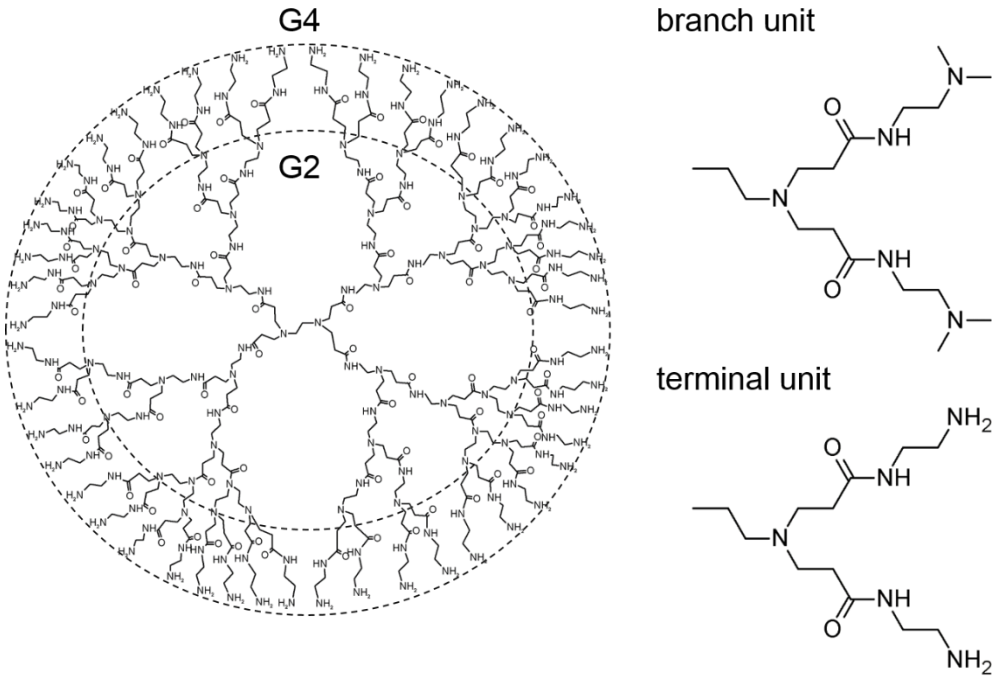

Fig. 3 Schematic drawing of the molecular structure of PAMAM dendrimers.

Table 1 Structural characteristics of the G2 and G4 PAMAM dendrimers

	G2 PAMAM dendrimer	G4 PAMAM dendrimer
primary amine (terminal group)	16	64
tertiary amine (branch point)	14	62
diameter / nm	2.9[a]	4.5[a]
configuration	planar-elliptical shape[b]	spherical shape[b]

[a]Ref. [26]. [b]Ref. [33]. Approximate hydrodynamic diameters based on gel electrophoresis [26]. MD calculations of configurations with AMBER force field [33].

1-3 Aim of This Study

Recently, the interfacial mechanism and molecular encapsulation behavior of the dendrimer have been investigated by using the fluorescence probes. In this study, in order to develop applications of dendrimers for medical sciences and analytical sciences, the interfacial mechanism and the molecular encapsulation behavior of the PAMAM dendrimers with a different generation for the anionic porphyrins and bioactive species are studied through the spectroelectrochemical analysis at the water|DCE interface. The effect of metal ions, hydrogen bonding, electrostatic and hydrophobic interaction on the encapsulation behavior of the dendrimers were investigated.

This thesis consists of two parts. In PART I, the association behavior between amino-terminated G4 and G2 PAMAM dendrimer and the anionic porphyrin at polarized liquid|liquid interfaces is spectroelectrochemically characterized.

In PART II, in order to extend the biological applications of dendrimers, the interfacial behavior of bioactive species, i.e. ionizable drugs and flavin derivatives, affected by PAMAM dendrimers are investigated.

2 Methodology

2-1 Voltammetric Measurements

At ITIES, an ion (x^{z+}) which have the intermediate property of a hydrophilicity and hydrophobicity of electrolytes dissolved in each phases can be transferred between water and organic phases within the electrochemical potential window.

$$x_w^{z+} \rightleftharpoons x_o^{z+} \tag{1}$$

where subscripts w and o refer to water and organic phases, respectively. In voltammetric techniques, ion transfer reactions are observed through current responses. Ion transfer reactions can be controlled by the Galvani potential ($\Delta_o^w\phi$) difference across the interface:

$$\Delta_o^w\phi = \phi^w - \phi^o \tag{2}$$

where ϕ^w and ϕ^o are the inner potential of each phases. In case the ion transfer is fast without adsorption, $\Delta_o^w\phi$ dominates the partitioning of x^{z+} between water and organic phases according to the Nernst equation:

$$\Delta_o^w\phi = \Delta_o^w\phi_t^\circ + \frac{RT}{zF}\ln\frac{a_x^o}{a_x^w} \tag{3}$$

where z, F, $\Delta_o^w\phi_t^\circ$, a_x^w and a_x^o are charge number of transferring ion, Faraday constant, the standard transfer potential, the activities in the aqueous and the organic phases, respectively. $\Delta_o^w\phi_t^\circ$, which is intrinsic value to the ionic species, is associated with the standard Gibbs free energy of ion transfer ($\Delta G_{t,x}^{\circ,w\to o}$) (**Scheme 1**):

$$\Delta G_{t,x}^{\circ,w\to o} = zF\Delta_o^w\phi_t^\circ \tag{4}$$

The hydrophilicity and hydrophobicity of the ion can be quantitatively evaluated from $\Delta G_{t,x}^{\circ,w\to o}$.

Charge transfer processes at ITIES can be represented as the equivalent circuit. **Fig. 4** shows the equivalent circuit of a liquid|liquid interface associated with ion transfer. R_u is the solution resistance. C_{dl} is the interfacial double-layer capacitance. Z_b and Z_t are the electrolyte and the ion transfer impedance, respectively. Using the dc voltammetric

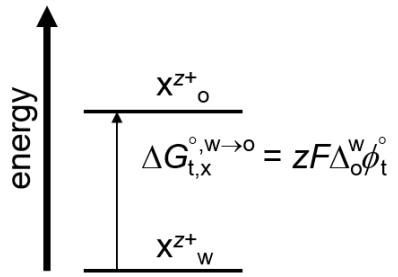

Scheme 1 Energy diagram of ion transfer.

technique, it is difficult to investigate interfacial reactions including an ion transfer and interfacial adsorption processes separately. The ac voltammetric technique provides us various electrochemical parameters in the circuit by analyzing the dependence of impedance on ac frequency. In the ac voltammetric technique, an ac potential modulation is superimposed on the controlled dc bias. In the case that a potential-dependent process of an ion takes place at the polarized liquid|liquid interface, the ac current signal is modulated with the same frequency as the potential modulation. Z_b and Z_t are given by:[37]

$$Z_b = R_u + \left[j\omega C_{dl} + \frac{1}{R_b} \right]^{-1} \tag{5}$$

$$Z_t = R_u + \left[j\omega C_{dl} + \frac{1}{R_b} + \frac{1}{R_{ct} + (1-j)\sigma\omega^{-0.5}} \right]^{-1} \tag{6}$$

where R_b is the electrolyte resistance. j and ω are imaginary number and the angular frequency ($\omega = 2\pi f$), respectively. The charge transfer resistance, R_{ct}, is described as:[38]

$$R_{ct} = \frac{RT}{z^2F^2Sk_tc_0^w} \tag{7}$$

where k_t is the ion transfer rate constant.σ is the Warburg term described as:[38]

$$\sigma = \frac{4RT\cosh^2(\xi/2)}{z^2F^2Sc^w\sqrt{2D^w}} \tag{8}$$

$$\xi = zF\left(\Delta^w_o\phi - \Delta^w_o\phi^{\circ\prime}_t\right)/RT \tag{9}$$

where c^w and D^w are the concentration and the diffusion coefficient of the transferring ion

in water phase, respectively. $\Delta_o^w\phi_t^{o'}$ is the formal ion transfer potential. In this study, the ac current signal is analyzed as the admittance. The admittance (Y) is represented as the inverse of impedance.

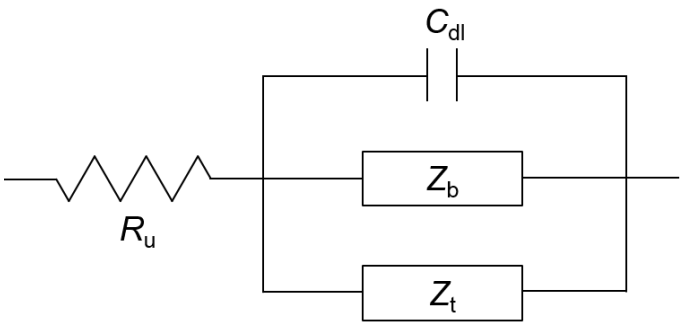

Fig. 4 Equivalent circuit of liquid|liquid interfaces in the presence of the reactant ions.

2-2 Potential Modulated Fluorescence (PMF) Spectroscopy

In this technique, the interfacial process of fluorescent ions can be selectively studied as a function of ac potential modulation superimposed on the dc bias defined as:

$$\Delta_o^w\phi = \Delta_o^w\phi_{dc} + \Delta_o^w\phi_{ac}\exp(j\omega t) \quad (10)$$

where $\Delta_o^w\phi_{ac}$ is the amplitude of the ac potential modulation. In the case that a potential-dependent process of the fluorescent ion takes place at the polarized liquid|liquid interface, the fluorescence intensity from the interfacial region is modulated with the same frequency as the potential modulation. By analyzing the phase shift and its frequency response, the ion transfer and adsorption processes are readily distinguishable.

2-2-1 PMF Responses for a Quasi-Reversible Ion Transfer Process

The PMF signal associated with a quasi-reversible ion transfer (ΔF_t) is correlated with the faradaic ac current ($i_{f,ac}$). In the case of the total internal reflection (TIR) excitation condition, ΔF_t is described as:[38, 39]

$$\Delta F_t = \frac{4.606\varepsilon\Phi_f I_0}{j\omega zFS\cos\psi} i_{f,ac} \quad (11)$$

where ε, Φ_f, I_0, S and Ψ, respectively, are the molar absorption coefficient, the fluorescence quantum yield, the intensity of excitation light, interfacial area and the angle of incidence. Eq. (10) can be separated to the real ($\Delta F_{t,re}$) and imaginary part ($\Delta F_{t,im}$):[38]

$$\Delta F_{t,re} = \frac{4.606\varepsilon\Phi_f I_0}{zFS\cos\psi}\left[\frac{\Delta_o^w\phi_1\sigma\omega^{-3/2}}{\left(R_{ct}+\sigma\omega^{-1/2}\right)^2+\left(\sigma\omega^{-1/2}\right)^2}\right] \quad (12)$$

$$\Delta F_{t,im} = -\frac{4.606\varepsilon\Phi_f I_0}{zFS\cos\psi}\left[\frac{\Delta_o^w\phi_1\left(R_{ct}+\sigma\omega^{-1/2}\right)\omega^{-1}}{\left(R_{ct}+\sigma\omega^{-1/2}\right)^2+\left(\sigma\omega^{-1/2}\right)^2}\right] \quad (13)$$

where σ and $\Delta_o^w\phi_1$ are the Warburg term and the amplitude of potential. It has been established that the real and imaginary components of the PMF signal for an ion transfer

of a cationic species across the interface are expressed as positive and negative values at an ion transfer potential, respectively (**Fig. 5**). In case the ion transfer rate constant is fast (k_t = 0.1 cm s^{-1}), the magnitude of the real and imaginary components of the PMF response is almost same. The relative magnitude of the real component decreases with small k_t values. Then, a PMF complex plane for cationic species with a large k_t value, k_t = 0.1 cm s^{-1}, appears in the fourth quadrant (**Fig. 6**). On the other hand, the 180° phase shift, negative real and positive imaginary components, is obtained for an anionic species.

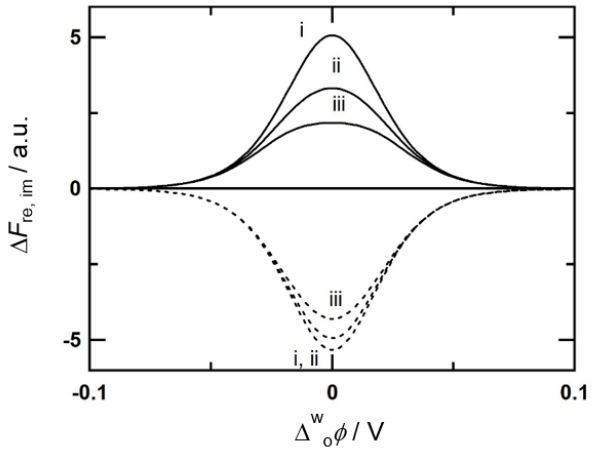

Fig. 5 Numerical simulations of PMF for a quasi–reversible ion transfer. The solid and dashed lines denote the real and imaginary components. The ion transfer rate constant, k_t = 0.1 (i), 0.01 (ii), 0.005 (iii) cm s^{-1}, respectively. Adopted from Ref. [38] and [39].

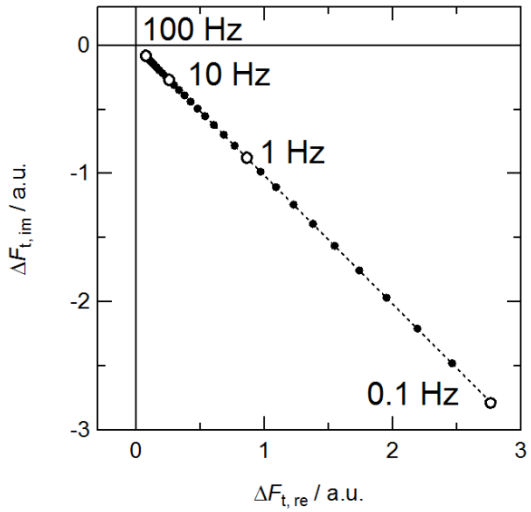

Fig. 6 Complex representation of the PMF for a quasi–reversible transfer of a monocation. k_t, = 0.1 cm s^{-1}. The diffusion coefficient in the aqueous phase, D^W,was taken as 5×10^{-6} cm^2 s^{-1}. Adapted from Ref. [38].

2-2-2 PMF Responses for an Adsorption Process

The PMF signal associated with the adsorption (ΔF_a) from the aqueous phase to the interface is expressed as a function of the ac surface coverage (θ_{ac}):[38]

$$\Delta F_a = 2.303\varepsilon\Phi_f I_0 \Gamma_s \theta_{ac} \tag{14}$$

where Γ_s is the saturated interfacial concentration. θ_{ac} is described as:[38]

$$\theta_{ac} = \frac{bzF\Delta_o^w\phi_{ac}}{RT}\left[\frac{k_{a,dc}\alpha c_{dc}(1-\theta_{dc}) - k_{d,dc}(\alpha-1)\theta_{dc}}{k_{a,dc}c_{dc} + k_{d,dc} + j\omega}\right] \tag{15}$$

where b is the portion of applied potential employed for adsorption process ($b^w + b^o \leq 1$), α is overall transfer coefficient for adsorption process (~0.5), c_{dc} is the bulk concentration, θ_{dc} is dc surface coverage, $k_{a,dc}$ and $k_{d,dc}$ are the dc components of adsorption and desorption rate constants at given potentials, respectively. The appropriate reverse sign is applied to Eq. (14) for the adsorption process from the organic phase because of an opposite potential dependence of the surface concentration. Then Eq. (14) is rewritten as:[38]

$$\Delta F_{a,re}^w = \frac{2.303\varepsilon\Phi_f I_0 \Gamma_s SbzF}{RT}\left[\frac{\Delta_o^w\phi_1\left(k_{a,0}\alpha c_0(1-\theta_0) - k_{d,0}(\alpha-1)\theta_0\right)\left(k_{a,0}c_0 + k_{d,0}\right)}{\left(k_{a,0}c_0 + k_{d,0}\right)^2 + \omega^2}\right] \tag{16}$$

$$\Delta F_{a,im}^w = -\frac{2.303\varepsilon\Phi_f I_0 \Gamma_s SbzF}{RT}\left[\frac{\Delta_o^w\phi_1\left(k_{a,0}\alpha c_0(1-\theta_0) - k_{d,0}(\alpha-1)\theta_0\right)\omega}{\left(k_{a,0}c_0 + k_{d,0}\right)^2 + \omega^2}\right] \tag{17}$$

The potential dependence of the PMF signals for adsorption processes of a cationic species is shown in **Fig. 7**. A PMF complex plane of adsorption processes from the aqueous and organic sides of the interface appears in the fourth and second quadrants (**Fig. 8**).

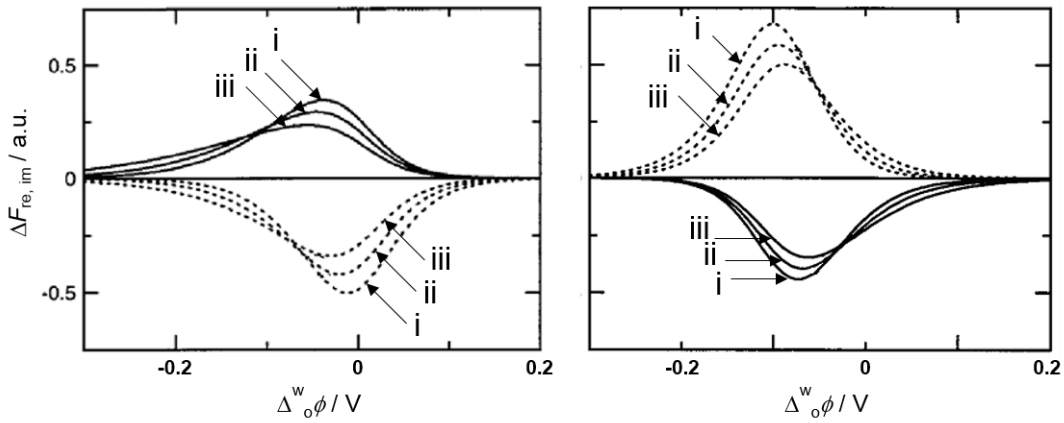

Fig. 7 Potential dependence of the PMF responses for a kinetically controlled adsorption from (left) the aqueous and (right) organic sides of the interface. The solid and dashed lines denote the real and imaginary components. b^{w} and b^{o} were taken as (i) 0.5 and 0.5, (ii) 0.4 and 0.6, (iii) 0.3 and 0.7, respectively. Adopted from Ref. [38].

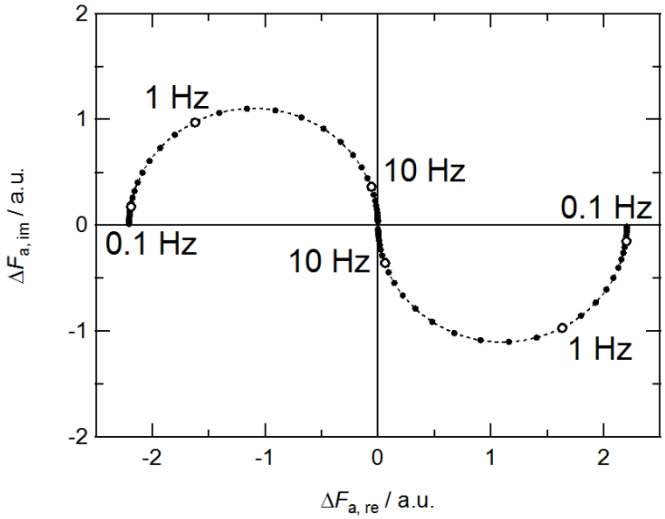

Fig. 8 Frequency dependence of the PMF responses for a kinetically controlled adsorption process. The adsorption rate constant, $k_{a,0} = 1\times10^{8}$ dm^{3} mol^{-1} s^{-1}. $k_{d,0}$ was fixed to 10 s^{-1}. Adopted from Ref. [38]

2-3 Photocurrent Transient Responses

The photoinduced electron transfer reaction between a sensitizer (S) and a quencher (Q), the product separation of the intermediate ion pair ($S^{-}\cdots Q^{+}$) as competition process with the recombination process generally would significantly affect the determination of overall electron transfer efficiency. In the case that S and Q are initially dissolved in the aqueous and the organic phase, respectively, the hydrophile-lipophile intermediate ion pair can be formed only at the liquid|liquid interface and the following product separation process readily takes place, since the decomposition products of the intermediate ion pair are diffused into each preferable liquid phase (**Scheme 2**).

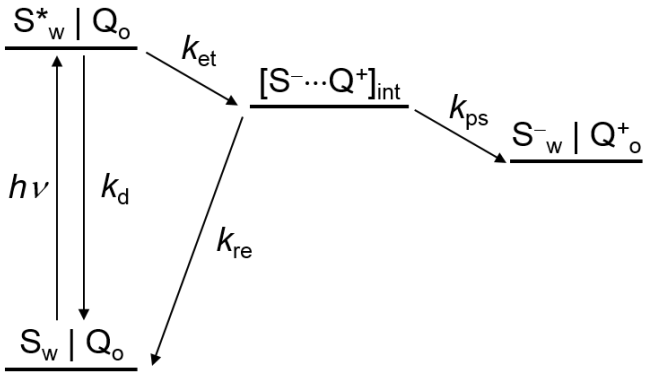

Scheme 2 Schematic representation of the photoinduced heterogeneous electron transfer reaction between a photoactive electron acceptor in the aqueous phase (S) and electron donner in the organic phase (Q). k_d, k_{et}, k_{ps} and k_{re} are the rate constant associated with the decay of the excited state, bimolecular electron transfer, product separation and back electron transfer steps, respectively.

3 EXPERIMENTAL SECTION

3-1 Reagents

The amino-terminated G4, G2 and carboxylate-terminated G3.5 PAMAM dendrimers with an ethylenediamine core were purchased from Aldrich (10 and 20 wt% in methanol) and prepared as an aqueous solution after removing methanol by drying in ultrapure argon (> 99.999%). The anionic porphyrins, 5,10,15,20-tetrakkis(4-sulfonatophenyl)porphyrin (H_2TPPS^{4-}) disulfuric acid tetrahydrate (Dojindo Laboratories) and the tetrasodium salt of its zinc(II) complex ($Na_4ZnTPPS$) (Frontier Scientific/Porphyrin Products), were used as received. Decamethylferrocene (DMFc, Wako Chemicals, >98%) as a lipophilic quencher for the photocurrent transient measurement was dissolved in the organic phase. Ionizable drugs, dipyridamole (DIP), propranolol (PRO) and warfarin (WAR) were received from TCI (> 98.0%), Aldrich (> 99%) and Nacalai Tesque (> 98%). Riboflavin (RF), lumichrome (LC) and its derivative flavin mononucleotide (FMN) were received from Kanto Chemical Co., Inc. (> 98.0%), TCI (> 95.0%) and Wako (> 95.0%). The composition of the electrochemical cell was represented in **Fig. 9**. In PART I, the dendrimers and the porphyrins were dissolved in the aqueous phase when the PMF measurement was carried out (**Fig. 9a**). In order to measure the photocurrent transient, DMFc as the electron donner was dissolved in the organic phase (**Fig. 9b**). In PART II, the dendrimers and bioactive species were dissolved in the aqueous phase (**Fig. 9c**). It should be noted that DIP was initially dissolved in the organic phase under the neutral and alkaline conditions because of its low solubility in water. The supporting electrolytes were 1.0×10^{-2} mol dm^{-3} LiCl for the aqueous phase and 5.0×10^{-3} mol dm^{-3} bis(triphenylphosphoranylidene)ammonium tetrakis(pentafluorophenyl)borate (BTPPATPFB) for the organic phase, respectively. BTPPATPFB was prepared by metathesis of bis(triphenylphosphoranylidene)ammonium chloride (BTPPACl) (Aldrich, > 97%) and lithium tetrakis(pentafluorophenyl)borate ethyl ether complex (TCI, ≥ 70%). In briefly, the molar ratio of BTPPACl : LiTPFB = 3 : 2 were prepared and dissolved in

methanol-water mixed solvent. LiTPFB solution was gradually added into BTPPACl solution. Precipitation was filtered with membrane filter (PTFE, pore size of 0.5 μm) and rinsed with water. Product was dried, dissolved in acetone and recrystallized at least two times. The organic solvent, 1, 2-dichloroethane (DCE), was of HPLC grade (Nacalai Tesque, > 99.7%). All other reagents were of the highest grade available and used without further purification. The aqueous solutions were prepared with purified water from a Milli-Q system (Millipore Simpli Lab-UV/Direct-Q 3 UV). The pH of the aqueous phase was controlled by the addition of HCl for acidic conditions, and LiH_2PO_4/LiOH, H_3BO_3/LiOH buffers and LiOH for neutral and alkaline conditions, respectively.

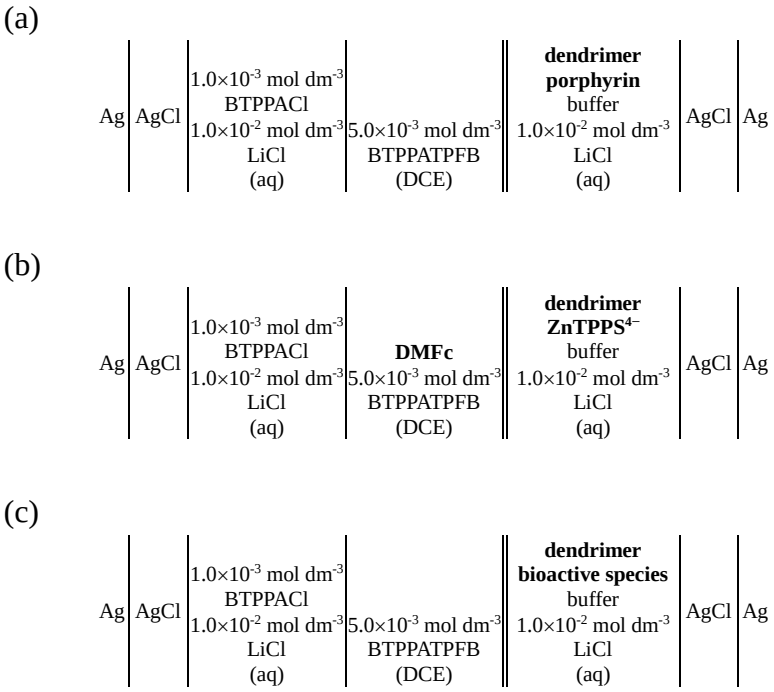

Fig. 9 The composition of the electrochemical cells for (a) porphyrin derivatives, (b) photocurrent transient and (c) bioactive species systems.

3-2 Apparatus

The electrochemical cell used in all measurements was shown in **Fig. 10**. The water|DCE interface with a geometrical area of 0.50 cm^2 was polarized by a four-electrode potentiostat (Hokuto Denko HA1010 mM1A). Platinum wires were used as counter electrodes in both aqueous and organic phases. The Luggin capillaries were provided for the reference electrodes (Ag/AgCl) in both phases. The Galvani potential difference ($\Delta_o^w\phi \equiv \phi^w - \phi^o$) was estimated by taking the formal transfer potential ($\Delta_o^w\phi^\circ$) of tetramethylammonium as 0.160 V.[40] UV-Vis absorption and fluorescence spectra of the aqueous solution were measured by UV-Vis spectrophotometer (JASCO, V-630) and fluorescence spectrophotometers (Hitachi, F-2500 for porphyrin derivatives and ionizable drugs systems, JASCO, FP-8300 for flavin derivtives system).

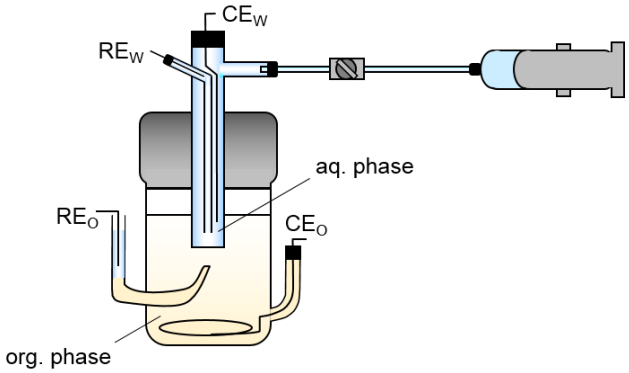

Fig. 10 Schematic drawing of the electrochemical cell.

3-3 Potential-Modulated Fluorescence Spectroscopy

The water|DCE interface under electrochemical control was illuminated from the organic phase by a cw laser of 50 mW at 404 nm (Coherent, CUBE 405-50C) in total internal reflection (TIR) mode. It should be noted that the laser power was attenuated to 10 mW for measuring the DIP system. The angle of incidence (ψ) of the *p*-polarized laser beam was set as ca. 75°. The fluorescence emitted from the interfacial region was collected perpendicularly to the interface by an optical fiber fitted to a photomultiplier tube through a monochromator (Shimadzu, SPG-120S). The ac modulated fluorescence signal at 1 Hz was analyzed as a function of ac potential modulation by a digital lock-in amplifier (NF LI5640) for potential dependence measurements at 5 mV s^{-1}, while a frequency response analyzer (NF FRA5022) was employed for frequency dependence measurements from 0.1 to 100 Hz. The PMF setup is shown in **Fig.11**. All of the experiments were carried out in a thermostated room at 298±2 K.

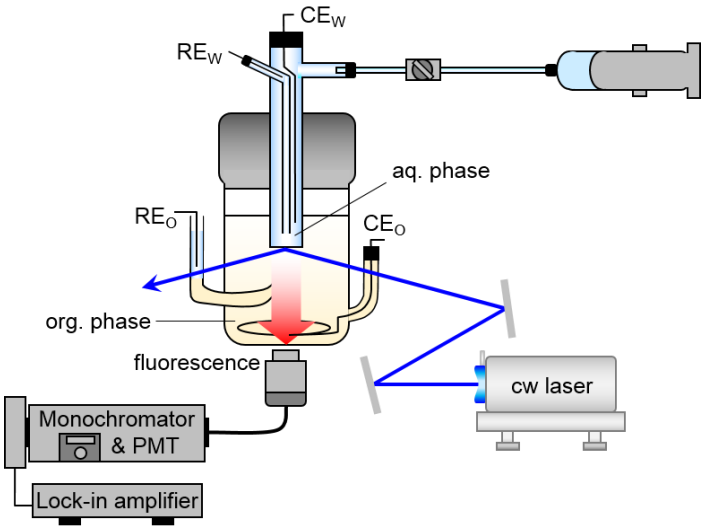

Fig. 11 Schematic drawing of the PMF apparatus.

3-4 Photocurrent Transient and Action Spectra Measurement

In the photocurrent transient measurement, the water|DCE interface under electrochemical control was illuminated from the organic phase by a cw laser at 410 nm (Neoark, TC20-4030S-2F-4.5)[41] in TIR mode. The photocurrent action spectra were measured by using a Xe lamp (Hamamatsu Photonics, LC8-03, 150 W) with a monochromator (Jobin-Yvon, H10VIS). The monochromatized excitation light was irradiated perpendicularly to the interface at 3.2 Hz. The setup is shown in **Fig.12**.

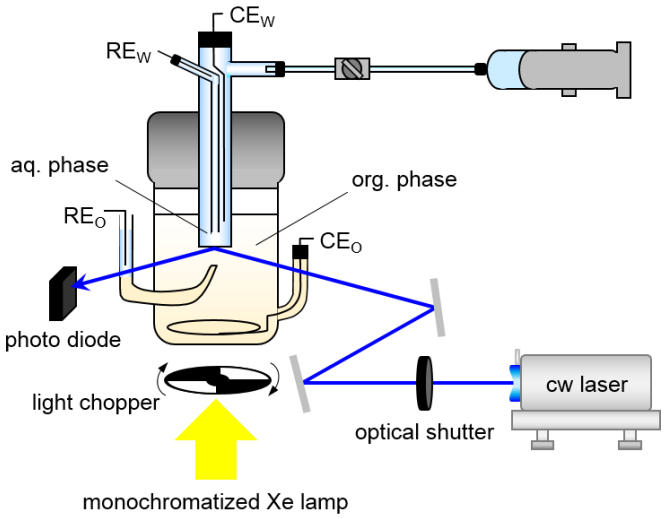

Fig. 12 Schematic drawing of the apparatus for measuring the photocurrent transient and action spectra.

PART I
Spectroelectrochemical Characterization of Dendrimer-Porphyrin Associates at Polarized Liquid|Liquid Interfaces

In PART I, the molecular encapsulation behavior of the free base and zinc(II) complex of water-soluble porphyrin, 5,10,15,20-tetrakis(4-sulfonatophenyl)porphyrin (TPPS, **Fig. 1-1**) in the amino-terminated G4 and G2 PAMAM dendrimers at the polarized water|DCE interface is described. Porphyrins have been extensively studied as biomimetic reactants, dye sensitizers, catalysts, spectrophotometric reagents and so on.[42] The physicochemical property and reactivity of porphyrin compounds strongly depend on peripheral substituted groups and metal center. The porphyrins and metalloporphyrins are readily protonated (via demetalation for metalloporphyrins) in acidic solutions inducing considerable spectral changes.[43] On the other hand, the molecular size and net charges of the free base porphyrin are identical to its divalent metal complex. The porphyrin molecules are therefore suitable for a contrastive evaluation of the contribution of the metal center in molecular encapsulation systems. Spectroscopic and spectroelectrochemical measurements are carried out for evaluating the molecular encapsulation behavior of the dendrimers for the zinc(II) complex of TPPS ($ZnTPPS^{4-}$) and its free base (H_2TPPS^{4-}). In addition, the stabilization of porphyrin molecules in the PAMAM dendrimer is discussed by estimating the Gibbs free energy of ion association between the dendrimers and porphyrins ($\Delta G_{D\cdots porphyrin}$).

The photochemical applications of the PAMAM dendrimer have been developed through the formation of nanocomposites with various organic molecules and quantum dots.[44-48] Unique characteristics of these dendrimer-based nanocomposites result from the molecular encapsulation ability as well as improvements to the photostability and reactivity of dye species. The dendrimers have, however, not been applied to the heterogeneous photoinduced electron-transfer system where the electron donor and acceptor located in their respective liquid phases can react each other only in the interfacial region under photoexcitation. The photoreactivity of the ion associates between the PAMAM dendrimer and $ZnTPPS^{4-}$ is described at the polarized water|DCE interface.

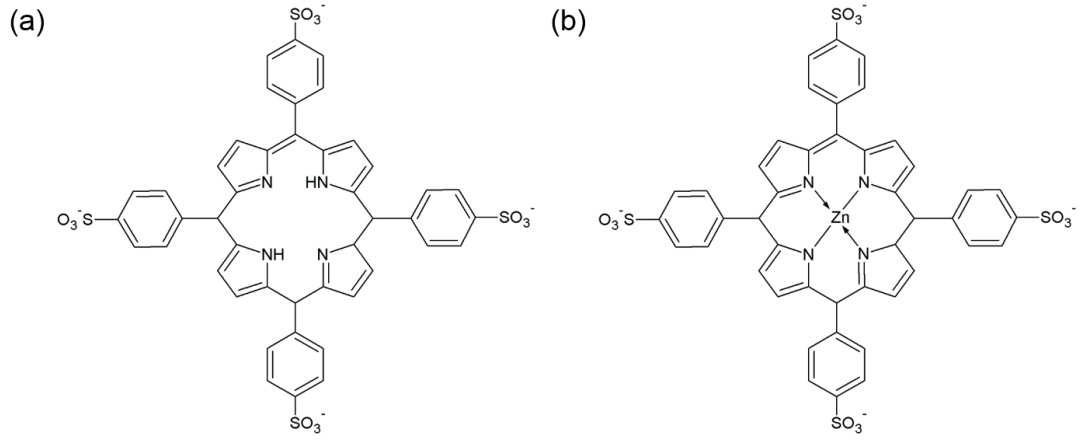

Fig. 1-1 Molecular structures of (a) H_2TPPS^{4-} and (b) $ZnTPPS^{4-}$.

I-1 Porphyrin Derivatives

I-1-1 Ion Association Behavior between PAMAM Dendrimers and Anionic Porphyrins in the Aqueous Solution

As a preliminary, spectroscopic properties of the porphyrins in the aqueous solution were investigated in the absence of the dendrimers. **Fig. 1-2** shows UV-Vis absorption and fluorescence spectra of the porphyrin species examined in this study. Porphyrin derivatives have two types of the absorption peaks, i.e., the Soret band and the Q band. Soret band and Q band correspond to the electron transition from the grand singlet state (S_0) to the second (S_2) and the first excited singlet states (S_1), respectively.[49, 50] At pH 7.2, the Soret bands of $ZnTPPS^{4-}$ and H_2TPPS^{4-} were observed at 421 nm and 413 nm, respectively. Under acidic conditions, $ZnTPPS^{4-}$ and H_2TPPS^{4-} in aqueous solution were changed to the diacid form (H_4TPPS^{2-}) by demetalation and protonation. In the present condition, the characteristic absorption bands for the monomeric H_4TPPS^{2-} without forming aggregates were measured, respectively, at 434 nm (Soret band), 645 and 594 nm (Q bands) (**Fig. 1-2a**). The corresponding changes of fluorescence spectra were also obtained as shown in **Fig. 1-2b**.

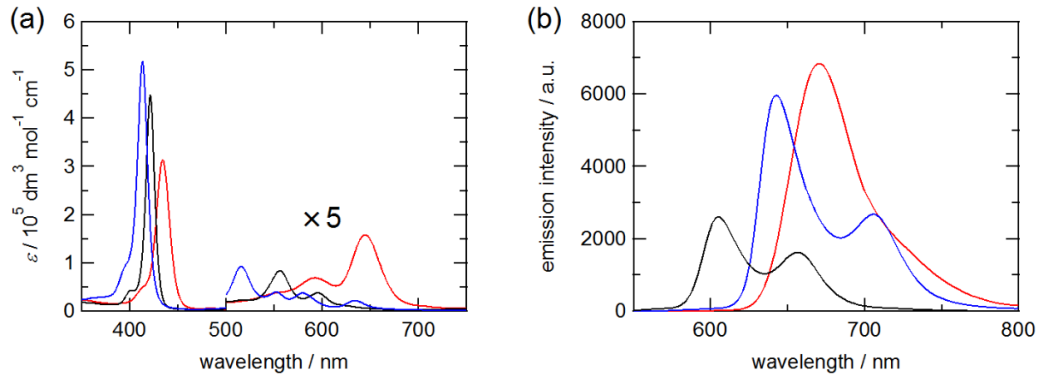

Fig. 1-2 (a) UV-Vis absorption and (b) fluorescence spectra of the porphyrins in the aqueous solution. The red, blue and black lines refer to H_4TPPS^{2-} at pH 2.0, H_2TPPS^{4-} and $ZnTPPS^{4-}$ at pH 7.2, respectively. The concentration of the porphyrins was 1.0×10^{-6} mol dm^{-3}.

The intermolecular interaction between the dendrimers and the anionic porphyrins in the aqueous phase was investigated at various pHs. **Fig. 1-3(a,b)** shows UV-Vis absorption and fluorescence spectra of $ZnTPPS^{4-}$ in the absence and presence of equimolar dendrimer at pH 7.2. The absorption maximum wavelength at the Soret band (421 nm) of $ZnTPPS^{4-}$ was significantly red-shifted to 428 nm and 427 nm, respectively, in the presence of the G4 and G2 PAMAM dendrimers. The corresponding red-shifts were also observed in the fluorescence spectra. The spectral changes demonstrate the effective ion association between the cationic dendrimer and the anionic porphyrin in the aqueous phase. In addition, the red-shift of the G4 PAMAM dendrimer system was larger than that of the G2 PAMAM dendrimer. These spectral shifts would indicate that the encapsulation environment of the porphyrin molecules such as hydration and/or axial coordination is not identical in the G4 and G2 PAMAM dendrimer systems, in which the higher generation dendrimer seems to isolate $ZnTPPS^{4-}$ from homogeneous solution phase. The G4 PAMAM dendrimer is regarded as spherical shape with diameters reported between 4.3 and 4.9 nm under various conditions, while the G2 PAMAM dendrimer is flat-elliptical shape with a diameter around ~2.9 nm.[26, 51] $ZnTPPS^{4-}$, whose longest diagonal axes are ~1.9 nm,[52] could be penetrated into the hydrophobic interior of the G4 PAMAM dendrimer in terms of the molecular dimension. On the other hand, the $ZnTPPS^{4-}$ molecules associated with the small G2 PAMAM dendrimer is exposed to the solution phase in any molecular arrangement. The change of solvation structure of $ZnTPPS^{4-}$ would be enhanced with the G4 PAMAM dendrimer. **Fig. 1-3(c,d)** shows the pH dependence of the spectra of $ZnTPPS^{4-}$ in the presence of equimolar G4 PAMAM dendrimer in the aqueous solution. The spectra measured at pH 10.7 were hardly modified from those of pH 7.2. The net charges on the G4 PAMAM dendrimer depend on protonation equilibria of 64 primary amines in the periphery moiety ($pK_{a,1}$: 9.20) and 62 tertiary amines as branch points ($pK_{a,2}$: 6.65).[53] The G4 PAMAM dendrimer thus has only few positive charges, ~+2, at pH 10.7. The apparent spectral changes of $ZnTPPS^{4-}$ in the

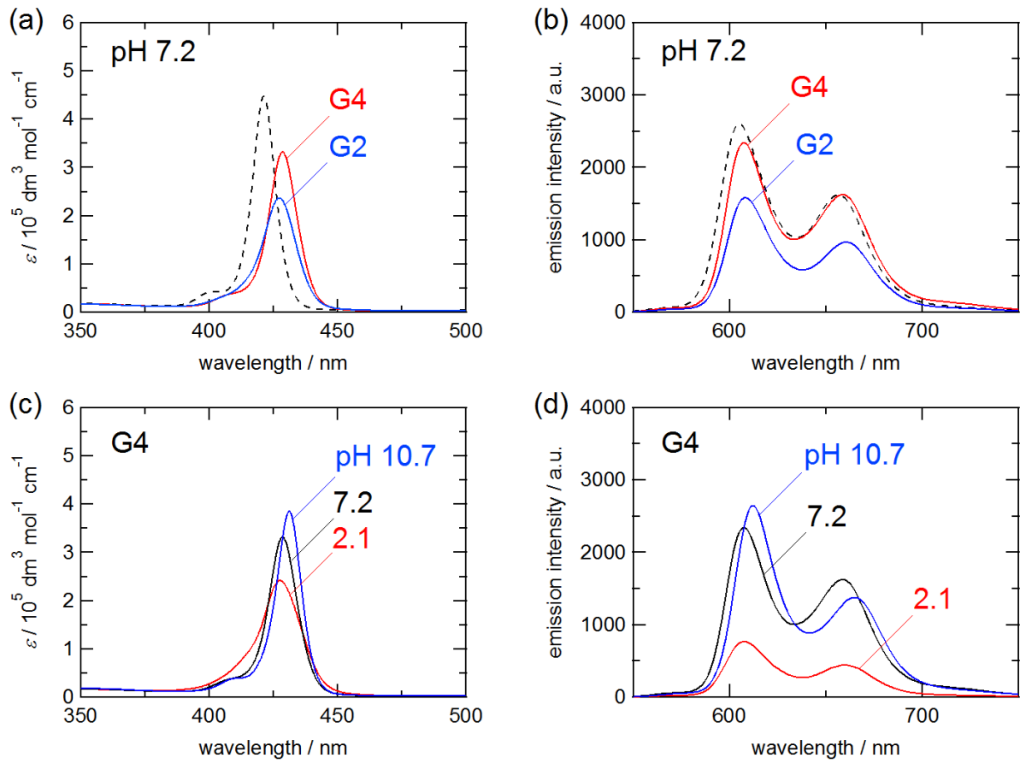

Fig. 1-3 UV-Vis absorption and florescence spectra of $ZnTPPS^{4-}$ in the presence of the equimolar dendrimers in the aqueous solution. (a, b) The spectra measured in the G4 and G2 PAMAM dendrimer systems at pH 7.2. (b, d) The pH dependences of the spectra in the presence of the G4 PAMAM dendrimer. The dashed lines are the spectra measured in the absence of the dendrimer. The concentration of $ZnTPPS^{4-}$ and the dendrimer was 1.0×10^{-6} mol dm^{-3}.

alkaline condition exhibit that the ion association between the anionic porphyrin and the dendrimer is promoted not only by the electrostatic interaction. Under acidic conditions, $ZnTPPS^{4-}$ was demetalated and protonated to the diacid form (H_4TPPS^{2-}) in the absence of the dendrimer. H_4TPPS^{2-} showed the Soret band at 434 nm and the Q bands at 645 and 594 nm (**Fig. 1-2**). The spectra taken at pH 2.1 indicated that $ZnTPPS^{4-}$ was effectively stabilized in the acidic aqueous solution by associating with the dendrimer. The broadening of the Soret band accompanied by relative decreases of the fluorescence intensity at pH 2.1, however, might be indicative of slight demetalation of $ZnTPPS^{4-}$. The

similar stability enhancement of $ZnTPPS^{4-}$ was also reported in the electrostatic formation of complex micelles with poly(ethyleneglycol)-*b*-poly(4-vinylpyridine) (PEG-*b*-P4VP) by Wang et al.[54] At pH 2.1, the G4 PAMAM dendrimers exist as fully protonated cationic species in the aqueous solution. The considerable decrease in the fluorescence intensity at pH 2.1 could thus be associated with the fluorescence quenching by the favorable electrostatic interaction between the $ZnTPPS^{4-}$ molecule and the positively charged dendrimer rather than slight demetalation of $ZnTPPS^{4-}$.[55]

As shown in **Fig. 1-4**, the analogous spectral changes were observed for the free base porphyrin under neutral and alkaline conditions, in which the Soret band at 413 nm was red-shifted to 419 nm in the presence of equimolar G4 PAMAM dendrimer. A slight shoulder response around 408 nm at pH 7.2 possibly relates to the H-aggregation of H_2TPPS^{4-}.[56, 57] The red-shifted fluorescence spectra at pH 7.2 and 10.7 are also attributable to the dendrimer-H_2TPPS^{4-} association. The spectral results at pH 2.1 showed rather complex features in which the UV-Vis absorption spectra indicated the appearance of new absorption peaks at 424, 483 and 699 nm (**Fig. 1-4a**, red line). The H_2TPPS^{4-} molecules strongly associated with the fully protonated dendrimers could be responsible

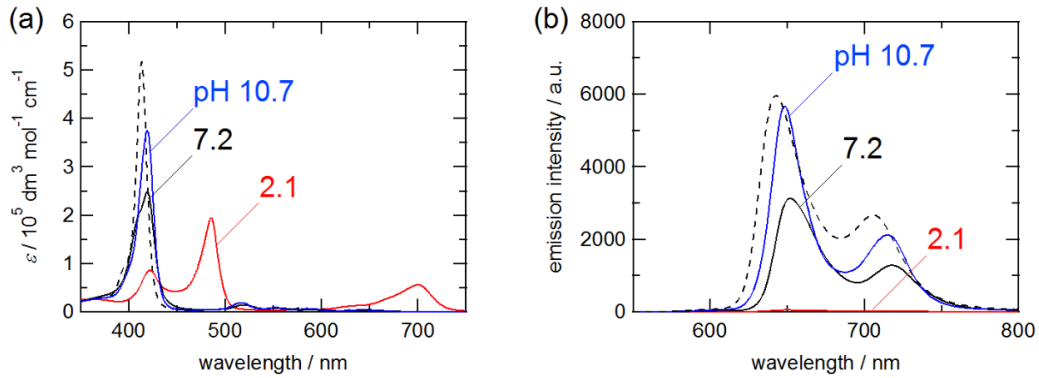

Fig. 1-4 (a) UV-Vis absorption and (b) florescence spectra of H_2TPPS^{4-} in the presence of equimolar G4 PAMAM dendrimer in the aqueous solution. The dashed lines are the spectra measured in the absence of the dendrimer at pH 7.2. The concentration of H_2TPPS^{4-} and the dendrimer was 1.0×10^{-6} mol dm^{-3}.

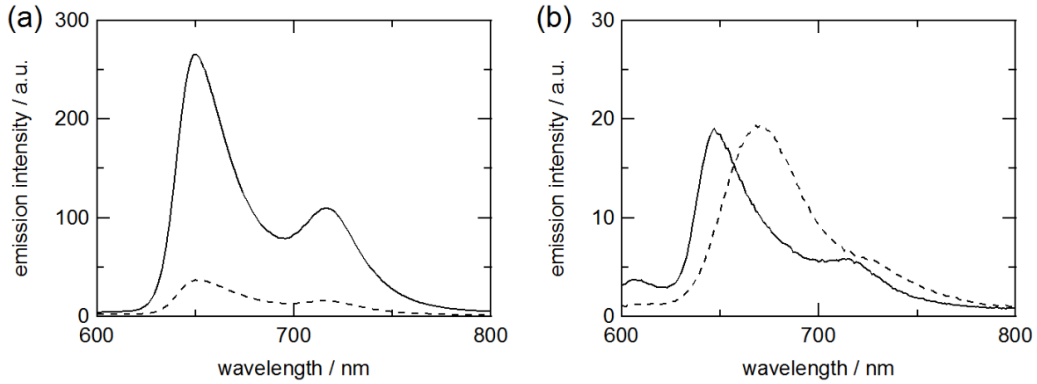

Fig. 1-5 Fluorescence spectra of the H_2TPPS^{4-} system at pH 2.0 in the presence of (a) G4 and (b) G2 PAMAM dendrimers in the aqueous solution. The initial concentration of H_2TPPS^{4-} was 1.0×10^{-6} mol dm^{-3}. The dendrimer was added with molar ratios 1:1 (dashed lines: 1.0×10^{-6} mol dm^{-3}) and 1:10 (solid lines: 1.0×10^{-5} mol dm^{-3}) with respect to the porphyrin.

for the absorption band at 424 nm. The other absorption bands were, however, apparently different from that of diprotonated monomers (H_4TPPS^{2-}) (**Fig. 1-2**) but would be attributed to the Soret and Q bands of J-aggregates of H_4TPPS^{2-}.[57, 58] A drastic decrease in the fluorescence intensity at pH 2.1 (**Fig. 1-4b**, red line) also coincides with the formation of J-aggregates since the aggregates of the porphyrin diacids are effectively the non-fluorescent species. The aggregation behavior of the H_4TPPS^{2-} monomers is strongly affected by porphyrin concentration, kinds of coexisting ions and ionic strength.[59] It should also be noted that the fluorescence response assigned to H_2TPPS^{4-} was relatively recovered even at pH 2 by adding an excess amount of the dendrimer, i.e., [TPPS]:[dendrimer] = 1:10. The porphyrins in the presence of the G2 PAMAM dendrimer exhibited spectral features similar to the G4 PAMAM dendrimer systems (**Fig. 1-5**). Fluorescence spectra associated with H_4TTPPS^{2-} was shifted to H_2TPPS^{4-} under [TPPS]:[G2 dendrimer] = 1:10 condition. On the other hand, Fluorescence intensity of H_2TPPS^{4-} was increased under [TPPS]:[G4 dendrimer] = 1:10 condition. This result suggests that H_2TPPS^{4-} molecule could be surrounded by a number of the G2 PAMAM

dendrimers. The spectral results indicate that a lower protecting ability of the dendrimer for the free base porphyrin as compared to the zinc(II) complex.

I-1-2 Ion Transfer Behavior of Dendrimer-Porphyrin Associates at the Water|DCE Interface

Cyclic voltammograms (CVs) in the presence of the dendrimers are shown in **Fig. 1-6**. The CVs were significantly dependent on the pH conditions. The charge number of the G4 PAMAM dendrimer can be calculated as +126 at pH 2.1 due to full protonation of both 62 tertiary and 64 primary amines. The positive peak current under all pH conditions was almost proportional to the square root of the potential sweep rate, while the positive peak at pHs 2.1 and 10.7, buried on the gradual increase of the voltammetric responses, could not be analyzed. As reported previously, the positive peak observed around 0.40 V assigned as ion transfer of the G4 PAMAM dendrimer from the aqueous to the organic phases, and negative peak around 0.30 V as the back transfer from the organic to the aqueous phases.[34, 36] In addition, a gradual increase of current response at the positive edge of the potential window was attributed to the transfer of the organic supporting electrolyte ($TPFB^-$) facilitated by the cationic dendrimer accumulated at the interface. While the tertiary amines of the dendrimer are hardly protonated in neutral conditions, similar voltammetric responses were obtained at pH 7.3, in which well-defined transfer responses were measured at 0.35 V. At pH 10.7 where the dendrimer has almost no positive charges, the voltammetric responses were significantly decreased, and only the small negative responses associated with a back transfer of the dendrimer from the organic phase were found around 0.40 V. As shown in **Fig. 1-6b**, the profile of CVs obtained for the G2 PAMAM dendrimer system was analogous to the G4 PAMAM dendrimer system. The net charge on the G2 PAMAM dendrimer with 16 amino terminal groups and 14 tertiary amines as branch points is reduced by almost quarter as compared with the G4 dendrimer under comparable conditions. Therefore, the relatively small voltammetric responses were observed at potentials close to the positive edge of potential window ($\Delta_o^w\phi > 0.25$ V).

Fig. 1-7 shows CVs and ac voltammograms in the presence of the porphyrins.

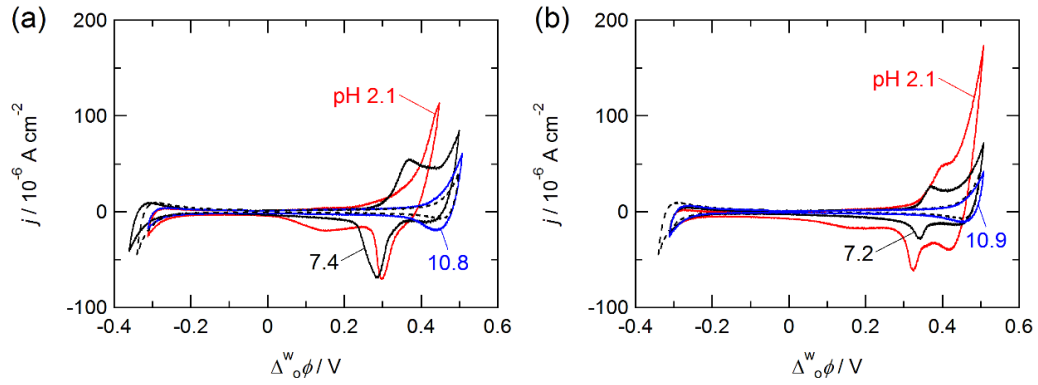

Fig. 1-6 CVs measured for the (a) G4 and (b) G2 PAMAM dendrimers. The dashed lines refer to the CVs measured in the absence of the dendrimer. The potential sweep rate was 50 mV s^{-1}. The concentration of the dendrimer was 1.0×10^{-5} mol dm^{-3}.

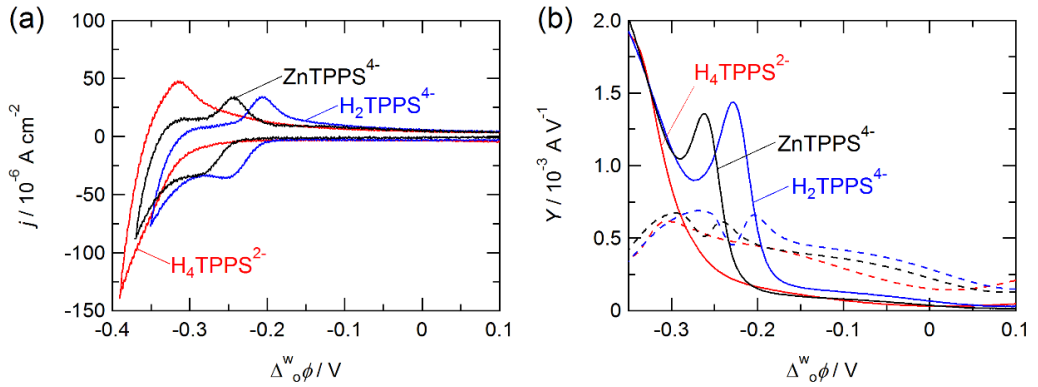

Fig. 1-7 (a) CVs and (b) ac voltammograms measured for the porphyrins at the water|DCE interface. The black, blue and red lines refer to $ZnTPPS^{4-}$ at pH 7.1, H_2TPPS^{4-} at pH 7.2 and H_4TPPS^{2-} at pH 2.1, respectively. (b) The solid and dashed lines refer to the real and imaginary components of admittance. The amplitude of ac potential modulation was 10 mV at 7 Hz. The concentration of the porphyrins was 5.0×10^{-5} mol dm^{-3}.

The intrinsic formal ion transfer potential ($\Delta^{w}_{o}\phi^{o'}$) of the porphyrins, respectively, as −0.26 V for $ZnTPPS^{4-}$ and –0.22 V for H_2TPPS^{4-} in agreement with the previous reports.[39, 60] On the other hand, the transfer response of H_4TPPS^{2-} formed under acidic conditions was not observed within the potential window, indicating a high hydrophilicity

of H_4TPPS^{2-}.

Fig. 1-8 shows CVs in the presence of the dendrimers and $ZnTPPS^{4-}$. The CVs were significantly dependent on the pH conditions. The net charges on the dendrimer-porphyrin associate should be reduced from the bare dendrimer because of the negative charges of the porphyrins. The voltammetric responses of the ion associates were, nevertheless, similar to those measured for the bare dendrimers as described above. Since the dendrimers has a number of charges as compared with the porphyrins, the change of the net charges on the dendrimer associated with the porphyrin could be almost negligible. The CVs measured for the dendrimers associated with H_2TPPS^{4-} were essentially the same as the system involving $ZnTPPS^{4-}$. The voltammetric responses of the porphyrins were vanished within the polarizable potential window by the addition of the dendrimer. (**Fig. 1-9**). The absence of apparent transfer responses in the corresponding potential region would demonstrate that the porphyrin molecules are stably associated with the dendrimers even at the polarized water|DCE interface.

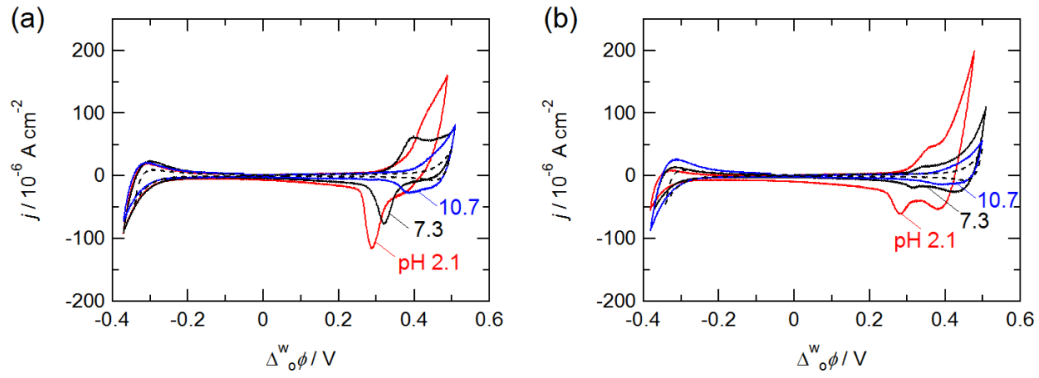

Fig. 1-8 Typical cyclic voltammograms measured for (a) G4 and (b) G2 PAMAM dendrimers in the presence of $ZnTPPS^{4-}$ at various pHs. The dashed lines are the CVs measured in the absence of $ZnTPPS^{4-}$ and the dendrimer. The potential sweep rate was 50 mV s^{-1}.

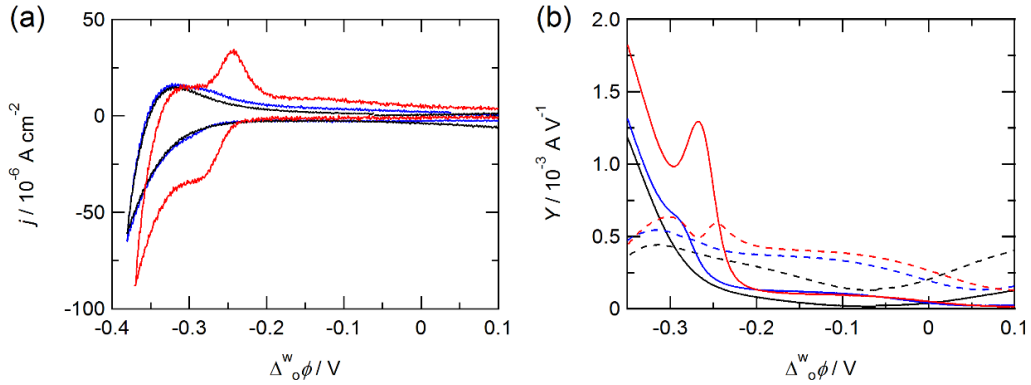

Fig. 1-9 (a) CVs and (b) ac voltammograms measured for $ZnTPPS^{4-}$ and the G4 PAMAM dendrimer-$ZnTPPS^{4-}$ associate at pH 7. The black, blue and red lines refer to 1.0×10^{-5} mol dm^{-3} dendrimer-$ZnTPPS^{4-}$ associate at pH 7.3, 1.0×10^{-5} and 5.0×10^{-5} mol dm^{-3} $ZnTPPS^{4-}$ at pH 7.1, respectively. (b) The solid and dashed lines refer to the real and imaginary components of admittance. The amplitude of ac potential modulation was 10 mV at 7 Hz. The potential sweep rates were (a) 50 mV s^{-1} and (b) 5 mV s^{-1}, respectively.

I-1-3 Spectroelectrochemical Analysis of Interfacial Mechanism of Dendrimer-Porphyrin Associates

PMF spectroscopy was employed in order to elucidate the interfacial mechanism of the dendrimer-porphyrin associates. The PMF technique basically cannot directly be applied to the bare PAMAM dendrimer including no fluorophore. The highly fluorescent dendrimer-porphyrin associates were, however, stable even at the positively polarized water|DCE interface. The PMF analysis of the interfacial mechanism was thus successfully performed both in the dendrimer-$ZnTPPS^{4-}$ and dendrimer-H_2TPPS^{4-} systems. The potential dependence and complex plane of the PMF responses in the presence of 1.0×10^{-5} mol dm^{-3} G4 PAMAM dendrimer and $ZnTPPS^{4-}$ at pH 7.3 are displayed in **Fig. 1-10**. In the potential dependence measurements, the real (ΔF_{re}) and imaginary components (ΔF_{im}) of the PMF response were obtained as positive and negative signs around 0.32 V, where the characteristic voltammetric responses were observed in CVs (c.f. **Fig. 1-8a**). The frequency dependent PMF responses measured at 0.32 V was expressed as a distorted linear response in the fourth quadrant of the complex plane (**Fig. 1-10b**). Therefore, the PMF responses around 0.32 V correspond to the ion transfer of the positively charged dendrimer associated with $ZnTPPS^{4-}$ (cf. Methodology section). The distortion of the complex plane could be considered due to the contributions of the adsorption step and the uncompensated solution resistance. A complicating PMF feature was also observed at potentials more positive than 0.35 V, where the real and imaginary components were obtained mainly as negative and positive signs. The complex plane of PMF responses at 0.37 V exhibited a semicircle in the second quadrant **(Fig. 1-10c**), demonstrating that the positively charged ion associates are transferred across the interface accompanied by the adsorption process at the organic side of the interface (cf. Methodology section). The high-frequency features in the first quadrant could be associated with an attenuation of the ac potential modulation due to the uncompensated resistance across the reference electrodes. On the conventional equivalent circuit for a

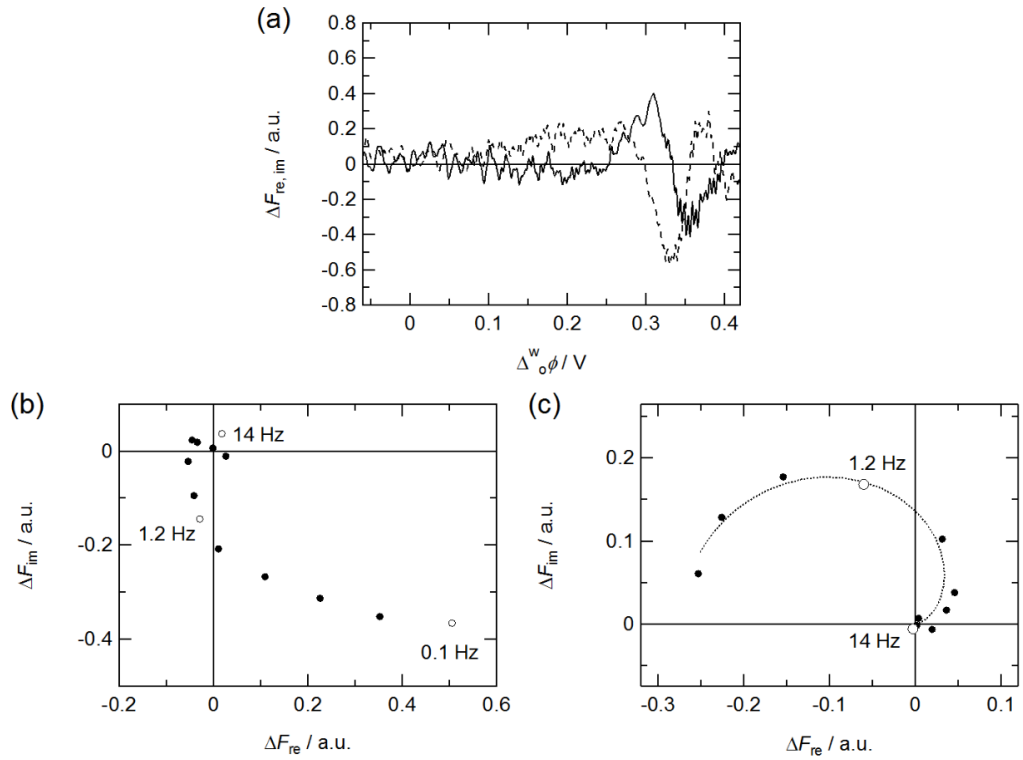

Fig. 1-10 Dependences of the PMF responses for the G4 PAMAM dendrimer in the presence of $ZnTPPS^{4-}$ at pH 7.3 on (a) the Galvani potential difference and the potential modulation frequency at (b) 0.32 and (c) 0.37 V. (a) The solid and dashed lines refer to the real and imaginary components, respectively. (c) The dotted line was obtained by a least-squares curve-fitting with the theoretical equation derived from Eqs (14)-(21). The amplitude of ac potential modulation was 20 mV.

liquid|liquid interface, the total impedance (Z_t) is described as:[37]

$$Z_t = R_u + \left[j\omega C_{dl} + \frac{1}{R_b} + \frac{1}{R_{ct} + (1-j)\sigma\omega^{-0.5}} \right]^{-1} \tag{18}$$

Taking into account that the ac potential can be attenuated by a magnitude proportional to the ac current and R_u, the effective potential modulation across the interface ($\Delta^{w}_{o}\phi^{eff}_{ac}$) can be estimated as:[38, 39]

$$\Delta^{w}_{o}\phi^{eff}_{ac} = \Delta^{w}_{o}\phi_{ac}\left(1 - \frac{R_u}{Z_t}\right) \tag{19}$$

The expression for the PMF response of the adsorption process at the aqueous side of interface (Eqs. (16) and (17)) can be rewritten as:[38, 39]

$$\Delta F_{\mathrm{a,re}}^{\mathrm{w}} = \frac{2.303\varepsilon\Phi_{\mathrm{f}} I_0 \Gamma_{\mathrm{s}} SbzF}{RT} \left[\frac{\left(k_{\mathrm{a},0}\alpha c_0\left(1-\theta_0\right) - k_{\mathrm{d},0}\left(\alpha-1\right)\theta_0\right)\left(\Delta_{\mathrm{o}}^{\mathrm{w}}\phi_{1,\mathrm{re}}^{\mathrm{eff}}\left(k_{\mathrm{a},0}c_0 + k_{\mathrm{d},0}\right) + \Delta_{\mathrm{o}}^{\mathrm{w}}\phi_{1,\mathrm{re}}^{\mathrm{eff}}\omega\right)}{\left(k_{\mathrm{a},0}c_0 + k_{\mathrm{d},0}\right)^2 + \omega^2} \right] \tag{20}$$

$$\Delta F_{\mathrm{a,im}}^{\mathrm{w}} = -\frac{2.303\varepsilon\Phi_{\mathrm{f}} I_0 \Gamma_{\mathrm{s}} SbzF}{RT} \left[\frac{\left(k_{\mathrm{a},0}\alpha c_0\left(1-\theta_0\right) - k_{\mathrm{d},0}\left(\alpha-1\right)\theta_0\right)\left(\Delta_{\mathrm{o}}^{\mathrm{w}}\phi_{1,\mathrm{re}}^{\mathrm{eff}}\omega - \Delta_{\mathrm{o}}^{\mathrm{w}}\phi_{1,\mathrm{im}}^{\mathrm{eff}}\left(k_{\mathrm{a},0}c_0 + k_{\mathrm{d},0}\right)\right)}{\left(k_{\mathrm{a},0}c_0 + k_{\mathrm{d},0}\right)^2 + \omega^2} \right] \tag{21}$$

As shown in **Fig. 1-10c**, the frequency responses of PMF were reproduced by the theoretical model (the dotted line). However, the kinetic parameters could not be determined with the acceptable error because of unknown conditional factors associated with an optical setup and "exact" charges on the dendrimer-porphyrin associate. **Fig. 1-11** shows the PMF response measured in the presence of 1.0×10^{-5} mol dm^{-3} the G4 PAMAM dendrimer and ZnTPPS^{4-} at various pHs. The broad PMF response around 0.10 V at pH 2.1 could be due to the weak adsorption process of the dendrimer-porphyrin associates prior to the ion transfer observed at 0.33 V. In addition, the PMF response around 0.40 V with an opposite sign to the ion transfer response should be the adsorption process at the organic side of the interface. No PMF responses for the adsorption process at the aqueous side were observed at pH 7.3. At pH 10.7, the PMF response for the ion transfer of the ion associates alone was observed at 0.38 V. The net charges on the ion associates dramatically decreases at pH 10.7. Since the potential dependent adsorption process of ionic species at the polarized liquid|liquid interface is substantially dominated by the bulk concentration and the Galvani potential difference,[38, 61] the driving force for the adsorption process could be inefficient for less charged ions at a given potential. The

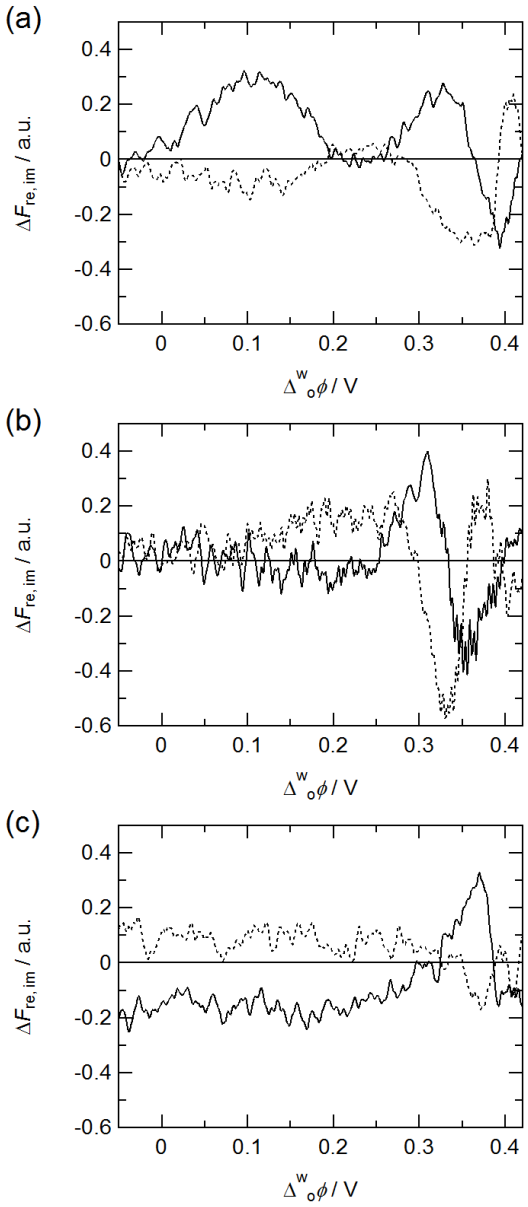

Fig. 1-11 Potential dependences of the PMF responses for the G4 PAMAM dendrimer-ZnTPPS^{4-} associates at various pHs. The solid and dotted lines relate to the real and imaginary components, respectively. The amplitudes of ac potential modulation were 50 mV at pH 2.1 (a) and 20 mV at pH 7.3 (b) and 10.7 (c), respectively.

disappearance of the adsorption responses at higher pH conditions, hence, results from the decrease in positive charges on the ion associates. The PMF responses of the H_2TPPS^{4-} systems were almost similar to that of the ZnTPPS^{4-} systems (**Fig. 1-12**). In a

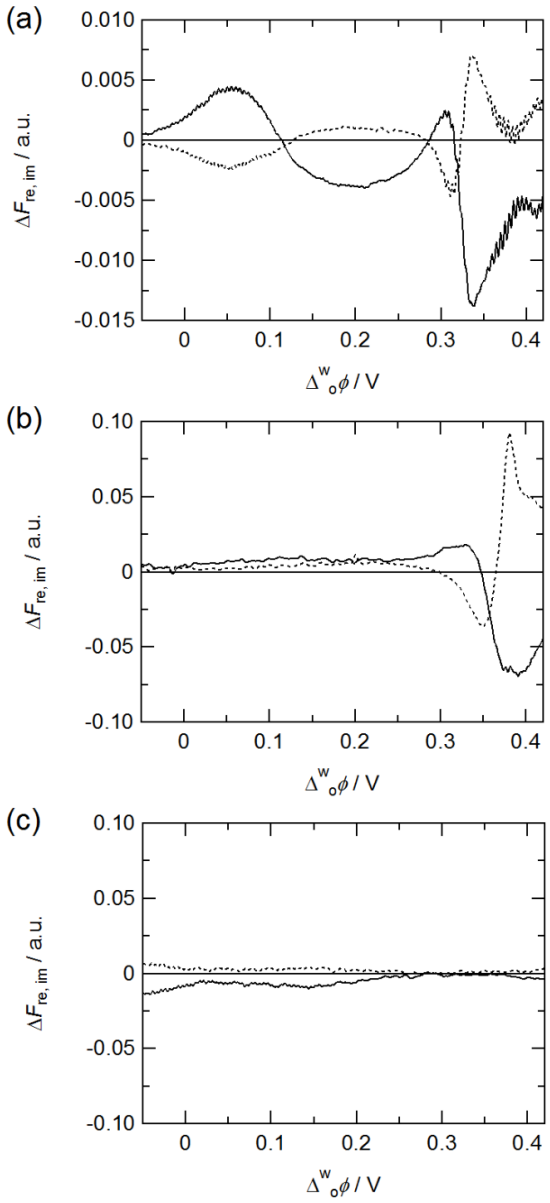

Fig. 1-12 Potential dependences of the PMF responses for the G4 PAMAM dendrimer-H_2TPPS^{4-} associates at various pHs. The solid and dotted lines relate to the real and imaginary components, respectively. The amplitudes of ac potential modulation were 20 mV at pH 2.1 (a) and 10 mV at pH 7.4 (b) and 10.7 (c), respectively.

potential region between 0.10 and 0.45 V, a further broad response with an opposite sign was superimposed on the ion transfer peak around 0.33 V in the G4 PAMAM dendrimer-H_2TPPS^{4-} system at pH 2.1 (**Fig. 1-12a**). As a result, the broad response apparently splits

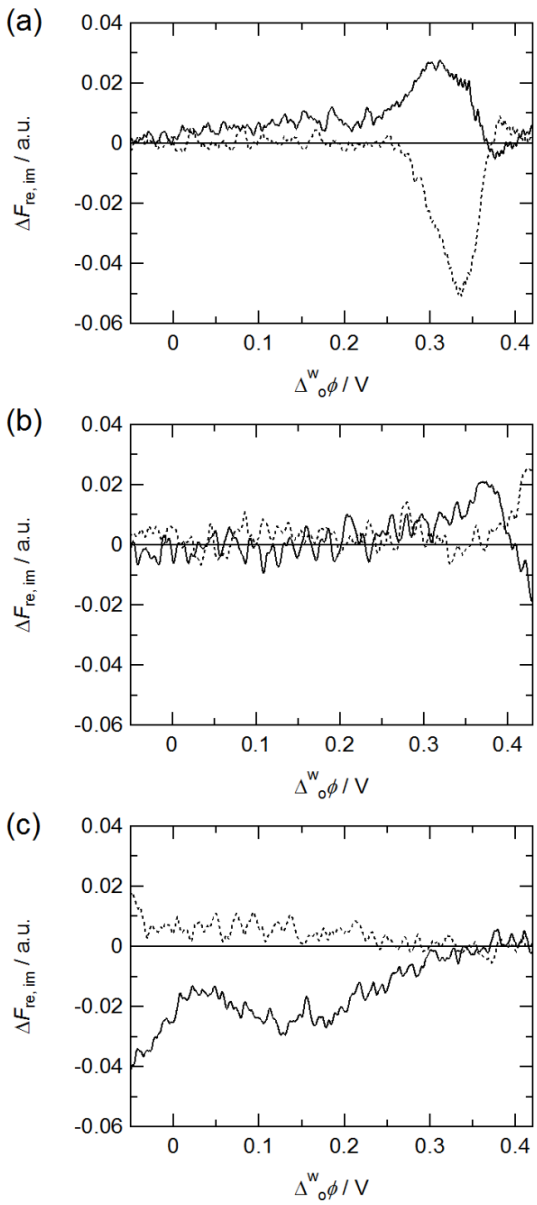

Fig. 1-13 Potential dependences of the PMF responses for the G2 PAMAM dendrimer-$ZnTPPS^{4-}$ associates at various pHs. The solid and dotted lines relate to the real and imaginary components, respectively. The amplitudes of ac potential modulation were 50 mV at pH 2.1 (a) and 20 mV at pH 7.3 (b) and 10.7 (c), respectively.

to two peaks at 0.25 V and 0.37 V. These PMF responses with opposite sign to the ion transfer responses could be due to the adsorption process of the cationic dendrimer at the organic side of the interface. At pH 10.7, the PMF responses of the ion transfer and the

adsorption processes were significantly decreased (**Fig. 1-12c**). This PMF result indicates that the ion association between the dendrimer and the porphyrin could be affected by the zinc(II) center of the porphyrin as well as the net charges on the dendrimer. The PMF responses of the ion transfer and the adsorption steps were also observed for the G2 PAMAM dendrimer in the presence of the porphyrins systems (**Fig. 1-13**). The G2 PAMAM dendrimer has less positive charges than the G4 PAMAM dendrimer. Therefore the effect of the Galvani potential difference on the interfacial processes of the G2 PAMAM dendrimer could be weak as compared with the G4 PAMAM dendrimer due to the less net charges on the dendrimer. In the alkaline condition, the G2 PAMAM dendrimer has almost no charges and no PMF responses were observed in the positively polarized interface (**Fig. 1-13c**). The PMF results demonstrated significant differences in the interfacial mechanism of the ion associates depending on pH.

In order to elucidate further details of the encapsulation behavior of the dendrimers for the anionic porphyrins the interface, the PMF analysis was performed in the negative potential region The PMF measurements for the porphyrins systems in the absence of the dendrimers were carried out prior to the dendrimers and the porphyrins coexistent systems. **Fig. 1-14** shows the potential dependences of the PMF responses measured for the porphyrins. Under acidic conditions in the absence of the dendrimer, the monomeric H_4TPPS^{2-} was preferentially formed in the aqueous phase, and the weak PMF signals for H_4TPPS^{2-} associated with the transfer and/or adsorption at the aqueous side of the interface were observed at the negative edge of the potential window ($\Delta_o^w\phi$ < –0.3 V). The negative real and positive imaginary components of the PMF signals observed around −0.26 V and −0.22 V, respectively, for $ZnTPPS^{4-}$ and H_2TPPS^{4-}. These potentials were nearly identical to the formal ion transfer potentials of each porphyrins determined from CVs (cf. **Fig. 1-7**). Although the voltammetric response for the porphyrins was effectively vanished in the presence of the dendrimer (**Fig. 1-9**), the buried charge transfer process

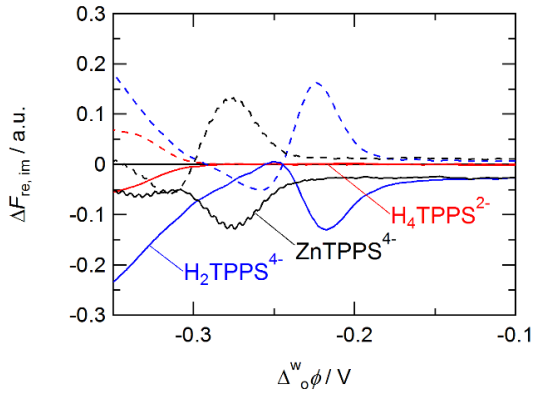

Fig. 1-14 Potential dependences of the PMF responses measured for the porphyrins. The black, blue and red lines refer to $ZnTPPS^{4-}$, H_2TPPS^{4-} at pH 7.1, and H_4TPPS^{2-} at pH 2.0, respectively. The solid and dotted lines refer to the real and imaginary components, respectively. The amplitudes of ac potential modulation were 10 mV for $ZnTPPS^{4-}$ and 20 mV for H_2TPPS^{4-} and H_4TPPS^{2-} at 1 Hz. The concentration of the porphyrins was 1.0×10^{-5} mol dm^{-3}.

in the negative edge region of the potential window was clarified by the PMF analysis. **Fig. 1-15** shows that the PMF responses of $ZnTPPS^{4-}$ with negative real and positive imaginary components at –0.26 V were negatively shifted to –0.37 V in the presence of the equimolar G4 PAMAM dendrimer. In addition, small PMF signals prior to the transfer response of $ZnTPPS^{4-}$, associating with the adsorption process at the aqueous side of the interface,[39, 60] were not observed in the presence of the dendrimer. The linear PMF response in the second quadrant (**Fig. 1-15b)** clearly indicates that the PMF responses at –0.37 V are associated with the ion transfer process of the anionic $ZnTPPS^{4-}$ without the adsorption step in the presence of the dendrimer. The negative shift of the $ZnTPPS^{4-}$ transfer in the presence of the dendrimer from its intrinsic transfer potential at –0.26 V can be considered as the result of the encapsulation of the porphyrin molecule in the dendrimer. The similar encapsulation and release behavior have been reported for the electrostatically formed ion associates between anionic anilinonaphthalenesulfonates and the carboxylate-terminated G3.5 PAMAM dendrimer at the polarized water|DCE

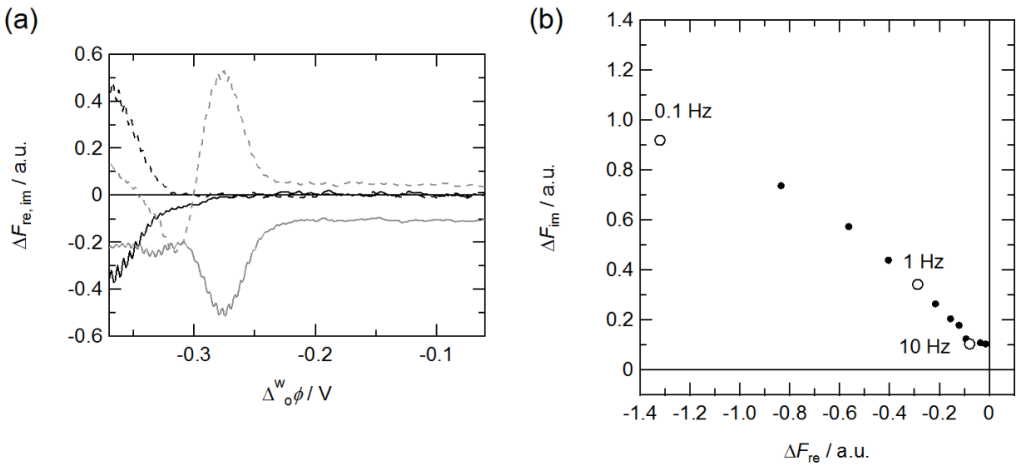

Fig. 1-15 Dependences of the PMF response for $ZnTPPS^{4-}$ in the presence of the G4 PAMAM dendrimer at pH 7.3 on (a) the Galvani potential difference and (b) the potential modulation frequency at –0.37 V. (a) The gray lines refer to PMF in the absence of the dendrimer at pH 7.1. The solid and dotted lines refer to the real and imaginary components, respectively. The amplitude of ac potential modulation was 20 mV.

interface.[35] The shift of the transfer potential is inseparably correlated to the association energy between the dendrimer and guest ions. The negative shifts of the PMF responses associated with the transfer of the released porphyrin anions were measured in all the dendrimer-porphyrin systems examined in this work (**Fig. 1-16**). It is noteworthy that the negative shift of the transfer responses of both the zinc(II) and free base porphyrins was enhanced in lower pH conditions, suggesting a stronger interaction of anionic porphyrins with highly protonated dendrimers. At pH 2.1, the PMF responses for the ion transfer of $ZnTPPS^{4-}$ and H_4TPPS^{2-} in the presence of the dendrimer were observed, respectively, at the negative edge ($\Delta^{w}_{o}\phi$ < –0.33 V) and out of the potential window as shown in **Fig. 1-16(a,b)** and **(c,d)**. Since $ZnTPPS^{4-}$ released from the dendrimer are possibly protonated via demetalation during the transfer process, the PMF signals measured for the $ZnTPPS^{4-}$ systems at pH 2 might include a certain contribution of the diacid formation. The potential dependent interfacial behavior of the dendrimer-porphyrin associates under neutral

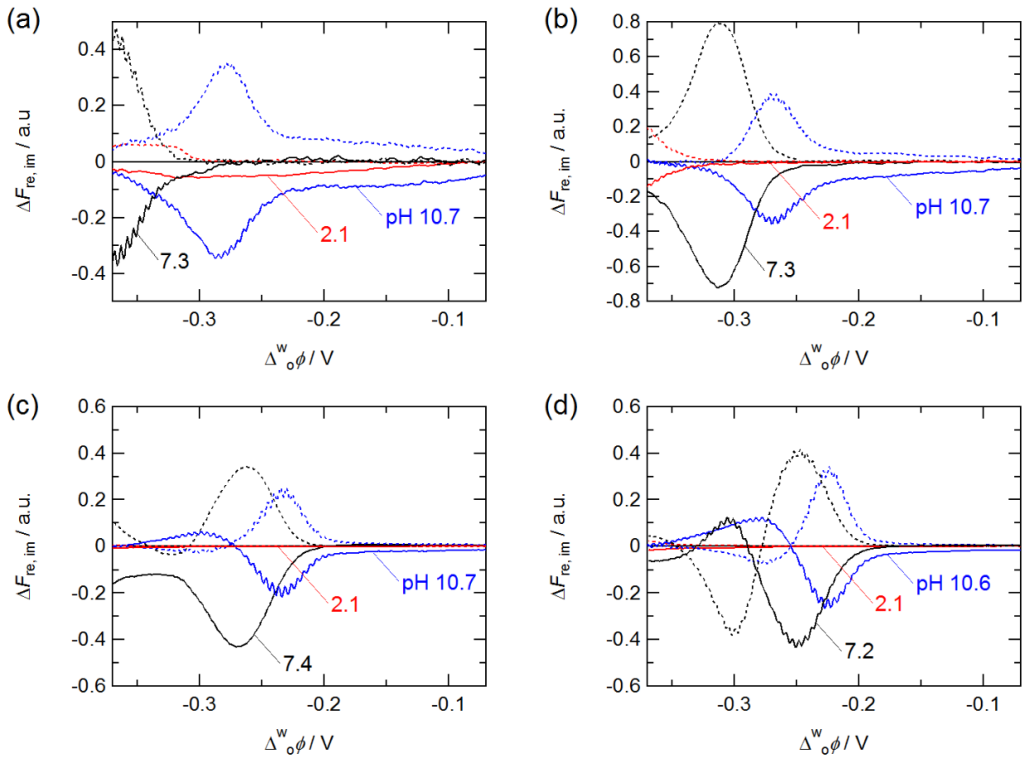

Fig. 1-16 Potential dependences of the PMF responses of (a, b) $ZnTPPS^{4-}$ and (c,d) H_2TPPS^{4-} in the presence of the (a,c) G4 and (b,d) G2 PAMAM dendrimers. The solid and dotted lines refer to the real and imaginary components, respectively. The amplitudes of ac potential modulation were (a,b) 50 mV at pH 2.1 and 20 mV at pH 7.3 and 10.7, (c) 20 mV at pH 2.1 and 10 mV at pH 7.4 and 10.7, and (d) 10 mV at pH 2.1, pH 7.2 and 10.6, respectively.

conditions can be schematically shown in **Fig. 1-17**. The cationic dendrimer incorporating the porphyrin molecule is transferred across the interface accompanied by the adsorption step at the positively polarized interface, while the ion transfer of the anionic porphyrin takes place at the negatively polarized interface.

The energy diagram of the porphyrins stabilized in the aqueous phase by forming the associate with the dendrimer is represented as **Scheme 1-1**. In the presence of the dendrimers system, the porphyrin are stabilized in the aqueous phase by forming the associates with the dendrimer. Taking into account Eq. (2), the Gibbs free energy of ion association between the dendrimers and porphyrins ($\Delta G_{D\cdots porphyrin}$) can be estimated from

Table 1-1 The Gibbs free energies of ion association between porphyrins and dendrimers ($\Delta G_{\mathrm{D}\cdots\mathrm{porphyrin}}$) estimated from the PMF measurement[a]

	$\Delta G_{\mathrm{D}\cdots\mathrm{porphyrin}}$ / kJ mol^{-1}			
	$ZnTPPS^{4-}$		H_2TPPS^{4-}	
pH	G4	G2	G4	G2
2	< −40	< −40	−	−
7	−30.1±0.9	−18.3±0.5	−15.4±0.9	−9.3±1.6
11	−6.3±0.7	−1.4±0.7	−3.2±1.3	−3.9±0.3

[a]Concentration of the dendrimers and the porphyrins was 1.0×10^{-5} mol dm^{-3}.

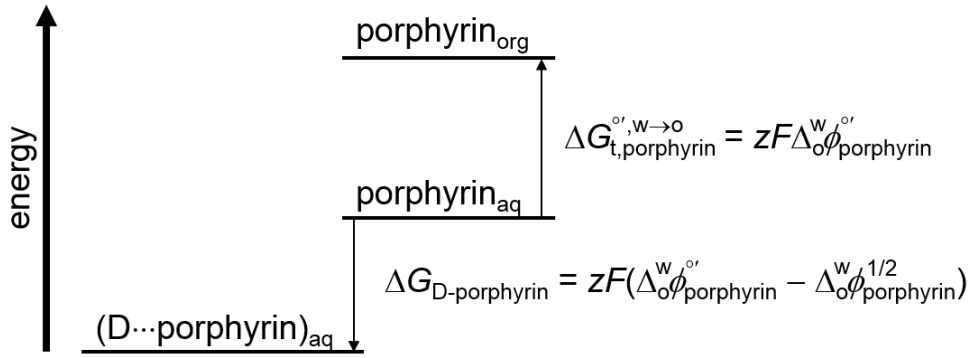

Scheme 1-1 Energy diagram of the porphyrin stabilized in the aqueous phase by forming the associate with the dendrimer.

following equation:[35]

$$\Delta_{\mathrm{o}}^{\mathrm{w}}\phi_{\mathrm{porphyrin}}^{1/2} = \Delta_{\mathrm{o}}^{\mathrm{w}}\phi_{\mathrm{porphyrin}}^{\circ\prime} - \frac{\left(\Delta G_{\mathrm{D}\cdots\mathrm{porphyrin}}\right)_{\mathrm{pH}}}{zF} \qquad (22)$$

where $\Delta_{\mathrm{o}}^{\mathrm{w}}\phi_{\mathrm{porphyrin}}^{1/2}$ is the half-wave potential for the transfer of porphyrin determined from the PMF analysis, $\Delta_{\mathrm{o}}^{\mathrm{w}}\phi_{\mathrm{porphyrin}}^{\circ'}$ is the formal ion transfer potential, z is the charge number of the porphyrin (−4). The $\Delta G_{\mathrm{D}\cdots\mathrm{porphyrin}}$ values summarized in **Table 1-1** were calculated from the PMF data measured in the presence of equimolar dendrimers and porphyrins (1.0×10^{-5} mol dm^{-3}). At pH 2.1, the $\Delta G_{\mathrm{D}\cdots\mathrm{porphyrin}}$ value was not precisely estimated from the PMF experiments because $ZnTPPS^{4-}$ was transferred across the interface at the negative edge of the potential window and H_2TPPS^{4-} formed non-

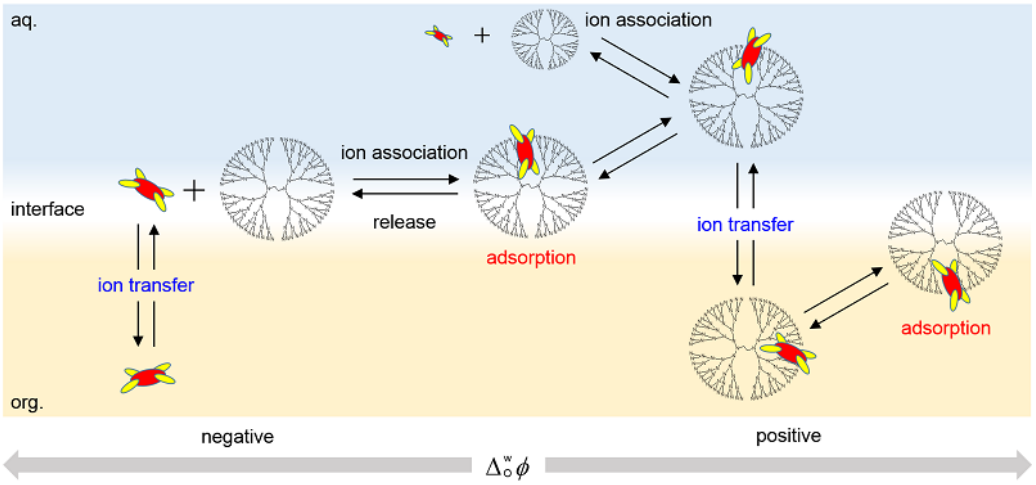

Fig. 1-17 Schematic representation of the interfacial mechanism of the dendrimer and porphyrin under neutral conditions.

fluorescent J-aggregates of the diacid species, $(H_4TPPS^{2-})_n$. Assuming that the self-aggregation and specific intermolecular interaction of the porphyrin molecules encapsulated in the dendrimer are negligible in the present condition, $\Delta G_{D\cdots porphyrin}$ can be used as a diagnostic criteria for the ion association stability. The lager negative values of $\Delta G_{D\cdots porphyrin}$ were obtained for the ion associates with the G4 PAMAM dendrimer in comparison with the G2 PAMAM dendrimer. As discussed in above section, the G4 PAMAM dendrimer is a sufficiently large molecule with internal cavities, where the encapsulated porphyrin molecules can effectively be isolated from the aqueous phase and protected from the proton attacks. On the other hand, the porphyrin molecule cannot be accommodated in a smaller interior of the G2 PAMAM dendrimer, although the interaction with the periphery groups seems to induce the red-shift of the spectra as shown in **Fig. 1-4a**. Another finding in **Table 1-1** is that $\Delta G_{D\cdots porphyrin}$ tends to be larger negative values for the $ZnTPPS^{4-}$ system. The $\Delta G_{D\cdots porphyrin}$ values therefore demonstrate the high stability of the zinc(II) porphyrin in the higher generation dendrimer. In the ion association system consisting of anilinonaphthalenesulfonates and the carboxylate-terminated G3.5 PAMAM dendrimer, it was reported that the electrostatic two-point

interaction of the dianionic species (bis-ANS^{2-}) enhance the ion association stability,[35] e.g., the $\Delta G_{\mathrm{D}\cdots\mathrm{bis-ANS}}$ values were −37 kJ mol^{-1} at pH 2.9 and −6 kJ mol^{-1} at pH 7.6, respectively. In the present system, the molecular size and four negative charges localized on *meso*-sulfonatophenyl groups of the zinc(II) porphyrin are essentially the same as the free base porphyrin, except for the acidic condition. In the case that only electrostatic (multipoint) interactions and size effects contribute to the formation of the dendrimer-porphyrin associates, $\Delta G_{\mathrm{D}\cdots\mathrm{porphyrin}}$ for the ZnTPPS^{4-} and H_2TPPS^{4-} systems should be identical each other. The $\Delta G_{\mathrm{D}\cdots\mathrm{porphyrin}}$ value for the G4 PAMAM dendrimer-ZnTPPS^{4-} associate at pH 7.2 was, however, ca. 15 kJ mol^{-1} more negative value than that for the G4 PAMAM dendrimer-H_2TPPS^{4-} associate. Gentle and coworkers have reported the structural analysis of the G4 PAMAM dendrimer-copper(II) ion complexes in the aqueous solution.[62] The X-ray absorption fine structure (XAFS) and NMR results indicated that the primary amine, amide and tertiary amine nitrogen atoms of the dendrimer were involved in bonding with the copper(II) ion to form five- and six-membered rings. The considerable stability enhancement for ZnTPPS^{4-} observed in the present study could be due to the axial coordination to the zinc(II) center of the porphyrin by amidoamine branch or tertiary amine of the dendrimer.

I-1-4 Photoreactivity of Dendrimer-ZnTPPS^{4-} Associates at the Water|DCE Interface

It was revealed that the positively charged PAMAM dendrimers spontaneously form stable ion associates with the anionic free base and zinc(II) porphyrins in the aqueous solution and the interfacial region over a wide pH range (*I-1-3*). The ion association stability was G4 PAMAM dendrime-ZnTPPS^{4-} > G2 PAMAM dendrime-ZnTPPS^{4-} > G4 PAMAM dendrime-H_2TPPS^{4-} > G2 PAMAM dendrime-H_2TPPS^{4-}. The ion association between the dendrimer and the anionic porphyrin is promoted mainly by the electrostatic interaction. In addition, ZnTPPS^{4-} could interact more strongly due to the axial coordination to the zinc(II) center by amidoamine branches or tertiary amines of the dendrimer. Recently, photoinduced electron transfer reactions between water-soluble porphyrin derivatives and lipophilic quenchers at the polarized water|DCE interface have been investigated.[63-65] For instance, the ion pair formed by ZnTPPS^{4-} and ZnTMPyP^{4+} located in the aqueous phase is reductively quenched by decamethylferrocene (DMFc) presents in the DCE phase.[63] In this case, the observed photocurrent is affected by the decay of the excited state and the rate of heterogeneous electron transfer. It has been reported that the photocurrent responses is enhanced in the presence of gold nanoparticles due to the plasmonic effect.[41] In this section, photoreactivity of the G4 PAMAM dendrimer-ZnTPPS^{4-} associates was evaluated by measuring the photocurrent transient responses at the polarized water|DCE interface.

Fig. 1-18a shows typical photocurrent transients in the presence and absence of the dendrimer at pH 5.2 and 5.4. The photoreactivity of the porphyrin derivatives at a polarized liquid|liquid interface is significantly influenced by the redox potential, lifetime of the excited state, molecular orientation at the interface and so on.[65-68] The photocurrent response of ZnTPPS^{4-} was negligibly small in the absence of the dendrimer (**Fig. 1-18a**). On the other hand, the large positive photocurrent was generated in the presence of the PAMAM dendrimers. The photocurrent in the presence of the G2 PAMAM dendrimer

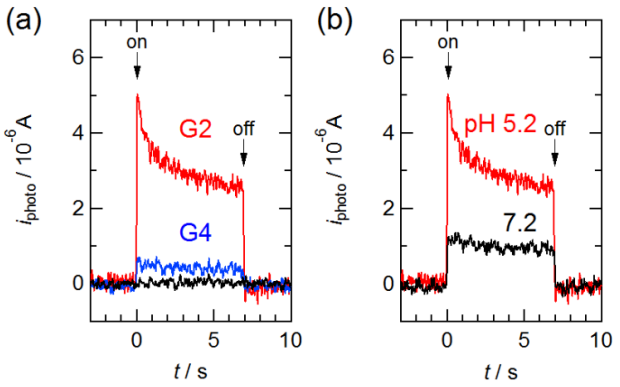

Fig. 1-18 Typical photocurrent transients of $ZnTPPS^{4-}$ at the water|DCE interface in the presence of the equimolar dendrimer at 0.20 V. (a) Photocurrent transients measured in the G2 and G4 PAMAM dendrimer-$ZnTPPS^{4-}$ systems at pH 5.2 and 5.4, respectively. The black line refers to the $ZnTPPS^{4-}$ system without adding the dendrimer at pH 5.1. (b) pH dependence for the G2 PAMAM dendrimer-$ZnTPPS^{4-}$ system.

was greatly enhanced as compared with the photocurrent in the presence of the G4 PAMAM dendrimer. In addition, the pH dependence for the G2 PAMAM dendrimer-$ZnTPPS^{4-}$ system shown in **Fig. 1-18b** indicated that larger photocurrents were generated under lower-pH conditions, at pH 5.2, where the terminal primary amines ($pK_{a,1}$ = 9.20) and interior tertiary amines of the dendrimer ($pK_{a,2}$ = 6.65) were almost protonated ($z \approx +29$). On the other hand, the protolytic demetalation of $ZnTPPS^{4-}$ was not take place at pH 5.2. It should be noted that no photocurrent was observed for the PAMAM dendrimer alone in the absence of $ZnTPPS^{4-}$. Because the chemical state of the $ZnTPPS^{4-}$ molecule is identical at pH > 5, the photocurrent enhancement should be attributed to the increase in the interfacial concentration of the photoreactive $ZnTPPS^{4-}$ or the improvement of electron-transfer kinetics in the presence of the dendrimer. The PAMAM dendrimers are effectively adsorbed at the water|DCE interface under acidic conditions,[36] and the interfacial concentration of $ZnTPPS^{4-}$ could be increased through the electrostatic interaction with the positively charged dendrimer. The photocurrent inceased

immediately in the on-transient from zero to pseudo-steady value, and the fast transient response excludes slow kinetic processes such as the ion transfer of photoproducts.[69, 70] Therefore, the positive photocurrent observed in the present system is associated with the heterogeneous electron transfer from the organic phase to the aqueous phase accompanied by the heterogeneous photoreduction of $ZnTPPS^{4-}$ of the ion associates ($D\cdots ZnTPPS^{4-}$) by DMFc in the interfacial region

$$D\cdots ZnTPPS^{4-}_{w} + DMFc_{o} \xrightarrow{h\nu} D\cdots ZnTPPS^{5-}_{w} + DMFc^{+}_{o} \qquad (23)$$

The photocurrent action spectra were measured to elucidate the wavelength dependence of the photoreactivity of the dendrimer-$ZnTPPS^{4-}$ associates at the interface. As shown in **Fig. 1-19**, the photocurrents were enhanced over the whole visible wavelength in the presence of the dendrimer, especially the G2 PAMAM dendrimer. The spectra of the photocurrent action spectra were quite similar to the bulk absorption spectra measured in the aqueous solution. The photocurrent maximum wavelengths ($\lambda_{i\text{photo,max}}$) observed under potentiostatic conditions are summarized in **Table 1-2**. The $\lambda_{i\text{photo,max}}$ values coincide roughly with the Soret band of $ZnTPPS^{4-}$ in each system. The photocurrent action spectra demonstrated that the photoreactive species at the polarized water|DCE interface were essentially identical to the bulk species in the aqueous solution, i.e., the dendrimer- $ZnTPPS^{4-}$ associate without dissociation. The relatively large effect by the G2 PAMAM dendrimer could be correlated with the preferable incomplete encapsulation of $ZnTPPS^{4-}$. As described above section (*I-1-3*), $\Delta G_{D\cdots\text{porphyrin}}$ values indicated explicitly a high stability of the G4 PAMAM dendrimer-$ZnTPPS^{4-}$ associate. The $ZnTPPS^{4-}$ molecule can penetrate into the interior of the large spherical G4 PAMAM dendrimer, whereas $ZnTPPS^{4-}$ associated with the small flat-elliptical G2 PAMAM dendrimer is exposed to the outer solution phase. The effective inhibition of the protolytic demetalation of $ZnTPPS^{4-}$ has also been attained even under acidic conditions by the G4 PAMAM dendrimer but not by the G2 PAMAM dendrimer. These findings indicate that the $ZnTPPS^{4-}$ molecule completely incorporated in the higher-generation dendrimer

seems not to react readily with DMFc located in the organic phase. As a result, the heterogeneous electron transfer from DMFc to $ZnTPPS^{4-}$ incorporated into the G4 PAMAM dendrimer at the interface was less efficient than the G2 PAMAM dendrimer-$ZnTPPS^{4-}$ system.

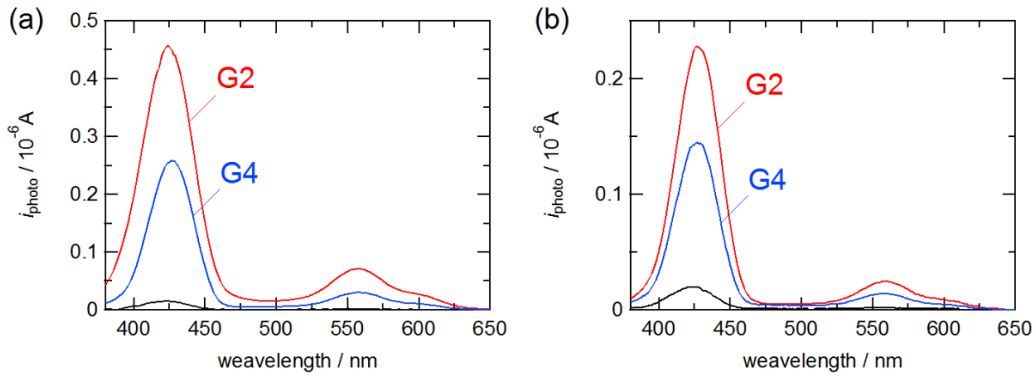

Fig. 1-19 Photocurrent action spectra measured at 0.20 V for the dendrimer-$ZnTPPS^{4-}$ systems at (a) pH 5.1-5.4 and (b) pH 7.2. The blue, red and black lines denote the G4 PAMAM dendrimer-$ZnTPPS^{4-}$, the G2 PAMAM dendrimer-$ZnTPPS^{4-}$ and $ZnTPPS^{4-}$ systems, respectively.

Table 1-2 Photocurrent maximum wavelengths ($\lambda_{iphoto,max}$) at the water|DCE interface

	$\lambda_{iphoto,max}$ / nm					
	pH 5			pH 7		
$\Delta^{w}_{o}\phi$ / V	G2-$ZnTPPS^{4-}$	G2-$ZnTPPS^{4-}$	G4-$ZnTPPS^{4-}$	G2-$ZnTPPS^{4-}$	G4-$ZnTPPS^{4-}$	$ZnTPPS^{4-}$
0.20	424	427	423	427	427	423
0.30	423	426	Ca. 423	427	427	Ca. 423
bulk aq.	425.8	427.8	421.2	426.8	428.4	421.2

I-2 Summary of PART I

The ion association behavior, interfacial mechanism of the PAMAM dendrimer-anionic porphyrin associates and its photoreactivity were investigated at the polarized water|DCE interface. Spectroelectrochemical analysis indicated that both $ZnTPPS^{4-}$ and H_2TPPS^{4-} favorably form the stable ion associates with the dendrimer in the aqueous solution. In particular, the G4 PAMAM dendrimer effectively inhibited demetalation of the zinc(II) porphyrin under acidic conditions. The ion association stability was estimated from $\Delta G_{D\cdots porphyrin}$ as: G4 PAMAM dendrimer-$ZnTPPS^{4-}$ > G2 PAMAM dendrimer-$ZnTPPS^{4-}$ > G4 PAMAM dendrimer-H_2TPPS^{4-} > G2 PAMAM dendrimer-H_2TPPS^{4-}. The relatively strong interaction for $ZnTPPS^{4-}$ could be result from the axial coordination to the zinc(II) center of the porphyrin molecule localized in the interior of the dendrimer. Furthermore, the encapsulation and release of $ZnTPPS^{4-}$ and H_2TPPS^{4-} at the liquid|liquid interface can be controlled as a function of the Galvani potential difference. Although the small positive photocurrent is generated intrinsically from the heterogeneous photoreduction of $ZnTPPS^{4-}$ by DMFc at the interface, the photocurrent response was drastically enhanced by the formation of the dendrimer-$ZnTPPS^{4-}$ associates. The high photoreactivity of the ion associates can be interpreted from the apparent increase of the interfacial concentration of $ZnTPPS^{4-}$ associated with the PAMAM dendrimers strongly adsorbed at the polarized water|DCE interface. In addition, the large photocurrent enhancement in the G2 PAMAM dendrimer-$ZnTPPS^{4-}$ system demonstrated that the higher-generation G4 PAMAM dendrimer which can incorporate the $ZnTPPS^{4-}$ molecule more completely is less efficient for the heterogeneous photoreaction system.

The present results clearly demonstrate that the dendrimer is capable as a molecular container as well as a protective agent for easily decomposable species. The intermolecular affinity of the dendrimer could enable development of highly functional

DDS with membrane potential sensitivity and selective separation systems. In addition, development of the optical-active molecule based on the dendrimer incorporating light sensitive dye and its use for the energy conversion device and the artificial photosynthesis system are accelerated.

PART II

Ion Transfer and Adsorption Behavior of Bioactive Species Affected by PAMAM Dendrimers at the Water|1,2-Dichloroethane Interface

In PART II, in order to evaluate the potential ability of dendrimers as a molecular capsule for DDS and separation sciences, the effect of the PAMAM dendrimers on the association behavior and interfacial mechanism of bioactive species at the water|DCE interface are discussed. Developing the highly effective DDS, it is significantly important to control the processes including encapsulation of drugs into a capsule, delivery and distribution to a target cell and release of drugs. In section II-1, ionizable drugs, i.e. dipyridamole (DIP), propranolol (PRO) and warfarin (HWAR) are described. The molecular structures of these drugs are shown in **Fig. 2-1.** These drugs are used for a coronary vasodilator, a coactivator of antitumor compounds, thromboembolism and so on.[71-75] It is significantly important to determine the physicochemical properties of drugs in biomimetic liquid-liquid distribution systems since the pharmacokinetics of drugs involves heterogeneous charge transfer and adsorption processes on or across a biomembrane. The ionic partition property of cationic PRO and anionic WAR molecules as common drugs has been widely investigated at ITIES. Characteristic of DIP in aqueous solution has been studied through conventional spectroscopic measurements.[76-78] In this section, the interfacial properties of these drugs in the presence of the G3.5 and G4 PAMAM dendrimers through the voltammetric and spectroelectrochemical techniques are discussed.

In section II-2, flavin derivatives, i.e. riboflavin (RF), lumichrome (LC) and flavin mononucleotide (FMN), are described. These flavin derivatives are ordinary in human body. RF is well known as vitamin B2 composed of isoalloxazine ring and ribitol chain. LC and FMN are generated from RF in the metabolic cycle *in vivo*. The molecular structures of the flavin derivatives are shown in **Fig. 2-2**. RF is a neutral species while FMN is an anionic species under neutral conditions due to the phosphate group located at the ribitol chain. It has been reported that the molecular recognition of RF by forming the complex through the hydrogen bond at the water|CCl_4 interface.[79] Therefore, RF could be associated with the dendrimers through the hydrogen bond and hydrophobic interaction.

In addition, FMN could be expected the molecular association thorough the electrostatic interaction as well as hydrogen bond with the dendrimers. Flavin derivatives are also known as light-sensitive fluorescent species.[80-83] Owing to these chemical and spectroscopic properties, flavin derivatives could interact with dendrimers and the PMF technique can be applied to investigate the interfacial mechanism and the molecular encapsulation behavior of the dendrimers for the bioactive species.

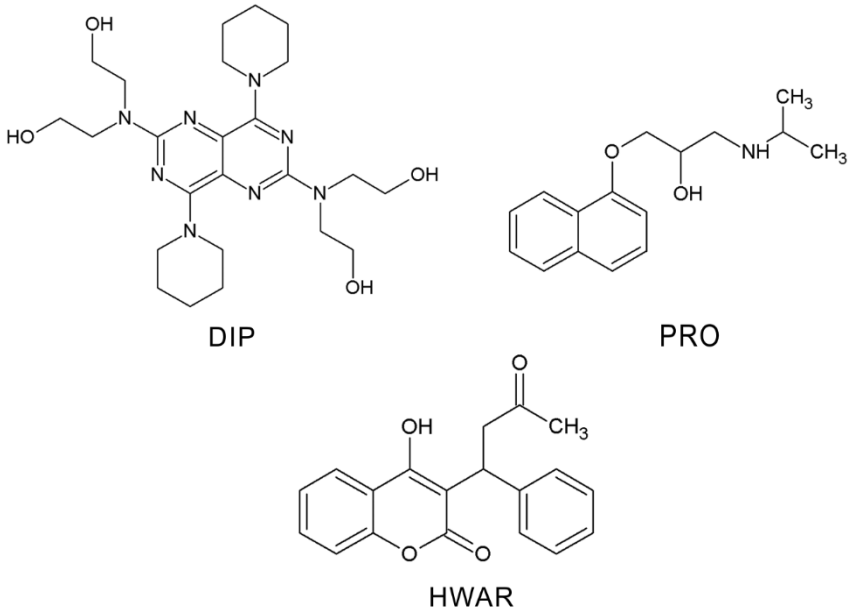

Fig. 2-1 Molecular structures of dipyridamole (DIP), propranolol (PRO) and warfarin (HWAR).

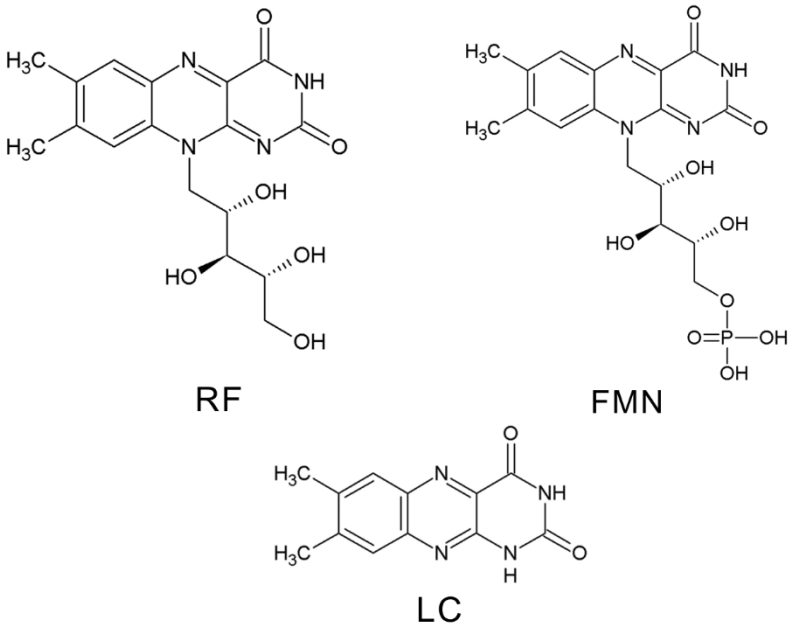

Fig. 2-2 Molecular structures of riboflavin (RF), flavin mononucleotide (FMN) and lumichrome (LC).

II-1 Ionizable Drugs System

II-1-1 Ion Partitioning of Ionizable Drugs in the Water|DCE System

The intrinsic ion transfer reactions of basic (DIP and PRO) and acidic drug (HWAR) molecules were preliminary investigated by cyclic voltammetry and admittance measurements in the absence of the dendrimers. Typical cyclic voltammograms (CVs) and ac voltammograms (ACVs) measured for DIP under various pH conditions are shown in **Fig 2-3**. The apparent ion transfer potential of the cationic DIP species was determined from the half-wave potential ($\Delta_o^w\phi^{1/2}$) observed in CVs and the peak potential of admittance in ACVs, in which the $\Delta_o^w\phi^{1/2}$ value was shifted toward positive potentials with increasing pH. For example, the $\Delta_o^w\phi^{1/2}$ values observed through the admittance measurements at pH 2.0, 7.0 and 9.1 were 0.02 V, 0.15 V and 0.28 V, respectively. At pH 7.1, an additional positive voltammetric response was found around 0.30 V and this post-

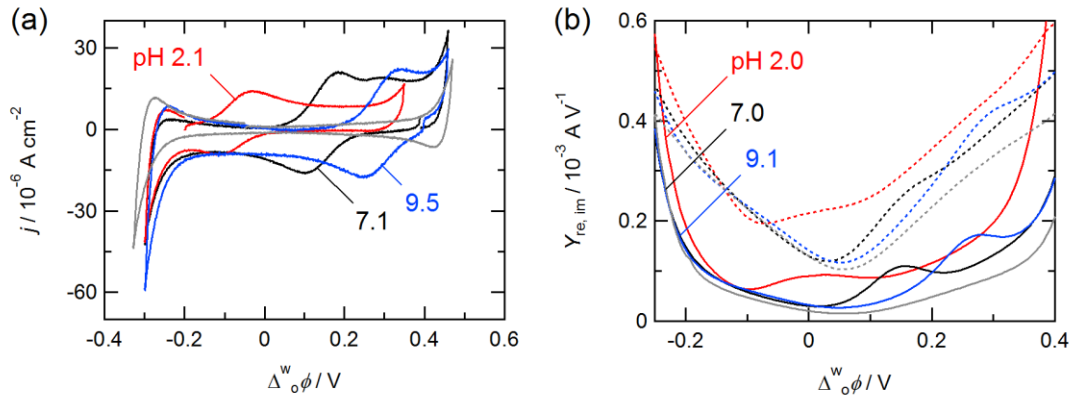

Fig. 2-3 (a) Cyclic and (b) ac voltammograms of DIP measured at the water|DCE interface. (a) The potential sweep rate was 100 mV s^{-1}. The gray line relates to CV at 100 mV s^{-1} in the absence of DIP at pH 7.1. The concentration of DIP was 8.0×10^{-5} mol dm^{-3}. (b) The solid and dashed lines refer to the rear (Y_{re}) and imaginary (Y_{im}) components of the admittance, respectively. The gray lines relate to the admittance in the absence of DIP at pH 7.1. The potential sweep rate was 5 mV s^{-1}. The amplitude of ac potential modulation was 10 mV at 7 Hz. The concentration of DIP was 1.0×10^{-5} mol dm^{-3}.

transfer response could be associated with the interfacial adsorption of cationic DIP species. The peak to peak separation for the ion transfer responses was 0.059 V at [DIP] = 1.0×10^{-5} mol dm^{-3} in agreement with the theoretical value for a monocationic species though slightly larger value (ca. 0.07 V) was observed at [DIP] = 8.0×10^{-5} mol dm^{-3} because of the partial overlap with the post-transfer adsorption response. The peak current was almost proportional to the square root of the potential sweep rate ($v^{1/2}$) for a quasi-reversible transfer of monocationic species. The voltammetric results indicated that the ion transfer of monoprotonated form, $HDIP^+$, takes place dominantly through the diffusion controlled process.

The ionic partition diagram is one of the most important data to evaluate the distribution property of ionic species and it allows us to trace the transfer potential and distribution equilibria of ionic species in the liquid|liquid system as a function of pH. The Nernst equation for the ion transfer of monobasic species, $HDIP^+$, is defined by:[12, 84]

$$\Delta_o^w\phi = \Delta_o^w\phi^{\circ'}_{HDIP^+} + \frac{2.303RT}{zF}\log\frac{[HDIP^+]_o}{[HDIP^+]_w} \quad (24)$$

where $\Delta_o^w\phi^{\circ'}_{HDIP^+}$ is the formal ion transfer potential. When the concentrations of $HDIP^+$ in the aqueous and organic phases are equal to each other, the term $\log([HDIP^+]_o/[HDIP^+]_w)$ is zero in Eq. (24) and then the Nernst equation is simplified into:

$$\Delta_o^w\phi = \Delta_o^w\phi^{\circ'}_{HDIP^+} \quad (25)$$

The acid-base equilibrium between $HDIP^+$ in the aqueous phase and DIP in the organic phase is described as:

$$DIP_o + H_2O \rightleftharpoons HDIP^+_w + OH^- \quad (26)$$

When the spontaneous distribution of the neutral DIP occurs in the water|DCE system, the acidity constant of DIP in water ($K_{a,HDIP^+}$) can be expressed as a function of pH and the partition coefficient of the neutral DIP (P_{DIP}):

$$K_{a,HDIP^+} = \frac{[DIP]_w[H^+]_w}{[HDIP^+]_w} = \frac{[DIP]_o}{[HDIP^+]_w}\frac{[H^+]_w}{P_{DIP}} \quad (27)$$

$$pK_{a,HDIP^+} = -\log\left(\frac{[DIP]_o}{[HDIP^+]_w}\right) + pH + \log P_{DIP} \quad (28)$$

where P_{DIP} is identical to $[DIP]_o/[DIP]_w$ under dilute conditions. The equiconcentration boundary line of $HDIP_w^+$ and DIP_o is given by:

$$pH = pK_{a,HDIP^+} - \log P_{DIP} \quad (29)$$

On the other hand, the boundary line of $HDIP_o^+$ and DIP_o is derived from Eqs. (24) and (27):

$$\Delta_o^w\phi = \Delta_o^w\phi^{\circ'}_{HDIP^+} + \frac{2.303RT}{zF}\log\left(\frac{[HDIP^+]_o}{[DIP]_o}\right) + \frac{2.303RT}{zF}\log\left(\frac{P_{DIP}K_{a,HDIP^+}}{[H^+]_w}\right) \quad (30)$$

In the case of equiconcentration of $HDIP_o^+$ and DIP_o, Eq. (30) can be rewritten as:

$$\Delta_o^w\phi = \Delta_o^w\phi^{\circ'}_{HDIP^+} + \frac{2.303RT}{zF}\left(\log P_{DIP} - pK_{a,HDIP^+}\right) + \frac{2.303RT}{zF}pH \quad (31)$$

As shown in **Fig. 2-4**, the transfer potentials experimentally obtained under the acidic conditions were approximately constant at $\Delta_o^w\phi^{\circ'}_{HDIP^+} = 0.00$ V, while the transfer potential exhibited a positive shift with a slope of 0.059 V (= 2.303*RT/F*) at pH > 5. These results bear out DIP as a monobasic species. Although a DIP molecule has eight possible protonation site (nitrogen atoms), a single protonation would only occur within the examined pH range ($0.0 \le pH \le 9.5$). According to the semi-empirical quantum calculations, the heats of formation (ΔH_f°) for monoprotonation of DIP at a pyrimidine nitrogen is estimated as ca. −58 kJ mol^{-1}, while ΔH_f° for second protonation is much higher value, 828 kJ mol^{-1}.[85] Hence, the additional protonation of $HDIP^+$ is unrealistic under the present conditions and theoretical predictions support our experimental results. The ($pK_{a,HDIP^+} - \log P_{DIP}$) value as a fitting parameter was evaluated as 4.52 from Eq. (31)

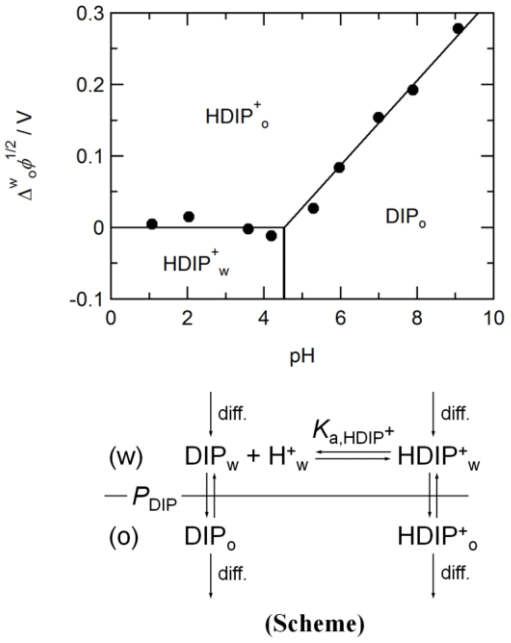

Fig. 2-4 Ionic partition diagram for DIP based on the ac voltammograms measured at various pHs. The vertical line represents the estimated value of ($pK_{a,HDIP^+} - \log P_{DIP}$). The concentration of DIP was 1.0×10^{-5} mol dm^{-3}. **(Scheme)** The reaction scheme for the partition of DIP associated with the acid-base equilibrium in the aqueous phase. The subscripts w and o denote the water and organic phases, respectively.

with $\Delta_o^w\phi^{\circ'}_{HDIP^+} = 0.00$ V and, thus, the $\log P_{DIP}$ value in the water|DCE system was estimated to be 1.2 by taking a literature value of $pK_{a,HDIP^+} = 5.7$.[78] The experimental values of $\Delta_o^w\phi^{\circ'}$ and log*P* for the drugs are summarized in **Table 2-1**. The simple ion transfer features were observed for $HPRO^+$ and WAR^- (**Fig. 2-5**). The ionic partition diagram of PRO system in **Fig. 2-6a** was analyzed in the same manner as the DIP system from the $\Delta_o^w\phi^{1/2}$ values. The $\Delta_o^w\phi^{\circ'}_{HPRO^+}$ and $\log P_{PRO}$ values were 0.12 V and 3.0, respectively, in good agreement with the literature values.[9, 10] In the WAR system, the ionic partition diagram for a lipophilic acid was obtained as shown in **Fig. 2-6b**, where the boundary lines for $HWAR_o / WAR^-_w$ and $HWAR_o / WAR^-_o$ are expressed by Eqs. (32) and (33):

$$\mathrm{pH} = \log P_{\mathrm{HWAR}} + \mathrm{p}K_{\mathrm{a,HWAR}} \tag{32}$$

$$\Delta_{\mathrm{o}}^{\mathrm{w}}\phi = \Delta_{\mathrm{o}}^{\mathrm{w}}\phi_{\mathrm{WAR}^-}^{\circ'} - \frac{2.303RT}{zF}\left(\log P_{\mathrm{HWAR}} + \mathrm{p}K_{\mathrm{a,HWAR}}\right) + \frac{2.303RT}{zF}\mathrm{pH} \tag{33}$$

$\Delta_{\mathrm{o}}^{\mathrm{w}}\phi_{\mathrm{WAR}^-}^{\circ'} = -0.10\ \mathrm{V}$ roughly coincides with the literature value, while the $\log P_{\mathrm{HWAR}}$ value estimated as 3.7 by taking $\mathrm{p}K_{\mathrm{a,HWAR}} = 5.1$[86] was relatively larger than the literature value.[86] The disparity in $\log P_{\mathrm{HWAR}}$ could result from the specific phase ratio of the spectroelectrochemical cell used in this study[84] or the difficulty in determining the precise ion transfer potential of WAR^- in the lower pH region, where the ion transfer peaks were observed at potentials close to the negative edge of the potential window (**Fig. 2-5**).

Table 2-1 Formal transfer potentials ($\Delta_{\mathrm{o}}^{\mathrm{w}}\phi^{\circ'}$) of drug ions and partition coefficients (log*P*) of neutral form determined by the electrochemical measurements

compounds	$\Delta_{\mathrm{o}}^{\mathrm{w}}\phi^{\circ'}$ / V	pK_{a}	log*P*
HDIP^+	0.00	5.7[a]	1.2
HPRO^+	0.12 (0.115[b])	9.5[b]	3.0 (3.1[b])
WAR^-	−0.10 (−0.112[b])	5.15[c]	3.7 (2.7[b])

[a]Ref. [78]. [b]Ref. [10]. [c]Ref. [86].

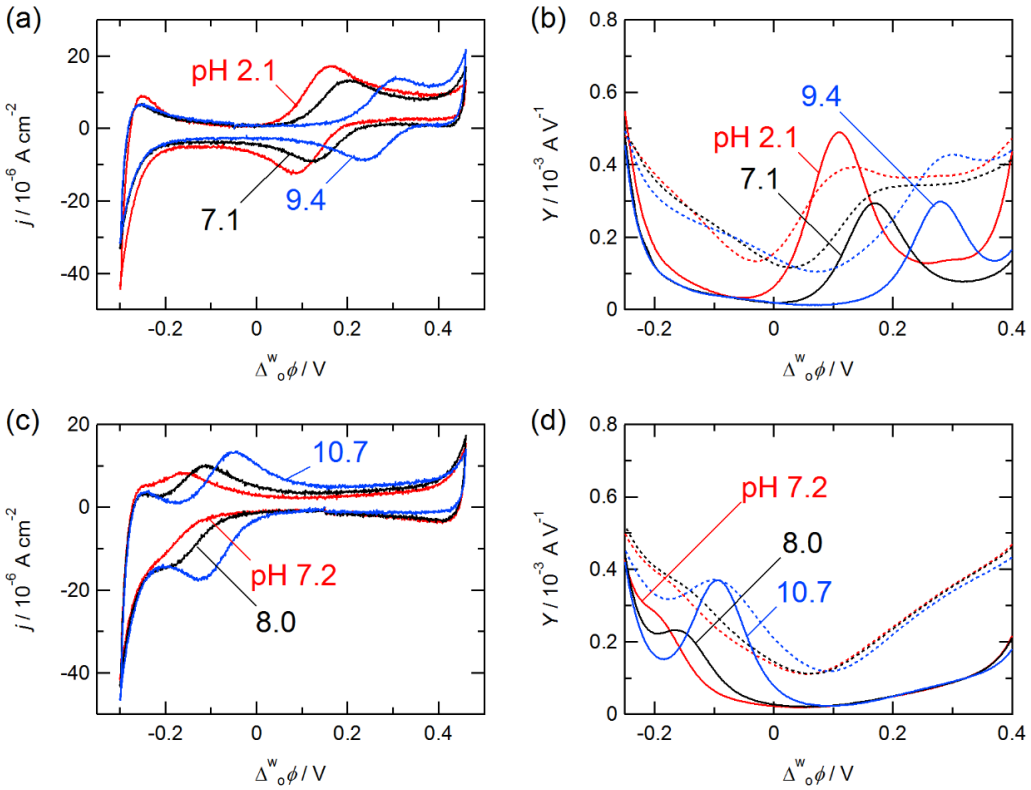

Fig. 2-5 Cyclic and ac voltammograms for (a, b) the PRO and (c, d) WAR systems at various pHs. The potential sweep rates were (a, c) 100 mV s^{-1} and (b, d) 5 mV s^{-1}, respectively. (b, d) The solid and dashed lines refer to the real (Y_{re}) and imaginary (Y_{im}) components of the admittance. The concentration of PRO and WAR was 1.0×10^{-4} mol dm^{-3}.

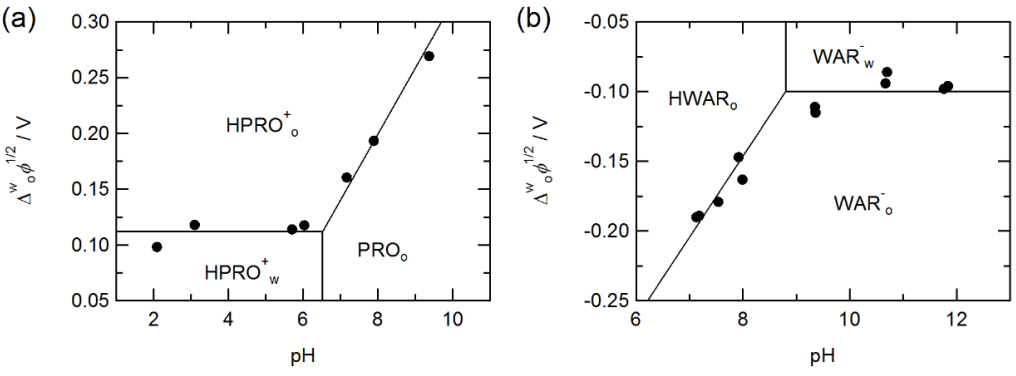

Fig. 2-6 Ionic partition diagram for (a) PRO and (b) WAR based on the voltammograms measured at various pHs. The concentration of PRO and WAR was 1.0×10^{-4} mol dm^{-3}.

II-1-2 Voltammetric Responses of Ionizable Drugs Affected by the Dendrimers

The intermolecular association between the ionizable drugs and the PAMAM dendrimers in the aqueous solution was investigated at various pHs by the UV-Vis absorption and fluorescence spectroscopies. **Fig. 2-7** shows typical emission and excitation spectra of the aqueous solution of DIP in the absence and presence of the equimolar dendrimers. The most abundant DIP species at pH 2.2, $HDIP^+$ was not efficient fluorescent species, while the neutral DIP with poor solubility in water at pH ≥ 7.2 exhibited strong fluorescence. Taking into account the acidity constants of terminal groups and tertiary amines of the dendrimers,[35, 53] the net charges (z) on the G3.5 and G4 PAMAM dendrimers are calculated as $+61 \geq z_{\text{G3.5 PAMAM}} \geq -64$ at $2.1 \leq \text{pH} \leq 9.5$ and $+126 \geq z_{\text{G4 PAMAM}} \geq +2$ at $2.1 \leq \text{pH} \leq 10.6$, respectively. Under the present pH conditions, the spectral profiles of DIP in the aqueous solution were not practically influenced by the presence of the dendrimers. In aqueous micellar systems, the DIP species located in a less polar environment such as micellar core indicate the intense fluorescence with a blue-shift of the emission maximum.[76, 87] The present spectral results would be indicative of no efficient interaction between DIP species and the hydrophobic interior of the

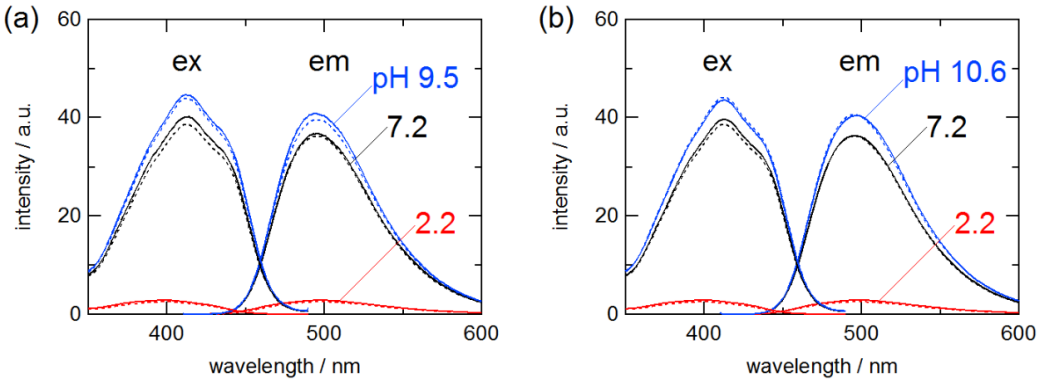

Fig. 2-7 Emission and excitation spectra of DIP in the absence (dashed) and presence (solid) of the equimolar (a) G3.5 and (b) G4 PAMAM dendrimer in the aqueous solution at various pHs. The concentration of DIP and the dendrimers was 1.0×10^{-5} mol dm^{-3}. The excitation wavelength was 404 nm.

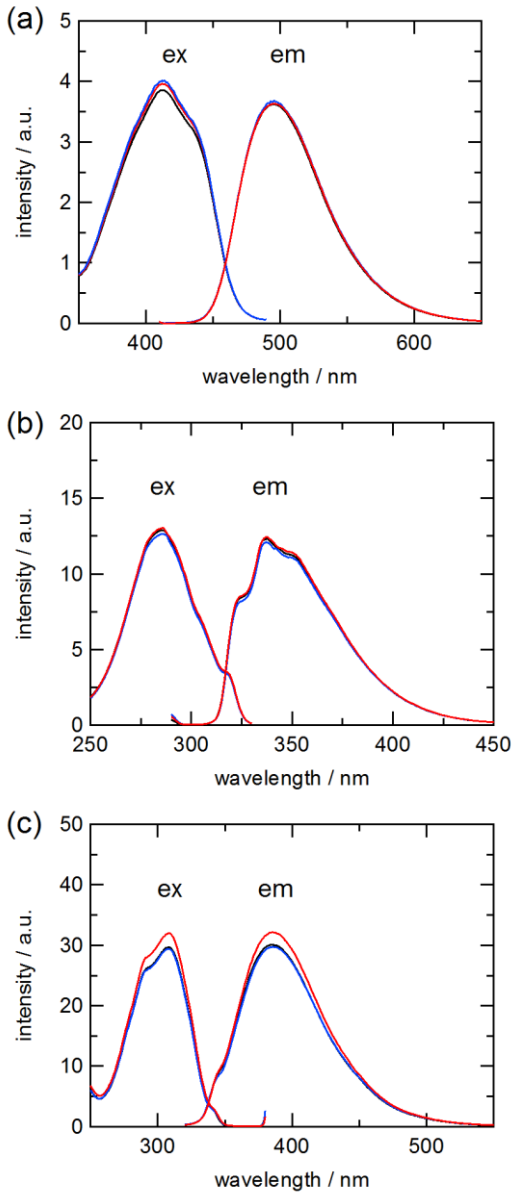

Fig. 2-8 Emission (solid) and excitation (dashed) spectra of (a) DIP at pH 7.2, (b) PRO at pH 7.1 and (c) WAR at pH 7.1 in the aqueous solution. The black, blue and red lines refer to the drug, drug−G3.5 PAMAM dendrimer, and drug−G4 PAMAM dendrimer systems, respectively. The concentration of drugs and the dendrimers was 1.0×10^{-5} mol dm^{-3}. The excitation wavelength was 404 nm.

dendrimers in the bulk aqueous phase. No spectral evidence for the association with the dendrimers were also observed for the PRO and WAR systems. (**Fig. 2-8**).

The voltammetric responses in the presence of the equimolar concentration of the drugs and dendrimers were significantly dependent on the pH conditions. The general features of CVs were analogous to those for the G3.5 and G4 PAMAM dendrimers reported previously.[35, 36] **Fig.2-9** shows the CVs measured for DIP with the G3.5 and G4 PAMAM dendrimer. In the G4 PAMAM systems (red lines), no significant changes of the electrochemical responses of DIP was observed since the current responses for the ion transfer and adsorption of the dendrimer superimposed even at pH 10.7. In the G3.5 PAMAM systems (blue lines), the electrochemical responses of DIP could be observed. At pH 2.2, the G3.5 PAMAM dendrimer exists as the cationic species ($z \approx +60$). The positive and negative current peaks observed around 0.35 V and 0.25 V could be assigned as the ion transfer of the positively charged G3.5 PAMAM dendrimer (**Fig. 2-9a**). In addition, the ion transfer response for $HDIP^+$ was observed at around 0 V. The broad voltammetric responses at $0 < \Delta_o^w\phi < 0.20$ V were also associated with the interfacial adsorption of the G3.5 PAMAM dendrimer.[35] In addition, the ion transfer response for $HDIP^+$ was observed at around 0 V. At pH 7.2 where the net charges on the dendrimer is ca. −53, the capacitive current was increased in the whole potential region (**Fig. 2-9b**), indicating the interfacial adsorption of the charged species. Under the alkaline condition at pH 9.5, the G3.5 PAMAM dendrimer showed no clear voltammetric responses (**Fig. 2-9c**), nevertheless the ion transfer currents of $HDIP^+$ at around 0.28 V were slightly decreased in the presence of the dendrimer. The similar current decrease was also observed for the cationic PRO system under the neutral and alkaline conditions in the presence of the G3.5 PAMAM dendrimer (**Fig. 2-10a**). On the other hand, the anionic WAR system showed no clear difference even in the presence of the cationic G4 PAMAM dendrimer with higher positive charges (**Fig. 2-10b**). These voltammetric results indicate that the ion transfer process of the cationic drugs could be affected by the oppositely charged G3.5 PAMAM dendrimer at the polarized interface. The ion transfer potentials and ionic partition diagrams of $HDIP^+$ and $HPRO^+$ were, however, not shifted in the

presence of the dendrimers. It has been reported that a multipoint electrostatic interaction of ionic species with the dendrimers could significantly enhance the ion association stability whereas a monovalent ion is appreciably associated with the dendrimer.[35, 88] The ambiguous effects of the dendrimer for the monovalent drug cations could be due to rather weak interaction with the negatively charged G3.5 PAMAM dendrimer.

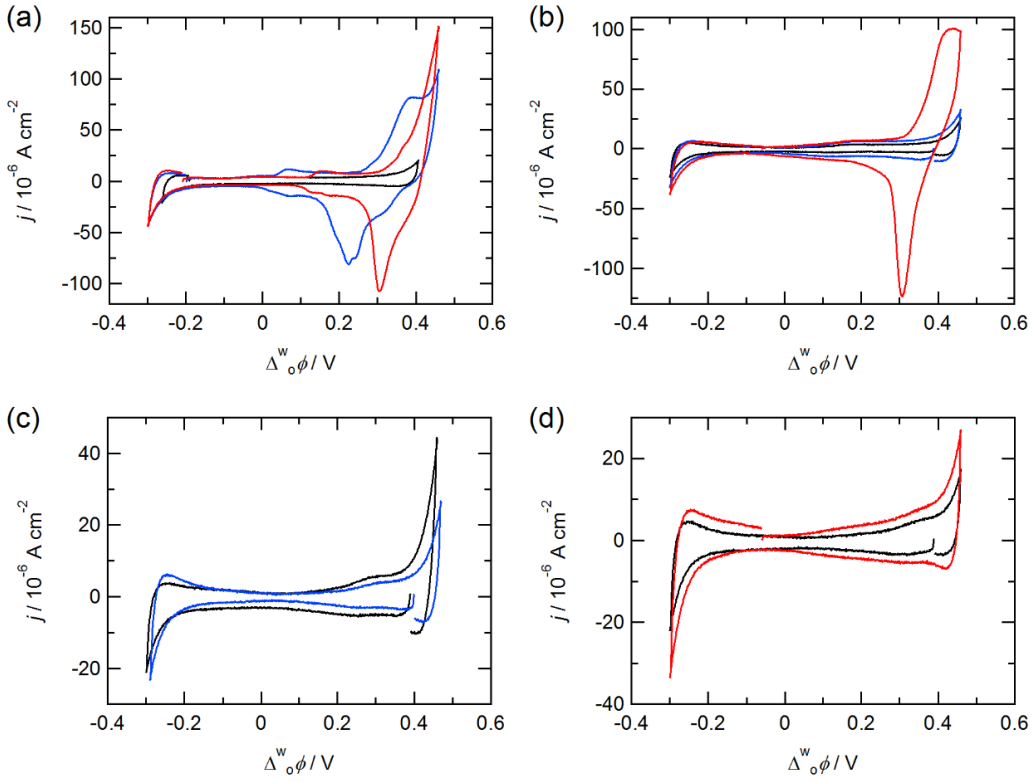

Fig. 2-9 Cyclic voltammograms measured for DIP in the absence and presence of the dendrimers at (a) pH 2.1, (b) 7.1, (c) 9.5 and (d) 10.7. The black, blue and red lines refer to the DIP, DIP−G3.5 PAMAM dendrimer, and DIP−G4 PAMAM dendrimer systems, respectively. The potential sweep rate was 100 mV s^{-1}. The concentration of DIP and the dendrimers was 1.0×10^{-5} mol dm^{-3}.

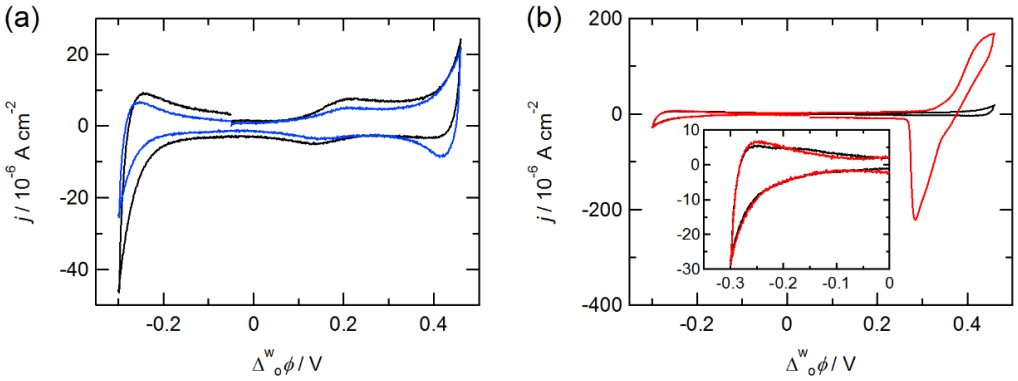

Fig. 2-10 Cyclic voltammograms measured for (a) PRO and (b) WAR at pH 7.1 in the presence of the equimolar dendrimers. The black lines refer to CVs in the absence the dendrimers. The blue and red lines refer to CVs in the presence of the G3.5 and G4 PAMAM dendrimer, respectively. The potential sweep rate was 100 mV s^{-1}. The concentration of PRO, WAR and the dendrimers was 2.0×10^{-5} mol dm^{-3}.

II-1-3 PMF Analysis of Interfacial Behavior of DIP in the presence of the Dendrimers

As shown in **Figs. 2-9** and **10a**, the electrochemical responses associated with the cationic drugs ($HDIP^+$ and $HPRO^+$) were slightly affected by the negatively charged G3.5 PAMAM dendrimer, in which the peak currents under neutral and alkaline conditions decreased in the presence of the dendrimer. Under the acidic condition at pH 2.2 (**Fig. 2-9a**), the voltammetric responses of DIP were totally buried in those of the dendrimer. In order to study the effect of the dendrimer on the interfacial behavior of cationic drugs in detail, the PMF analysis was carried out for the DIP species which indicates the distinct fluorescence emission in the visible wavelength region. **Fig. 2-11** shows the potential dependence and complex plane of the PMF responses of DIP at pH 2.1. In the potential dependence measurements, the real (ΔF_{re}) and imaginary components (ΔF_{im}) of the PMF response were obtained as positive and negative signs around −0.06 V, where the characteristic voltammetric responses were observed in CVs (**Fig. 2-11a**). A PMF complex plane for the ion transfer of cationic species appears in the fourth quadrant with linearity (cf. Methodology section). The frequency dependent PMF responses measured at −0.06 V was expressed as a distorted linear response in the fourth quadrant of the complex plane due to the contribution of the adsorption process (**Fig. 2-11b**). Therefore, the PMF responses around −0.06 V correspond to the ion transfer of $HDIP^+$. In addition, the PMF signals with the negative ΔF_{re} and positive ΔF_{im} were observed at $0\ \mathrm{V} \le \Delta_o^w\phi \le 0.20\ \mathrm{V}$. The complex plane of PMF responses at 0.07 V exhibited a semicircle in the second quadrant **(Fig. 2-11c**), demonstrating that $HDIP^+$ are transferred across the interface accompanied by the adsorption process at the organic side of the interface. At pH 7.2 and 9.5, the neutral DIP was initially dissolved in the organic phase because of the low solubility in water. **Fig. 2-12** shows the potential dependence and complex plane of the PMF responses of DIP at pH 7.2. In the potential dependence measurements at [DIP] = 8.0×10^{-5} mol dm^{-3}, ΔF_{re} and ΔF_{im} of the PMF response were obtained as positive and negative signs around 0.14 V (**Fig. 2-12c**), although it is difficult

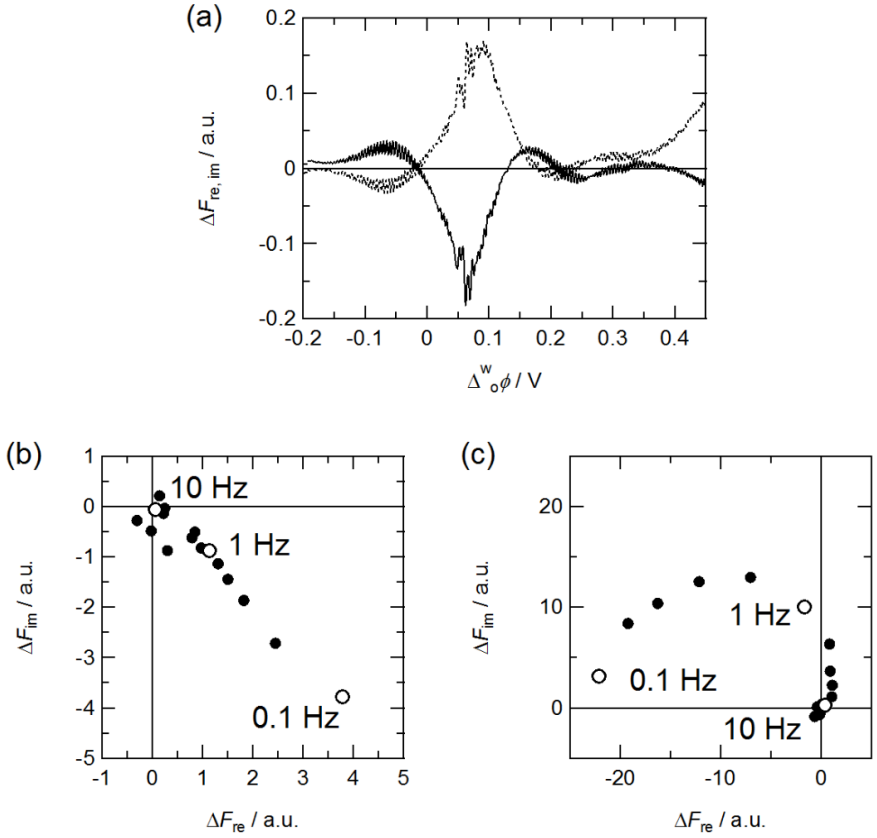

Fig. 2-11 Dependences of the PMF responses for DIP at pH 2.1 on (a) the Galvani potential difference and the potential modulation frequency at (b) −0.06 V and (c) 0.07 V. (a) The solid and dashed lines refer to the real and imaginary components, respectively. The amplitude of ac potential modulation was 10 mV. The concentration of DIP was 1.0×10^{-5} mol dm^{-3}.

to analyze the frequency dependence of the PMF responses at [DIP] = 1.0×10^{-5} mol dm^{-3} due to the low and complicated PMF responses. In addition, the complex PMF responses were observed at $\Delta^{w}_{o}\phi \geq 0.25$ V as negative ΔF_{re} and positive ΔF_{im} signs which were indicative of the adsorption process of $HDIP^{+}$ at the organic side of the interface. These PMF results indicate that $HDIP^{+}$ are transferred across the interface accompanied by the adsorption process at the organic side of the interface (**Fig. 2-16**). **Fig. 2-13** shows the potential dependence and complex plane of the PMF responses of DIP at pH 9.5. The simple PMF responses were obtained in more positive potential region than at pH 2.1 and

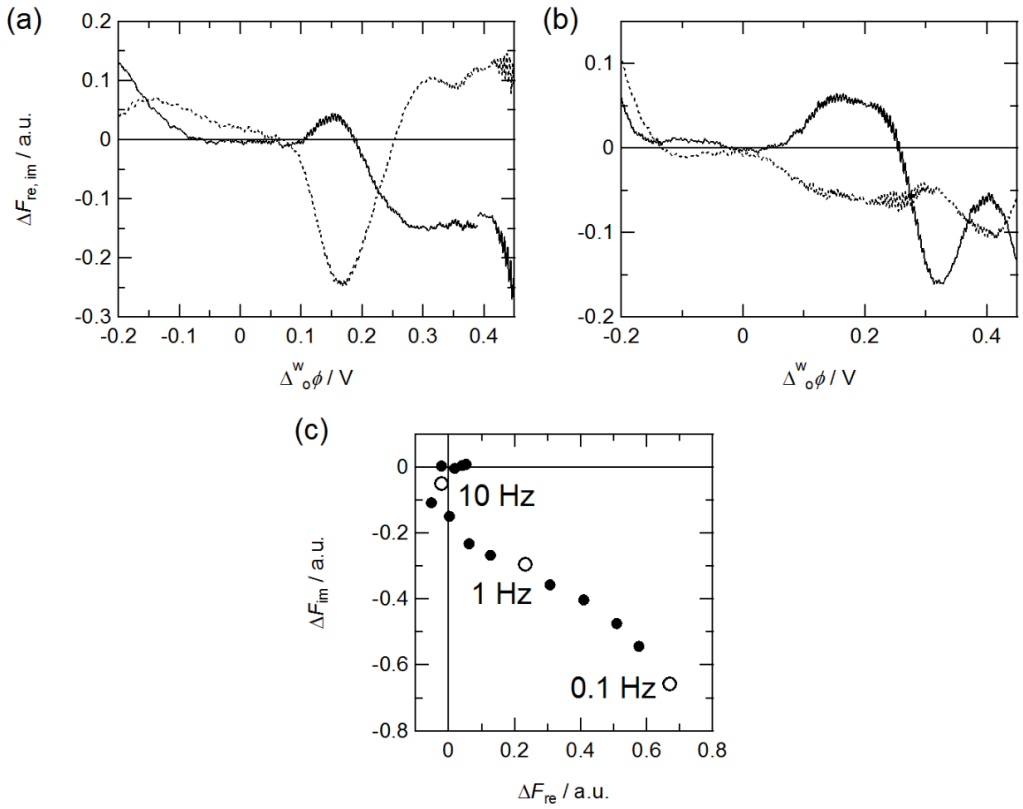

Fig. 2-12 Dependences of the PMF responses for DIP at pH 7.2 on (a, b) the Galvani potential difference and (c) the potential modulation frequency at 0.14 V. (a, b) The solid and dashed lines refer to the real and imaginary components, respectively. The amplitude of ac potential modulation was 20 mV. The concentration of DIP was (a) 1.0×10^{-5} mol dm^{-3} and (b, c) 8.0×10^{-5} mol dm^{-3}, respectively.

7.2. The frequency dependences of the PMF responses for the ion transfer and adsorption process of $HDIP^+$ were observed around 0.26 V and 0.44 V, respectively. The positively shift of the ion transfer potential in alkaline conditions was corresponding to the result of electrochemical measurements (**Figs. 2-3** and **2-4**).

These PMF responses of DIP alone systems were changed in the presence of the G3.5 and G4 PAMAM dendrimer. **Fig. 2-14a** shows the potential dependences of the PMF signals for $HDIP^+$ in the presence and absence of the equimolar G3.5 PAMAM dendrimer at pH 2.2. The PMF responses for the adsorption process of $HDIP^+$ exhibited

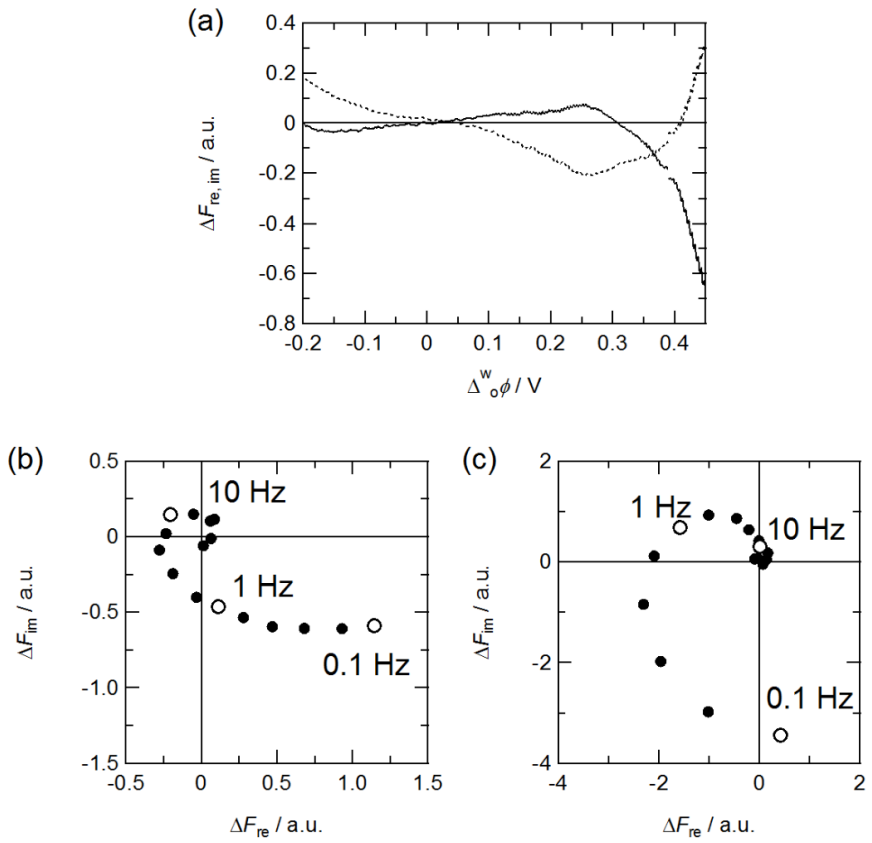

Fig. 2-13 Dependences of the PMF responses for DIP at pH 9.5 on (a) the Galvani potential difference and the potential modulation frequency at (b) 0.26 V and (c) 0.44 V. (a) The solid and dashed lines refer to the real and imaginary components, respectively. The amplitude of ac potential modulation was 20 mV. The concentration of DIP and was 1.0×10^{-5} mol dm^{-3}.

apparent negative shifts in the presence of the G3.5 PAMAM dendrimer. At pH 2.2, the estimated net charges on the G3.5 PAMAM dendrimer is ca. +60. The strong adsorption of the positively charged G3.5 PAMAM dendrimer at the water|DCE interface has been reported in the positive potential region.[35] The negative shift of the adsorption responses of $HDIP^+$, therefore, could result from the electrostatic repulsion by the positively charged dendrimers adsorbed at the interface. On the other hand, the PMF response of the adsorption of $HDIP^+$ was hardly changed in the presence of the G4 PAMAM dendrimer at pH 2.2 (**Fig. 2-15a**). As reported previously,[88] the interfacial adsorption of the G4

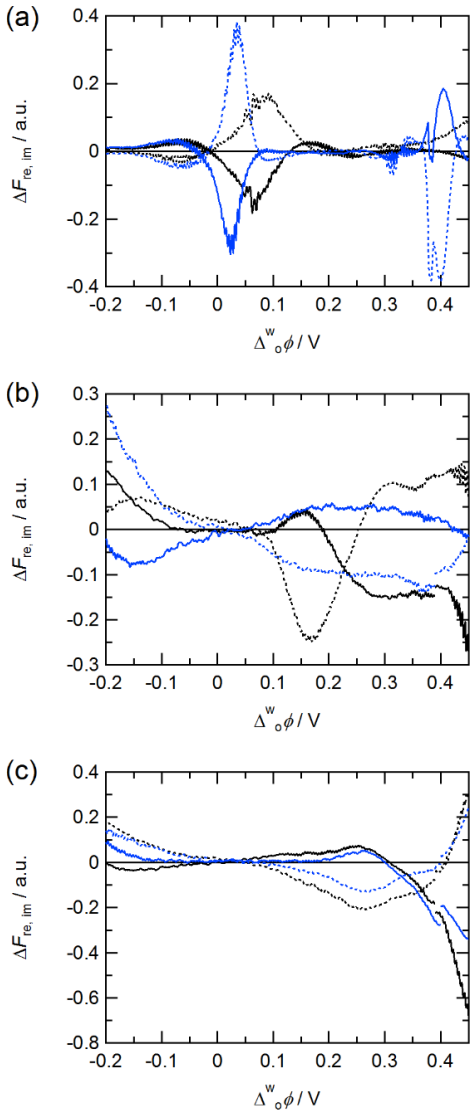

Fig. 2-14 Potential dependences of the PMF responses measured for DIP at pH (a) 2.2, (b) 7.2 and **(c)** 9.5 in the presence of the equimolar G3.5 PAMAM dendrimer. The black lines refer to the PMF responses in the absence of the dendrimer. The potential sweep rate was 5 mV s^{-1}. The amplitudes of ac potential modulation were (a) 10 mV and (b, c) 20 mV at 1 Hz. The solid and dashed lines refer to the real and imaginary components, respectively. The concentration of DIP and the G3.5 PAMAM dendrimer was 1.0×10^{-5} mol dm^{-3}.

PAMAM dendrimer is observed at $\Delta^{w}_{o}\phi > 0.10$ V under acidic conditions, where this potential region is more positive than that of the adsorption of the G3.5 PAMAM

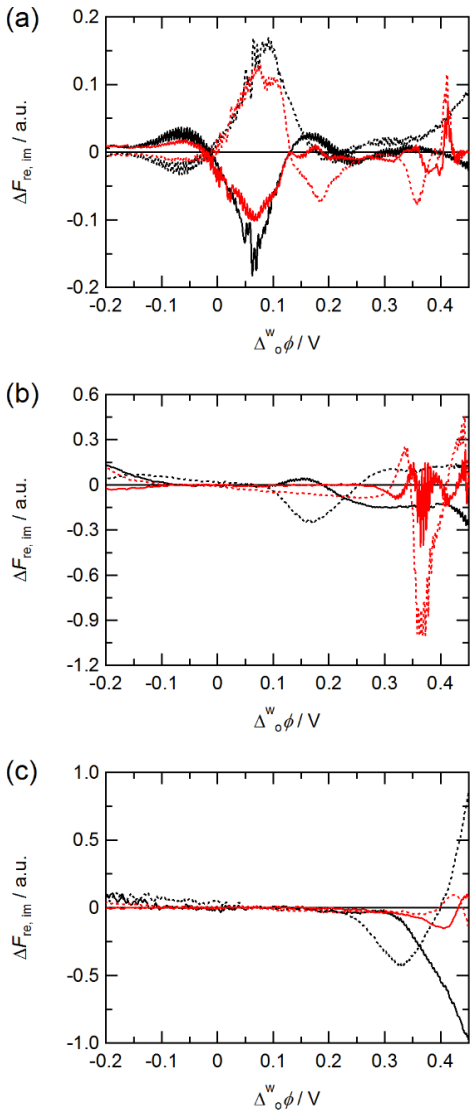

Fig. 2-15 Potential dependences of the PMF responses measured for DIP at pH (a) 2.2, (b) 7.3 and (c) 10.7 in the presence of the equimolar G4 PAMAM dendrimer. The black lines depict the data measured in the absence of the dendrimer. The potential sweep rate was 5 mV s^{-1}. The amplitudes of ac potential modulation were (a) 10 mV and (b, c) 20 mV at 1 Hz. The solid and dashed lines refer to the real and imaginary components, respectively. The concentration of DIP and the dendrimer was 1.0×10^{-5} mol dm^{-3}.

dendrimer. Therefore the electrostatic repulsion between $HDIP^{+}$ and the G4 PAMAM dendrimer seems not to be efficient. In the PMF measurements, in principle, the

interfacial process of only the fluorescence ions is detectable and the interfacial processes associated with non-fluorescent dendrimers should be excluded from the PMF response.[16, 36] The relatively weak PMF signals were, however, observed at $\Delta_o^w\phi > 0.30$ V, where the ion transfer and adsorption of the G3.5 PAMAM dendrimer take place at the water|DCE interface. The PMF responses observed at the positive edge of the potential window agreed with those of the G3.5 PAMAM dendrimer incorporating anilinonaphthalenesulfonates.[35] Taking into account the positive net charges on the dendrimer under acidic conditions, the only neutral DIP can be encapsulated into the hydrophobic interior of the dendrimer. The fluorescent DIP-G3.5 PAMAM dendrimer associates are therefore responsible for the PMF signals at $\Delta_o^w\phi > 0.30$ V. At pH 7.2, the PMF responses for the ion transfer process were broaden at $\Delta_o^w\phi > 0$ V and the adsorption responses of $HDIP^+$ were disappeared by adding the dendrimer in the aqueous phase (**Fig. 2-14b**). The broad PMF responses suggest the complex interfacial process involving the distribution of the neutral DIP from the organic phase into the hydrophobic interior of the dendrimers adsorbed at the interface and the protonation of DIP in the aqueous phase (**Fig. 2-16**). The additional bell-shaped PMF responses around the negative edge of the potential window relate to the adsorption process of the negatively charged dendrimer associated with $HDIP^+$ at the aqueous side of the interface.[35] In the G4 PAMAM dendrimer system (**Fig. 2-15b)**, the distorted PMF signals associated with the ion transfer and adsorption of the dendrimer were observed at $\Delta_o^w\phi > 0.30$ V similarly to the G3.5 PAMAM dendrimer system at pH 2.2. Under alkaline conditions, the 62 tertiary amines and 64 carboxylate groups of the G3.5 PAMAM dendrimer were totally deprotonated and the dendrimer has −64 charges on the periphery moiety. As shown in **Fig. 2-14c**, the well-defined PMF responses for the transfer of $HDIP^+$ across the interface were observed around 0.26 V in the presence of the dendrimer at pH 9.5. The PMF intensities were slightly weakened in the presence of the dendrimer in agreement with the voltammetric features in **Fig. 2-9c**. These results suggest that the transfer process of

$HDIP^+$ was depressed through the intermolecular association between the neutral DIP (or $HDIP^+$) and the hydrophobic interior (or the negatively charged periphery) of the G3.5 PAMAM dendrimer. The PMF signals associated with the transfer process of $HDIP^+$ were also attenuated in the presence of the G4 PAMAM dendrimer under alkaline conditions (**Fig. 2-15c**). The hydrophobic interaction between the neutral DIP and the dendrimer is presumed to be the principal effect in the G4 PAMAM dendrimer system. Although the interfacial mechanism of the non-fluorescent PRO species could not be analyzed in detail, the similar attenuation of the ion transfer response observed in the CVs for $HPRO^+$ might be interpreted as analogous mechanism (**Fig. 2-10a**)

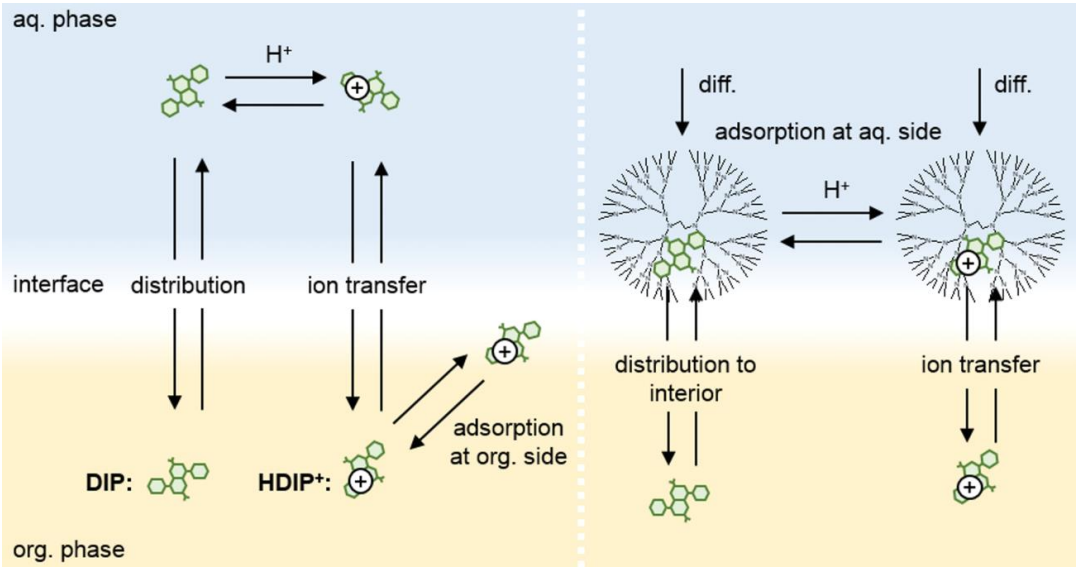

Fig. 2-16 Schematic representation of the interfacial mechanism of DIP in the absence (left) and presence (right) of the G3.5 PAMAM dendrimer adsorbed at the aqueous side of the interface under neutral conditions.

II-2 Flavin Derivatives System

II-2-1 Ion Association Behavior between the Dendrimer and Flavin Derivatives in the Aqueous Solution

RF and FMN are an important redox coenzyme which play a particularly important biological role in the electron transfer reactions of all living systems.[89] These flavin derivatives are decomposed to LC under illumination conditions.[90-92] It has been reported that lumiflavin is the dominant photoproduct of RF and FMN in alkaline solutions (pH > 8).[92] In this study, therefore, the pH condition of the aqueous solution was adjusted around pH 7 which is close to the pH condition *in vivo*. UV-Vis absorption and fluorescence spectra of RF, FMN and LC in the presence and absence of the G4 PAMAM dendrimer are shown in **Fig. 2-17**. RF in the aqueous solution gave two absorption peaks at 373 nm and 445 nm in the absence of the dendrimer (**Fig. 2-17a**). The spectroscopic property of RF have been widely investigated.[93] The peak wavelengths and associated molar absorptivities depend on the environment of flavin chromophore, e.g., solvent and pH. These absorbance characteristics are attributed to the π-π* electron transition. In addition, it has been reported that the absorbance at 373 nm could include the n-π* electron transition associated with electrons on nitrogen atoms.[93] The absorption peaks of RF were slightly blue-shifted to 370 nm and decreased, respectively, in the presence of the dendrimer. Spectroscopic studies of the interaction between RF and cyclodextrins or DNA in the aqueous solution have been reported.[94-96] The absorption peak around 370 nm is increased and blue-shifted, while the other peak around 440 nm is decreased in the presence of DNA.[94] These results demonstrated that RF molecules are intercalated into DNA double helix through the hydrophobic interaction. Our spectral results could indicate that RF interact with the interior moiety of the dendrimer in a similar manner of the DNA system. Fluorescence spectra were also affected in the presence of the dendrimer. In addition, NMR measurements were performed to confirm the interaction between RF

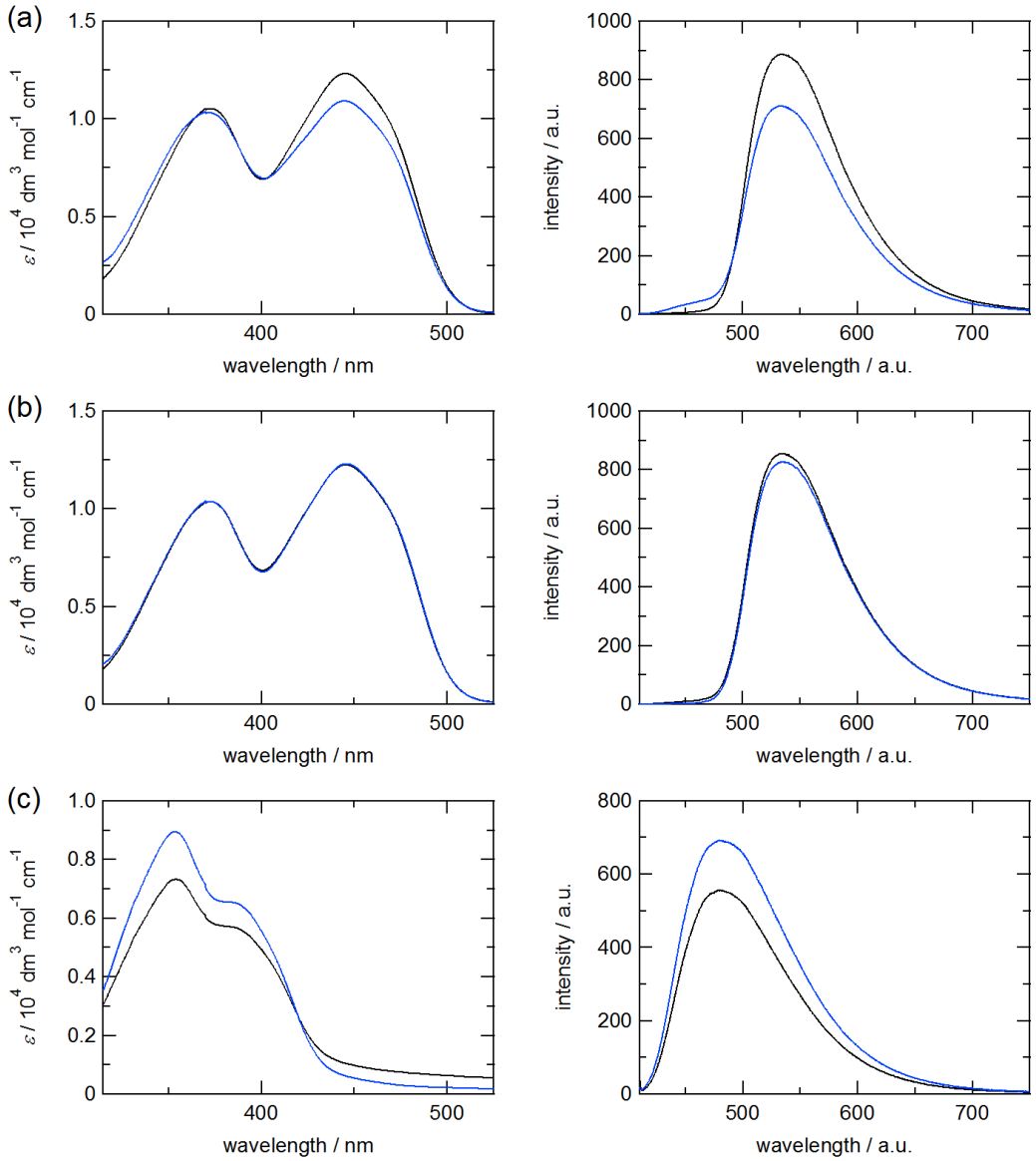

Fig. 2-17 UV-Vis absorption (left) and fluorescence (right) spectra of (a) RF, (b) FMN and (c) LC in the presence of the equimolar dendrimer in the aqueous solution at pH 7.1-7.3. The black lines refer to spectra in the absence of the dendrimer. The concentration of RF, FMN, LC and the dendrimer was 1.0×10^{-5} mol dm^{-3}. The excitation wavelength was 404 nm.

and the dendrimer. **Fig. 2-18** shows the dependence of ^{1}H NMR spectra of the G4 PAMAM dendrimer on RF concentration. The ^{1}H NMR spectrum of the PAMAM dendrimer consists of four broad ^{1}H peaks for the interior (a-d) and peripheral (b′, d′)

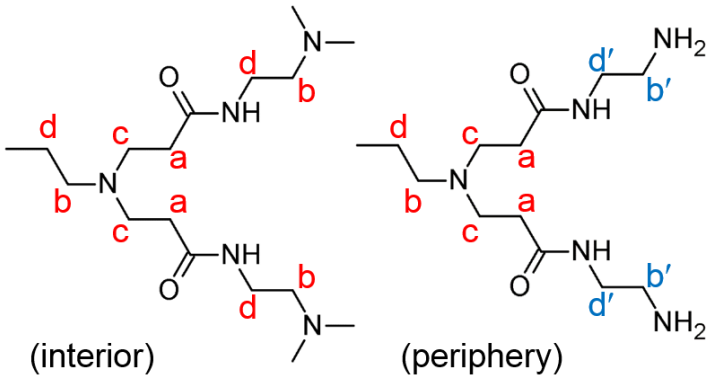

Scheme 2-1 Chemical structure and atom labeling of the branch and terminal units of the G4 PAMAM dendrimer. a-d refer to the interior methylene protons of the dendrimer. b′ and d′ refer to the peripheral methylene protons in the dendrimer.

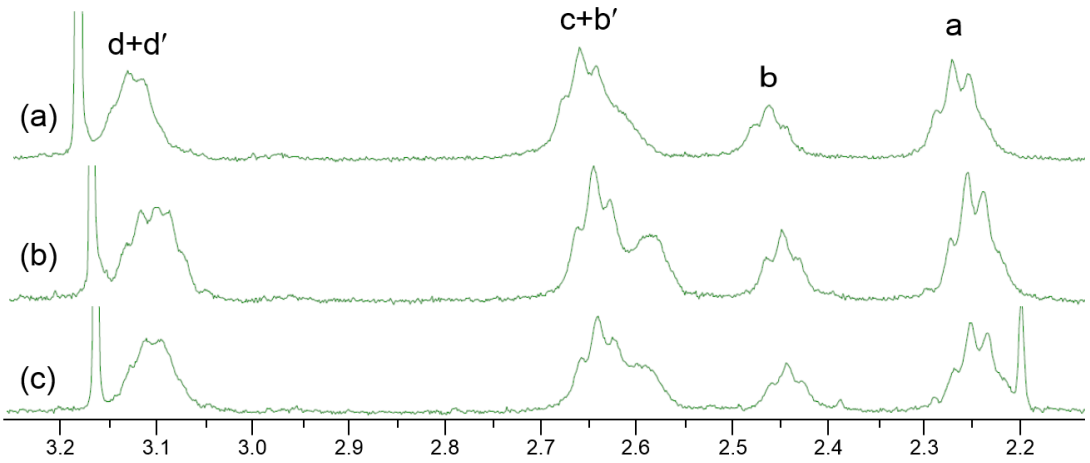

Fig. 2-18 ^{1}H NMR spectra of the G4 PAMAM dendrimer/RF in D_2O solutions at different molar ratios. The concentration of the dendrimer was 5.0×10^{-5} mol dm^{-3}. The concentrations of RF were (a) 0, (b) 5.0×10^{-5} mol dm^{-3} and (c) 1.0×10^{-4} mol dm^{-3}, respectively.

methylene in D_2O (**Scheme 2-1**).[97, 98] All these four peaks exhibited the slightly upfield shift and the new peak (shoulder) was observed around 2.6 ppm in the presence of RF caused by increasing of the electron density of methylene protons (**Table 2-2**). The interior moiety of the dendrimer is relatively hydrophobic. In addition, the PAMAM dendrimer has a number of amide groups in the interior moiety which can act as hydrogen

Table 2-2 Dependences of chemical shifts of ^{1}H NMR spectra for the G4 PAMAM dendrimer on the concentration RF

[RF] / 10^{-5} mol dm^{-3}	a	b	c+b′	d+d′
0	2.271	2.461	2.659	3.130
50	2.254	2.448	2.644	3.116
100	2.251	2.444	2.640	3.110

Table 2-3 Dependences of chemical shifts of ^{1}H NMR spectra for the G4 PAMAM dendrimer on the concentration FMN

[FMN] / 10^{-5} mol dm^{-3}	a	b	c+b′	d+d′
0	2.271	2.461	2.659	3.130
50	2.247	2.441	2.637	3.108
100	2.249	2.440	2.637	3.107

bonding sites. Therefore, NMR results suggested that the neutral RF could be encapsulated into the dendrimer by the hydrophobic interaction and/or hydrogen bonding. UV-Vis absorption and fluorescence spectra of LC were also changed in the presence of the dendrimer (**Fig. 2-17c**). The different association form of LC with the β-cyclodextrin (β-CD) and the human serum albumin (HSA) has been reported,[99] where the neutral LC is incorporated into the β-CD with the decrease of the fluorescence intensity. On the other hand, the anionic LC^- interact with HSA with the increase of fluorescence intensity. Taking into account the acidity constant of LC ($pK_{a,LC}$ = 8.28)[80], LC^- could exist in the present system (pH 7.3). Therefore, the enhancement of the fluorescence intensity may be due to the interaction between LC^- and the cationic G4 PAMAM dendrimer. On the other hand, UV-Vis absorption and fluorescence spectra of FMN were not significantly changed in the presence of the dendrimer (**Fig. 2-17b**). The anionic FMN could electrostatically interact with the positively charged periphery moiety of the dendrimer due to the negatively charged phosphate group in the aqueous solution, although ^{1}H NMR spectra of the G4 PAMAM dendrimer in the presence of the FMN indicated the upfield shift for all methylene protons (a-d′) as similar to those of RF systems (**Table 2-3**). It has

been reported that the interaction between the anionic mycophenolic acid (MPA) and the positively charged G5 PAMAM dendrimer induces the downfield shift of ^{1}H NMR peaks of the dendrimer due to the decrease of the electron density of methylene protons.[97] In the present NMR results indicated that the driving force of the interaction between FMN and the dendrimer could be the hydrophobic interaction and/or hydrogen bonding rather than the electrostatic interaction.

II-2-2 Adsorption Behavior of Flavin Derivatives in the presence of the Dendrimer at the Water|DCE Interface

CVs and capacitance curves of RF, FMN and LC in the absence of the dendrimer are shown in **Fig. 2-19**. At pH 7.1, the neutral RF ($pK_{a,RF}$ = 9.88)[100] and LC ($pK_{a,LC}$ = 8.28)[80] is dominant species while FMN ($pK_{a,FMN}$ = 6.18)[100] is anionic species. In the RF and LC system, CVs and capacitance curves were hardly changed as compared with those of base electrolyte systems (**Fig. 2-19a,c**). In principle, capacitive responses are decreased in case that the neutral species is adsorbed at the interface.[101, 102] According to electrochemical results, RF and LC exist as the neutral species, and transfer and adsorption of the ionic species do not take place at the interface. On the other hand, the capacitance of FMN system was increased in the whole potential region, although the current peak was not observed (**Fig. 2-19b**). These results indicated that the anionic FMN^- could not be transferred but adsorbed at the interface within the potential window.

Fig. 2-20 shows CVs and capacitance curves of the flavin derivatives in the presence of the G4 PAMAM dendrimer. Electrochemical responses of the flavin derivatives were not clearly observed due to the large current responses of the ion transfer of the positively charged dendrimer accompanied by the adsorption and facilitated transfer of the organic electrolyte anion in the positive potential region.[36]

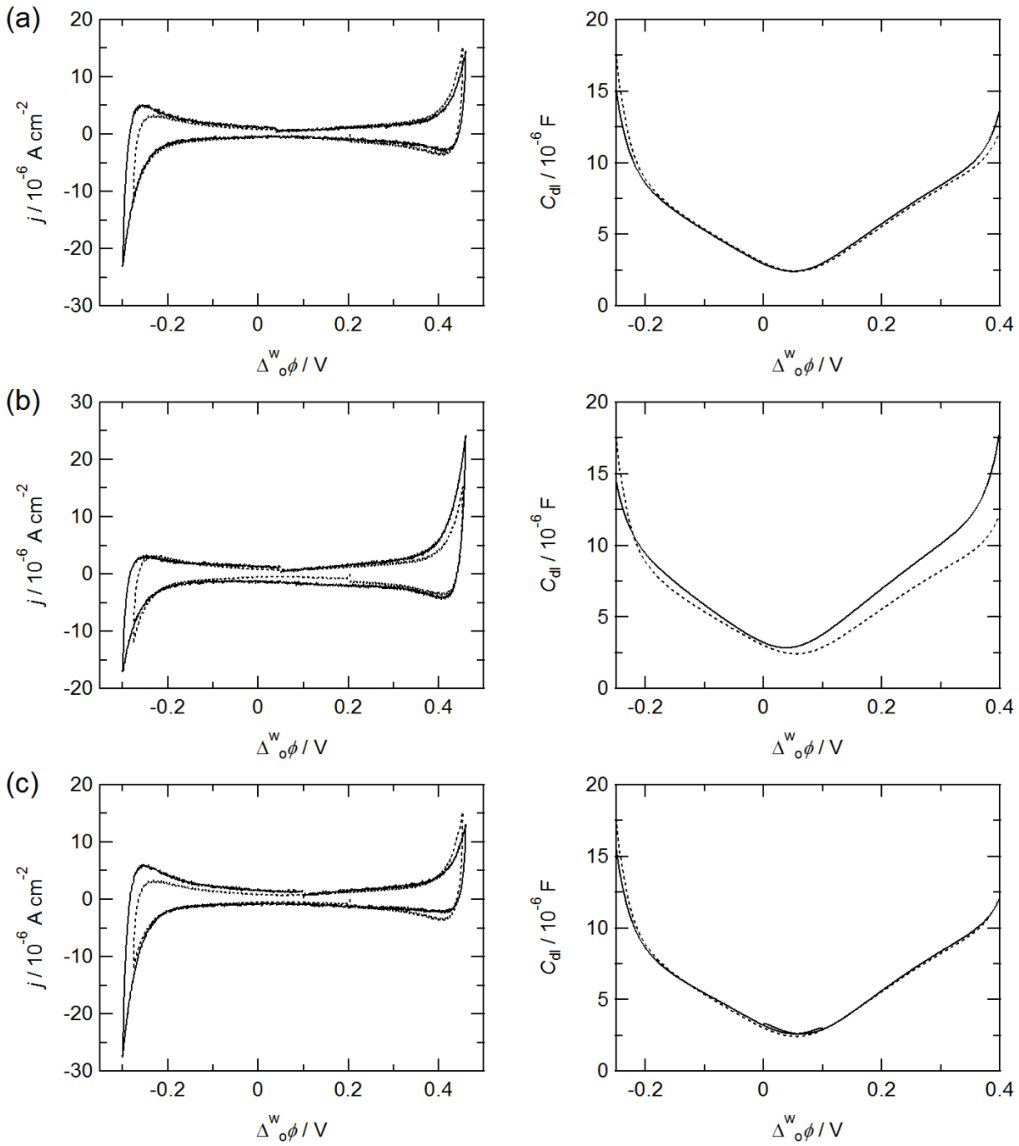

Fig. 2-19 CVs (left) and capacitance curves (right) measured for (a) RF, (b) FMN and (c) LC at pH 7.1. The dotted lines refer to the base electrolyte system at pH 7.1. (right) The amplitude of ac potential modulation was 10 mV at 7 Hz. The concentration of RF, FMN and LC was 1.0×10^{-5} mol dm^{-3}. The potential sweep rates were 50 mV s^{-1} for CVs and 5 mV s^{-1} for capacitance measurement, respectively.

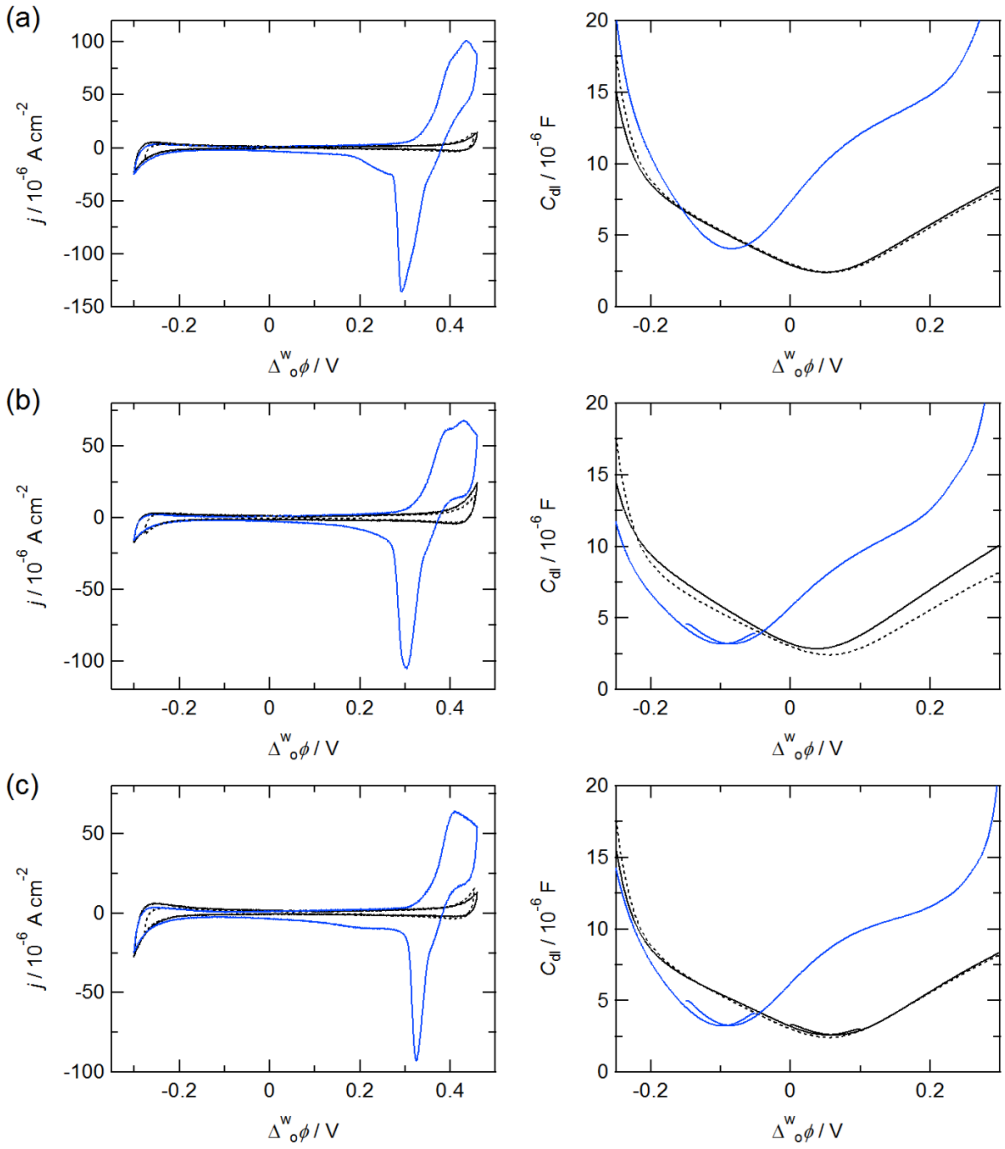

Fig. 2-20 CVs (left) and capacitance curves (right) measured for (a) RF, (b) FMN and (c) LC in the presence of the equimolar dendrimer at pH 7.3. The black and blue lines refer CVs and capacitance curves in the absence and presence of the dendrimer. (right) The dotted lines refer to the base electrolyte system at pH 7.1. The amplitude of ac potential modulation was 10 mV at 7 Hz. The concentration of RF, FMN, LC and the dendrimer was 1.0×10^{-5} mol dm^{-3}. The potential sweep rates were 50 mV s^{-1} for CVs and 5 mV s^{-1} for capacitance measurement, respectively.

II-2-3 Interfacial Mechanism of Flavin Derivatives Affected by the Dendrimer

The PMF spectroscopy was carried out in order to elucidate the interfacial mechanism of the flavin derivatives in the absence and presence of the G4 PAMAM dendrimer. The potential dependences of the PMF responses in the presence of the RF are shown in **Fig. 2-21**. The ambiguous PMF responses were obtained in the negative and positive potential regions. As shown in *II-2-2*, the electrochemical measurements indicated that the neutral RF is dominant species in the aqueous solution, and the ion transfer and adsorption could not be occurred. RF is well known as photosensitive dye. It has been reported that LC ($pK_{a,LC} = 8.29$) is one of the major photodegradation products of RF. Therefore, a relatively small amount of the negatively charged LC^- could exist in the interfacial region. The PMF signals, $\Delta F_{re} < 0$, $0 < \Delta F_{im}$, in the negative potential region could be attributed to the adsorption of LC^- at the aqueous side of the interface. **Fig. 2-22** shows the potential dependences and complex plane of the PMF responses of LC. The similar potential dependences of the PMF responses as RF were obtained in the negative and positive potential region. The frequency dependent PMF responses measured at −0.27 V were expressed as a distorted semicircle in the second quadrant (**Fig. 2-22b**). Therefore, the PMF responses in the negative potential region obtained in RF system were primarily associated with the adsorption process of the negatively charged LC^- at the aqueous side of the interface (**Fig. 2-25**). In both RF and LC systems, the gradual increase of the PMF responses, $\Delta F_{re} > 0$, $0 > \Delta F_{im}$, were observed in the positive potential region. These responses might be attributed to the adsorption of LC^- distributed into the organic phase. These PMF responses were decreased in the presence of the dendrimer (**Figs. 2-21** and **2-23**). The G4 PAMAM dendrimer which has the net charges of ca. +75 at pH 7.3 is not transferred and adsorbed in the negatively polarized interface.[36, 88] The decrease of the PMF responses in the negative potential region suggested that RF and LC^- are stabilized in the aqueous phase by associating with the dendrimer in agreement with spectroscopic results (**Fig. 2-17a**). The real and imaginary components of the PMF responses were

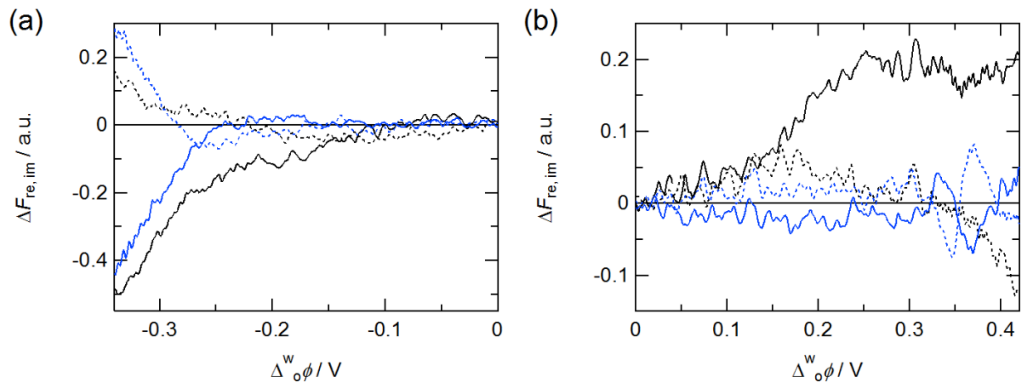

Fig. 2-21 Potential dependences of the PMF responses for RF at pH 7.1-7.3. The black and blue lines refer to the PMF responses in the absence and presence of the dendrimer, respectively. The solid and dotted lines relate to the real and imaginary components, respectively. The amplitudes of ac potential modulation was 20 mV at 1 Hz.

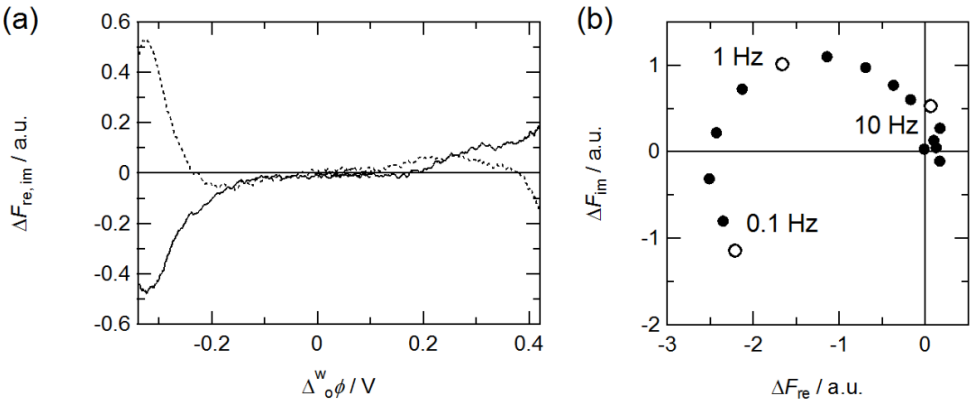

Fig. 2-22 Dependences of the PMF responses for LC at pH 7.1 on (a) the Galvani potential difference and (b) the potential modulation frequency at −0.27 V. (a) The solid and dashed lines refer to the real and imaginary components, respectively. The amplitude of ac potential modulation was 20 mV.

obtained as positive and negative signs around 0.33 V and vice versa around 0.36 V in the presence of RF and the dendrimer. These PMF responses were associated with the ion transfer of the dendrimer accompanied by the adsorption process at the organic side of

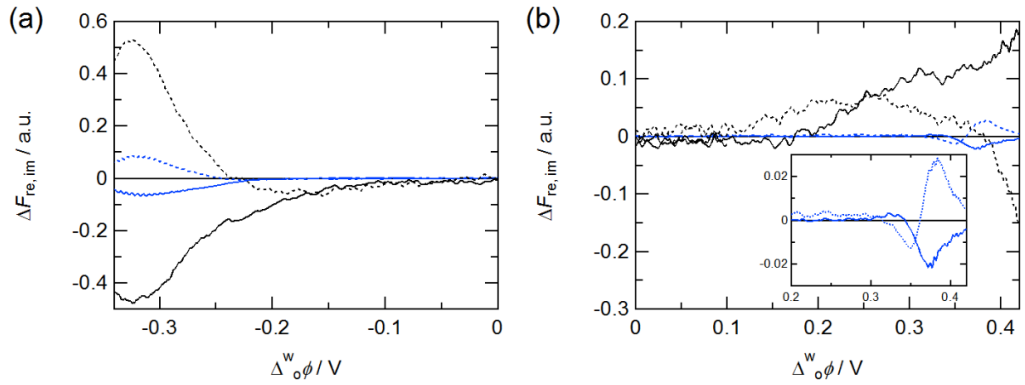

Fig. 2-23 Potential dependences of the PMF responses for LC at pH 7.1-7.3. The black and blue lines refer to the PMF responses in the absence and presence of the dendrimer, respectively. (inset) Extended PMF responses. The solid and dotted lines relate to the real and imaginary components, respectively. The amplitudes of ac potential modulation was 20 mV at 1 Hz.

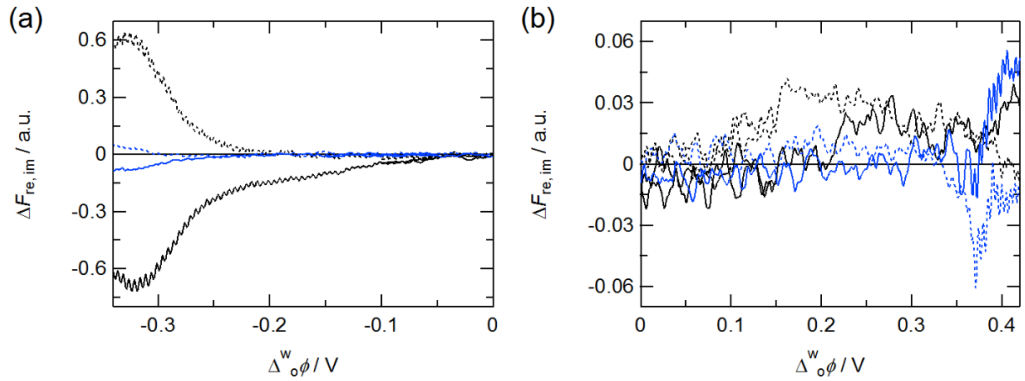

Fig. 2-24 Potential dependences of the PMF responses for FMN at pH 7.1-7.3. The black and blue lines refer to the PMF responses in the absence and presence of the dendrimer, respectively. The solid and dotted lines relate to the real and imaginary components, respectively. The amplitudes of ac potential modulation was 20 mV at 1 Hz.

the interface (*I-1-3*). The similar effect of the dendrimer was observed in the LC system (**Fig. 2-23**). The PMF responses for the adsorption of LC^{-} was decreased in the negative potential region due to the association with the dendrimer and its associates were transferred across the interface accompanied by the adsorption process at the organic side

of the interface in the positive potential region (**Fig. 2-25**).

The PMF analysis was also applied to the anionic FMN^- which has a phosphate group in the ribitol chain. The potential dependences of the PMF responses in the presence of the FMN^- are shown in **Fig. 2-24**. The well-defined PMF responses for the adsorption process at the aqueous side of the interface, $\Delta F_{re} < 0$, $0 < \Delta F_{im}$, were obtained around −0.33 V. These PMF responses were decreased in the presence of the dendrimer. The PMF results suggested that FMN^- could be stabilized in the aqueous phase by associating with the dendrimer, although no effective interactions with the dendrimer were observed through the spectroscopic measurements in the aqueous solution (**Fig. 2-17b**). Relatively weak positive real and negative imaginary components of the PMF responses were obtained in the positive potential region, $\Delta_o^w\phi > 0.35$ V. Similar to the RF, LC and the anionic porphyrins systems, the PMF responses could be due to the interfacial reactions of the dendrimer associated with FMN^-. Since the anionic FMN^- could be stabilized in the positively polarized interface, the dissociation of FMN^--dendrimer associates during the ion transfer of the associate could be attributed to the complexation of the PMF responses.

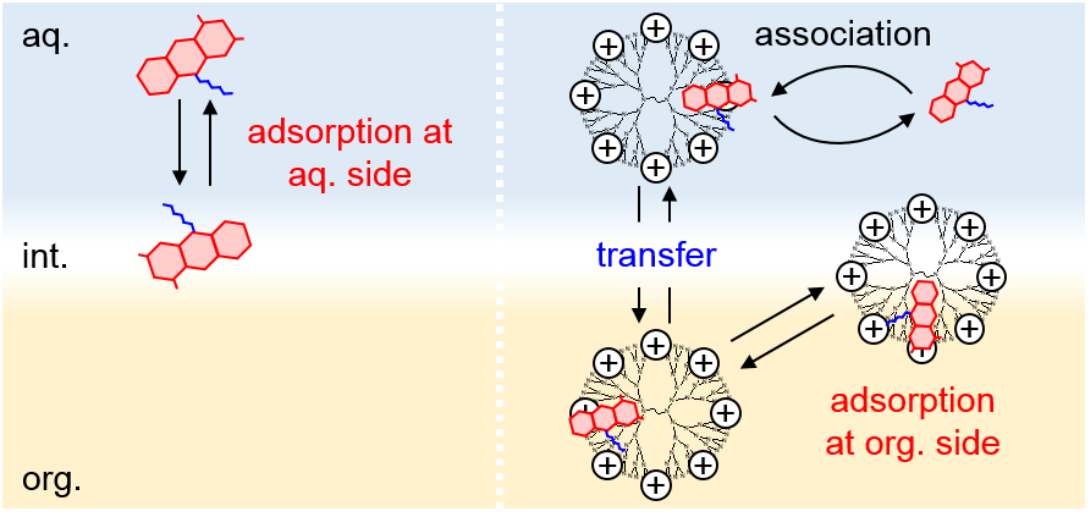

Fig. 2-25 Schematic representation of the interfacial mechanism of the flavin derivatives and the G4 PAMAM dendrimer proposed from the PMF measurements.

II-3 Summary of PART II

The interfacial behavior of the bioactive species in the presence of the PAMAM dendrimers was studied at the polarized water|DCE interface. The intrinsic interfacial mechanism of the bioactive species was significantly affected by acid-base equilibrium as well as liquid|liquid distribution of neutral species. The voltammetric results implied the weak interaction between the cationic drugs (DIP and PRO) and the dendrimers, while the electrochemical responses the anionic WAR and flavin derivatives were hardly affected by adding the dendrimers. The interfacial mechanism of the fluorescent DIP and flavin derivatives was analyzed in detail by the PMF spectroscopy. The charge transfer mechanism of the bioactive species was significantly changed by adding the dendrimers, in which the pH and potential dependencies of the reactivity of the dendrimers dominantly affected the transfer and adsorption processes of the bioactive species. The potential ability of the dendrimer as a modifier for the pharmacokinetic properties of bioactive species on a biomembrane was demonstrated through the present results. The detailed analysis of the interfacial association between the dendrimer and bioactive species will accelerate the development of highly functional DDS with the sensitivity to the pH conditions and membrane potentials *in vivo*.

CONCLUDING REMARKS

In this study, charge transfer reaction and molecular association behavior of the PAMAM dendrimer were investigated at the polarized water|DCE interface though the spectroelectrochemical techniques. Dendrimers, whose interior moiety provides a different environment from outer phase, showed the potential ability as molecular capsule (container) for various molecules. Although the porphyrins which are easily protonated in acidic solution, they were stabilized under acidic conditions by incorporating into the interior of the dendrimer. Some bioactive species also interacted with the dendrimer specifically at the interface. Those molecules were transferred across the interface by associating with the dendrimer. The molecule incorporated in the dendrimer could be released at the interface by applying appropriate potentials. In addition, the coordination to the metal center, generation of the dendrimer (size and shape), electrostatic and hydrophobic interaction, and hydrogen bonding play an important role for the molecular encapsulation behavior.

The present results clearly demonstrate that the dendrimer is capable as a molecular capsule as well as a protective agent for unstable or easily decomposable species. The intermolecular affinity of the dendrimer could enable development of highly functional DDS with membrane potential sensitivity and selective separation systems.

REFERENCES

1. Benjamin, I., *Chem. Rev.* **1996,** *96*, 1449-1475.
2. Girault, H. H., Electrochemistry at Liquid-Liquid Interfaces. In *Electroanalytical Chemistry*, Bard, A. J., Ed. CRC Press: 2010; Vol. 23, pp 1-104.
3. Samec, Z., *Pure Appl. Chem.* **2004,** *76*, 2147-2180.
4. Freiser, H., *Chem. Rev.* **1988,** *88*, 611-616.
5. Kihara, S.; Kasuno, M.; Okugaki, T.; Shirai, O.; Maeda, K., *Electrochmistry* **2012,** *80*, 390-400.
6. Senda, M.; Kubota, Y.; Katano, H., Voltammetric study of drugs at liquid-liquid interfaces. In *Liquid interfaces in chemical, biological, and pharmaceutical applications*, Volkov, A. G., Ed. New York, 2001; pp 683-698.
7. Reymond, F., Transfer mechanisms and lipophilicity of ionizable drugs. In *Liquid interfaces in chemical, biological, and pharmaceutical applications*, Volkov, A. G., Ed. Marcel Dekker: New York, 2001; pp 729-774.
8. Arai, K.; Kusu, F.; Takamura, K., *Electrochemical behavior of drugs at the oil/water interface*. CRC Press: 1996; p 375-400.
9. Deryabina, M. A.; Hansen, S. H.; Ostergaard, J.; Jensen, H., *J. Phys. Chem. B* **2009,** *113*, 7263-7269.
10. Deryabina, M. A.; Hansen, S. H.; Jensen, H., *Anal. Chem.* **2008,** *80*, 203-208.
11. Reymond, F.; Chopineaux-Courtois, V.; Steyaert, G.; Bouchard, G.; Carrupt, P. A.; Testa, B.; Girault, H. H., *J. Electroanal. Chem.* **1999,** *462*, 235-250.
12. Reymond, F.; Steyaert, G.; Carrupt, P. A.; Testa, B.; Girault, H. H., *J. Am. Chem. Soc.* **1996,** *118*, 11951-11957.

13. Kontturi, A. K.; Kontturi, K.; Murtomaki, L.; Schiffrin, D. J., *Acta Chem. Scand.* **1992,** *46*, 47-53.

14. Fermin, D. J., Linear and Non-linear Spectroscopy at the Electrified Liquid/Liquid interface. In *Diffraction and Spectroscopic Methods in Electrochemistry*, Alkire, R. C.; Kolb, D. M.; Lipkowski, J.; Ross, R. N., Eds. Wiley-VCH: 2006; pp 127-161.

15. Benjamin, I., *Chem. Rev.* **2006,** *106*, 1212-1233.

16. Nagatani, H.; Sagara, T., *Anal. Sci.* **2007,** *23*, 1041-1048.

17. Tomalia, D. A.; Christensen, J. B.; Boas, U., *Dendrimers, dendrons, and dendritic polymers: discovery, applications, and the future*. Cambridge University Press: Cambridge, 2012.

18. Cheng, Y. Y.; Zhao, L. B.; Li, Y. W.; Xu, T. W., *Chem. Soc. Rev.* **2011,** *40*, 2673-2703.

19. Tomalia, D. A., *Soft Matter* **2010,** *6*, 456-474.

20. Astruc, D.; Boisselier, E.; Ornelas, C., *Chem. Rev.* **2010,** *110*, 1857-1959.

21. Cheng, Y. Y.; Xu, T. W., *Eur. J. Med. Chem.* **2008,** *43*, 2291-2297.

22. Gillies, E. R.; Frechet, J. M. J., *Drug Discovery Today* **2005,** *10*, 35-43.

23. Kesharwani, P.; Jain, K.; Jain, N. K., *Prog. Polym. Sci.* **2014,** *39*, 268-307.

24. Tomalia, D. A.; Baker, H.; Dewald, J.; Hall, M.; Kallos, G.; Martin, S.; Roeck, J.; Ryder, J.; Smith, P., *Polym. J.* **1985,** *17*, 117-132.

25. Vögtle, F.; Richardt, G.; Werner, N., *Dendrimer Chemistry: Concepts, Syntheses, Properties, Applications*. Wiley-VCH: 2009.

26. Tomalia, D. A., *Prog. Polym. Sci.* **2005,** *30*, 294-324.

27. Morgan, M. T.; Carnahan, M. A.; Immoos, C. E.; Ribeiro, A. A.; Finkelstein, S.;

Lee, S. J.; Grinstaff, M. W., *J. Am. Chem. Soc.* **2003,** *125*, 15485-15489.

28. Hu, J. J.; Xu, T. W.; Cheng, Y. Y., *Chem. Rev.* **2012,** *112*, 3856-3891.

29. Han, J.; Gao, C., *Curr. Org. Chem.* **2011,** *15*, 2-26.

30. Prosa, T. J.; Bauer, B. J.; Amis, E. J., *Macromolecules* **2001,** *34*, 4897-4906.

31. Prosa, T. J.; Bauer, B. J.; Amis, E. J.; Tomalia, D. A.; Scherrenberg, R., *J Polym Sci Pol Phys* **1997,** *35*, 2913-2924.

32. Tomalia, D. A.; Naylor, A. M.; Goddard, W. A., *Angew Chem Int Edit* **1990,** *29*, 138-175.

33. Naylor, A. M.; Goddard, W. A.; Kiefer, G. E.; Tomalia, D. A., *J. Am. Chem. Soc.* **1989,** *111*, 2339-2341.

34. Berduque, A.; Scanlon, M. D.; Collins, C. J.; Arrigan, D. W. M., *Langmuir* **2007,** *23*, 7356-7364.

35. Nagatani, H.; Sakamoto, T.; Torikai, T.; Sagara, T., *Langmuir* **2010,** *26*, 17686-94.

36. Nagatani, H.; Ueno, T.; Sagara, T., *Electrochim. Acta* **2008,** *53*, 6428-6433.

37. Fermin, D. J.; Ding, Z.; Brevet, P. F.; Girault, H. H., *J. Electroanal. Chem.* **1998,** *447*, 125-133.

38. Nagatani, H.; Fermín, D. J.; Girault, H. H., *J. Phys. Chem. B* **2001,** *105*, 9463-9473.

39. Nagatani, H.; Iglesias, R. A.; Fermín, D. J.; Brevet, P. F.; Girault, H. H., *J. Phys. Chem. B* **2000,** *104*, 6869-6876.

40. Wandlowski, T.; Mareček, V.; Samec, Z., *Electrochim. Acta* **1990,** *35*, 1173-1175.

41. Nagatani, H.; Tonari, S.; Shibata, T.; Sagara, T., *Electrochem. Commun.* **2011,** *13*, 985-988.

42. Kadish, K. M.; Smith, K. M.; Guilard, R., *Handbook of Porphyrin Science*. World Scientific Publishing: Singapore, 2010.

43. Farajtabar, A.; Gharib, F.; Jamaat, P.; Safari, N., *J. Chem. Eng. Data* **2008,** *53*, 350-354.

44. Kim, Y.; Kim, J., *Anal. Chem.* **2014,** *86*, 1654-1660.

45. Perez-Tejeda, P.; Prado-Gotor, R.; Grueso, E. M., *Inorg. Chem.* **2012,** *51*, 10825-10831.

46. Ghosh, S.; Khan, A. H.; Acharya, S., *J Phys Chem C* **2012,** *116*, 6022-6030.

47. Myers, V. S.; Weir, M. G.; Carino, E. V.; Yancey, D. F.; Pande, S.; Crooks, R. M., *Chemical Science* **2011,** *2*, 1632-1646.

48. Bronstein, L. M.; Shifrina, Z. B., *Chem. Rev.* **2011,** *111*, 5301-5344.

49. Gouterman, M., *Jornal of Molecular Spectroscopy* **1961,** *6*, 138-163.

50. Gierszewski, M.; Wagniere, G. H., *J. Mol. Spectrosc.* **1963,** *11*, 108-127.

51. Maiti, P. K.; Cagin, T.; Lin, S. T.; Goddard III, W. A., *Macromolecules* **2005,** *38*, 979-991.

52. Da Costa, V. C. P.; Ribeiro, A. C. F.; Sobral, A. J. F. N.; Lobo, V. M. M.; Annunziata, O.; Santos, C. I. A. V.; Willis, S. A.; Price, W. S.; Esteso, M. A., *J. Chem. Thermodyn.* **2012,** *47*, 312-319.

53. Leisner, D.; Imae, T., *J. Phys. Chem. B* **2003,** *107*, 13158-13167.

54. Wang, X.; Zhao, L.; Ma, R.; An, Y.; Shi, L., *Chem. Commun.* **2010,** *46*, 6560-6562.

55. Paulo, P. M. R.; Costa, S. M. B., *J. Phys. Chem. B* **2005,** *109*, 13928-13940.

56. Paulo, P. M. R.; Gronheid, R.; De Schryver, F. C.; Costa, S. M. B., *Macromolecules* **2003,** *36*, 9135-9144.

57. Paulo, P. M. R.; Costa, S. M. B., *Photochemical and Photobiological Sciences* **2003,** *2*, 597-604.

58. Kubát, P.; Lang, K.; Zelinger, Z., *J. Mol. Liq.* **2007,** *131-132*, 200-205.

59. Choi, M. Y.; Pollard, J. A.; Webb, M. A.; McHale, J. L., *J. Am. Chem. Soc.* **2003,** *125*, 810-820.

60. Nagatani, H.; Ozeki, T.; Osakai, T., *J. Electroanal. Chem.* **2006,** *588*, 99-105.

61. Kakiuchi, T., *J. Electroanal. Chem.* **2001,** *496*, 137-142.

62. Tran, M. L.; Gahan, L. R.; Gentle, I. R., *J. Phys. Chem. B* **2004,** *108*, 20130-20136.

63. Eugster, N.; Fermin, D. J.; Girault, H. H., *J. Am. Chem. Soc.* **2003,** *125*, 4862-4869.

64. Fermin, D. J.; Duong, H. D.; Ding, Z. F.; Brevet, P. F.; Girault, H. H., *J. Am. Chem. Soc.* **1999,** *121*, 10203-10210.

65. Fermin, D. J.; Duong, H. D.; Ding, Z. F.; Brevet, P. F.; Girault, H. H., *PCCP* **1999,** *1*, 1461-1467.

66. Eugster, N.; Fermin, D. J.; Girault, H. H., *J. Phys. Chem. B* **2002,** *106*, 3428-3433.

67. Jensen, H.; Kakkassery, J. J.; Nagatani, H.; Fermin, D. J.; Girault, H. H., *J. Am. Chem. Soc.* **2000,** *122*, 10943-10948.

68. Kalyanasundaram, K.; Neumann-Spallart, M., *J. Am. Chem. Soc.* **1982,** *86*, 5163-5169.

69. Nagatani, H.; Dejima, S.; Hotta, H.; Ozeki, T.; Osakai, T., *Anal. Sci.* **2004,** *20*, 1575-1579.

70. Osakai, T.; Muto, K., *J. Electroanal. Chem.* **2001,** *496*, 95-102.

71. Shalinsky, D. R.; Jekunen, A. P.; Alcaraz, J. E.; Christen, R. D.; Kim, S.; Khatibi, S.; Howell, S. B., *Br. J. Cancer* **1993,** *67*, 30-36.

72. Bastida, E.; del Prado, J.; Almirall, L.; Jamieson, G. A.; Ordinas, A., *Cancer Res.* **1985,** *45*, 4048-52.

73. Rae, A. P.; Beattie, J. M.; Lawrie, T. D. V.; Hutton, I., *Br. J. Clin. Pharmacol.* **1985,** *19*, 343-352.

74. Porter, W. R., *J. Comput. Aided Mol. Des.* **2010,** *24*, 553-573.

75. Řehulková, O., *Biomedical Papers* **2001,** *145*, 27-38.

76. Karanikolopoulos, N.; Zamurovic, M.; Pitsikalis, M.; Hadjichristidis, N., *Biomacromolecules* **2010,** *11*, 430-438.

77. Tabak, M.; Borisevitch, I. E., *Biochim. Biophys. Acta* **1992,** *1116*, 241-249.

78. Borisevitch, I. E.; Tabak, M., *J. Lumin.* **1992,** *51*, 315-322.

79. Ishizaka, S.; Kitamura, N., *Anal. Sci.* **2004,** *20*, 1587-1592.

80. Tyagi, A.; Penzkofer, A., *Photochem. Photobiol.* **2011,** *87*, 524-533.

81. Drossler, P.; Holzer, W.; Penzkofer, A.; Hegemann, P., *Chem. Phys.* **2002,** *282*, 429-439.

82. Iseki, M.; Matsunaga, S.; Murakami, A.; Ohno, K.; Shiga, K.; Yoshida, K.; Sugai, M.; Takahashi, T.; Hori, T.; Watanabe, M., *Nature* **2002,** *415*, 1047-1051.

83. Christie, J. M.; Briggs, W. R., *J. Biol. Chem.* **2001,** *276*, 11457-11460.

84. Gobry, V.; Ulmeanu, S.; Reymond, F.; Bouchard, G.; Carrupt, P. A.; Testa, B.; Girault, H. H., *J. Am. Chem. Soc.* **2001,** *123*, 10684-10690.

85. Alves, C. N.; Castilho, M.; Mazo, L. H.; Tabak, M.; da Silva, A. B. F., *Chem. Phys. Lett.* **2001,** *349*, 146-152.

86. Otagiri, M.; Fokkens, J. G.; Hardee, G. E.; Perrin, J. H., *Pharm. Acta Helv.* **1978,**

53, 241-7.

87. Nassar, P. M.; Almeida, L. E.; Tabak, M., *Langmuir* **1998,** *14*, 6811-6817.

88. Sakae, H.; Nagatani, H.; Morita, K.; Imura, H., *Langmuir* **2014,** *30*, 937-945.

89. Massey, V., *Biochem. Soc. Trans.* **2000,** *28*, 283-296.

90. Holzer, W.; Shirdel, J.; Zirak, P.; Penzkofer, A.; Hegemann, P.; Deutzmann, R.; Hochmuth, E., *Chem. Phys.* **2005,** *308*, 69-78.

91. Ahmad, I.; Fasiliullah, Q.; Vaid, F. H. M., *J Photoch Photobio B* **2004,** *75*, 13-20.

92. Ahmad, I.; Fasihullah, Q.; Noor, A.; Ansari, I. A.; Ali, Q. N. M., *Int. J. Pharm.* **2004,** *280*, 199-208.

93. Ahmad, I.; Vaid, F. H. M., Photochemistry of Flavins in Aqueous and Organic Solvents. In *Flavins Photochemistry and Photobiology*, Silva, E.; Edwaards, A. M., Eds. RCS Publishing: Cambridge, 2006; Vol. 6, pp 13-40.

94. Wang, Q.; Wu, Q.; Wang, J.; Chen, D. D.; Fan, P.; Wang, B. X., *Spectrochim Acta A* **2014,** *117*, 754-762.

95. de Jesus, M. B.; Fraceto, L. F.; Martini, M. F.; Pickholz, M.; Ferreira, C. V.; de Paula, E., *J. Pharm. Pharmacol.* **2012,** *64*, 832-842.

96. Wang, X. M.; Chen, H. Y., *Spectrochim Acta A* **1996,** *52*, 599-605.

97. Hu, J. J.; Cheng, Y. Y.; Ma, Y. R.; Wu, Q. L.; Xu, T. W., *J. Phys. Chem. B* **2009,** *113*, 64-74.

98. Hu, J. J.; Cheng, Y. Y.; Wu, Q. L.; Zhao, L. B.; Xu, T. W., *J. Phys. Chem. B* **2009,** *113*, 10650-10659.

99. Marchena, M.; Gil, M.; Martin, C.; Organero, J. A.; Sanchez, F.; Douhal, A., *J. Phys. Chem. B* **2011,** *115*, 2424-2435.

100. Sigel, H.; Song, B.; Liang, G. G.; Halbach, R.; Felder, M.; Bastian, M., *Inorg. Chim. Acta* **1995,** *240,* 313-322.

101. Kakiuchi, T.; Kondo, T.; Senda, M., *Bull. Chem. Soc. Jpn.* **1990,** *63,* 3270-3276.

102. Kakiuchi, T.; Kotani, M.; Noguchi, J.; Nakanishi, M.; Senda, M., *J. Colloid Interface Sci.* **1992,** *149,* 279-289.

ACKNOWLEDGMENTS

Throughout the course of this study, I have received generous support from many people. Taking this opportunity, I would like to express my gratitude to the people.

I owe my deepest gratitude to Associate Professor Hirohisa Nagatani of Kanazawa University for his penetrating and constructive advice. He sincerely encouraged me in the research and his continuous support has been a great help for me. Without his encouragement, this dissertation would not have been accomplished.

I express my gratitude to all members of Kanazawa University Analytical Chemistry Laboratory for their support in everyday life.

I thank my parents, Yoshio and Yasuko Sakae, for continuous support and encouragement.

PUBLICATION LIST

[1] Hiroki Sakae, Hirohisa Nagatani, Kotaro Morita, Hisanori Imura, "Spectroelectrochemical Characterization of Dendrimer-Porphyrin Associates at Polarized Liquid|Liquid Interfaces", *Langmuir*, **30**, 937-945 (2014).

[2] Hirohisa Nagatani, Hiroki Sakae, Taishi Torikai, Takamasa Sagara, Hisanori Imura, "Photoinduced Electron Transfer of PAMAM Dendrimer-Zinc(II) Porphyrin Associates at Polarized Liquid|Liquid Interfaces", *Langmuir*, **31**, 6237-6244 (2015).

[3] Hiroki Sakae, Hirohisa Nagatani, Hisanori Imura, "Ion transfer and adsorption behavior of ionizable drugs affected by PAMAM dendrimers at the water|1,2-dichloroethane interface", *Electrochimica Acta*, **191**, 631-639 (January, 2016).

Following publication is not included in this dissertation:

[4] Hirohisa Nagatani, Makoto Harada, Hajime Tanida, Hiroki Sakae, Hisanori Imura, "Coordination structure of bromide ions associated with hexyltrimethylammonium cations at liquid/liquid interfaces under potentiostatic control as studied by total-reflection X-ray absorption fine structure", *The Journal of Chemical Physics*, **140**, 101101 (2014).